

**LEVEL II**

2



ADA 078670

**VARIABLE CYCLE ENGINE MULTIVARIABLE CONTROL SYNTHESIS**

**Interim Report --- Control Structure Definition**

STEPHEN M. ROCK  
RONALD L. DE HOFF

SYSTEMS CONTROL, INC. (VT)  
1801 PAGE MILL RD.  
PALO ALTO, CA 94304

FEBRUARY 1979

DDC  
RECEIVED  
DEC 27 1979  
E

TECHNICAL REPORT AFAPL-TR-79-2043  
INTERIM REPORT FOR PERIOD 1 SEPTEMBER 1977 - 31 AUGUST 1978

DDC FILE COPY

Approved for public release; distribution unlimited

AIR FORCE AERO-PROPULSION LABORATORY  
AIR FORCE WRIGHT-AERONAUTICAL LABORATORIES  
AIR FORCE SYSTEMS COMMAND  
WRIGHT-PATTERSON AIR FORCE BASE, OHIO 45433

79 12 27 15

NOTICE

When Government drawings, specifications, or other data are used for any purpose other than in connection with a definitely related Government procurement operation, the United States Government thereby incurs no responsibility nor any obligation whatsoever; and the fact that the government may have formulated, furnished, or in any way supplied the said drawings, specifications, or other data, is not to be regarded by implication or otherwise as in any manner licensing the holder or any other person or corporation, or conveying any rights or permission to manufacture, use, or sell any patented invention that may in any way be related thereto.

This report has been reviewed by the Information Office (OI) and is releasable to the National Technical Information Service (NTIS). At NTIS, it will be available to the general public, including foreign nations.

This technical report has been reviewed and is approved for publication.



CHARLES A. SKIRA  
Project Engineer



CHARLES E. BENTLEY  
Tech Area Manager, Controls

FOR THE COMMANDER



ERNEST C. SIMPSON  
Director  
Turbine Engine Division

"If your address has changed, if you wish to be removed from our mailing list, or if the addressee is no longer employed by your organization please notify AFAPL/TBC, W-PAFB, OH 45433 to help us maintain a current mailing list".

Copies of this report should not be returned unless return is required by security considerations, contractual obligations, or notice on a specific document.



20. ABSTRACT (Continued)

authority digital electronic controller must utilize demonstrated multi-variable design techniques to integrate adequately these complex system functions.

A preliminary design of a controller for this variable cycle engine is described. It is implementable on a small digital computer (less than 16K words of storage), and is modular in design (subroutine format). Specific controller functions of transient regulation, steady state regulation, trajectory generation, signal processing, and fault detection and accommodation are incorporated in a way which allows experimentation with different techniques for each function without affecting the overall structure. Promising techniques for implementing each function are discussed.



# TABLE OF CONTENTS

	Page
I. EXECUTIVE SUMMARY . . . . .	1
1.1 Introduction . . . . .	1
1.2 Multivariable Control Design Program for the GE-23 Variable Cycle Engine . . . . .	3
1.3 Summary . . . . .	5
II. CONTROL REQUIREMENTS FOR A VARIABLE CYCLE ENGINE . . . . .	7
2.1 Introduction . . . . .	7
2.2 The GE23-JTDE Variable Cycle Engine . . . . .	7
2.3 Control Hardware Characteristics . . . . .	10
2.4 Mission Definition . . . . .	16
2.5 Control Requirements . . . . .	19
2.6 Summary . . . . .	22
III. MULTIVARIABLE CONTROL DESIGN METHODOLOGY . . . . .	24
3.1 Introduction . . . . .	24
3.2 The Control Design Problem . . . . .	24
3.3 Feedforward and Transition Control . . . . .	25
3.4 Classical Control Synthesis . . . . .	29
3.5 Modern Control Synthesis Methods . . . . .	29
3.6 Model Generation . . . . .	39
3.7 Nonlinear Model Development . . . . .	52
3.8 Summary . . . . .	57
IV. CONTROL STRUCTURE DEFINITION . . . . .	58
4.1 Introduction . . . . .	58
4.2 Overview of System . . . . .	63
4.3 Nonlinear Model . . . . .	68
4.4 Reference Point Schedules . . . . .	69
4.5 Trajectory Generator . . . . .	77
4.6 Multivariable Regulator Logic . . . . .	81
4.7 Fault-Tolerant Filter . . . . .	84
4.8 Engine Limit Logic . . . . .	85
4.9 Failure Accommodation Logic . . . . .	86
4.10 Summary . . . . .	92
V. PRELIMINARY DESIGN RESULTS . . . . .	94
5.1 Linear Model Analysis . . . . .	94
5.2 Nonlinear Model Generation . . . . .	118
5.3 Actuator Servo Valve Compensation . . . . .	122
5.4 Transition Generator Demonstration . . . . .	134

TABLE OF CONTENTS (Continued)

	Page
VI. SUMMARY AND PROGRAM STATUS . . . . .	138
6.1 Summary . . . . .	138
6.2 Program Status . . . . .	139
APPENDIX A: DERIVATION OF $\frac{dJ}{dC}$ . . . . .	141
APPENDIX B: SECOND STAGE MODEL REDUCTION . . . . .	147
APPENDIX C: MODELING PROCEDURES FOR THE VARIABLE CYCLE ENGINE . . . . .	151
REFERENCES . . . . .	160

## LIST OF FIGURES

		Page
1.1	Variable Cycle Engine . . . . .	3
1.2	Multivariable Control Design Program for the GE-23 Variable Cycle Engine . . . . .	4
2.1	Variable Cycle Engine - Controls and Outputs . .	8
2.2	Grumman Design 623 VSTOL-B Fighter . . . . .	10
2.3	Functional Hardware Description . . . . .	10
2.4	Control System Diagram . . . . .	12
2.5	Fail-Fixed Servo Valve . . . . .	15
2.6	Grumman 623 Envelope . . . . .	16
2.7	Three Typical Mission Profiles for the GE23/623 Involving Air Combat, VTOL Intercept and Subsonic Surveillance . . . . .	17
2.8	Partition of Operating Envelope in Mission . . .	18
3.1	Block Diagram of Output Regulator Design . . . .	40
3.2	Generation of Design Models . . . . .	49
3.3	Comparison of Time Histories for Second Stage Reduction Example . . . . .	51
4.1	Controller Structure . . . . .	59
4.2	FADEC Hardware . . . . .	61
4.3	Control Signal Flow Diagram . . . . .	65
4.4	Reference Point Schedule Generator . . . . .	70
4.5	Control Criteria within Flight Envelope . . . . .	72
4.6	Control Saturation Effects on $N_p$ Schedule . . . .	75
4.7	Reference Point Calculation Flowchart . . . . .	75
4.8a	Trajectory Generator Logic - Large Transient Control Loop . . . . .	79
4.8b	Trajectory Generator Logic - Small Transient Loop	79
4.9a	$T_4$ Limit Schedule . . . . .	82
4.9b	$TB_4$ Limit Schedule for Increased Engine Life . .	82
4.10	Engine Limit Logic . . . . .	87
4.11	Overview of Engine Limit Logic . . . . .	88
4.12a	Normal Operation of Actuator Servo Loop . . . . .	91
4.12b	Operation of Actuator with Failed LVPT . . . . .	91
5.1a	Definition of Flight Points vs. Altitude and Mach Number . . . . .	96
5.1b	Definition of Flight Points vs. PT2 and TT2 . . .	96

LIST OF FIGURES (Continued)

	Page
5.2 Definition of Power Points 1 through 5 and A through D . . . . .	97
5.3 Variable Cycle Engine - Controls and Outputs . . .	103
5.4 Differential and Collective Spool Response Time Constants at Flight Points 1 through 6 . . . . .	107
5.5 Temperature Response Time Constants at Flight Points 1 through 6 . . . . .	107
5.6 Eigenvalues Corresponding to Engine Gas Dynamics at Each of Six Flight Conditions . . . . .	108
5.7 Eigenvalues (Gas Dynamics) vs. Flight Condition	108
5.8 Eigenvector Composition of the Five Principal Modes at SLS/Maximum Power (Table 5.7) . . . . .	109
5.9 Residue Spectra of Selected Transfer Functions. . .	111
5.10 Sensitivity of Mean Square Response to Elements in F-Matrix . . . . .	115
5.11 Nonlinear Model Generation Procedure . . . . .	118
5.12 Comparison of Linear Eigenvalue Locations and Root Locations Found by Linearizing the Nonlinear Model at 28 Flight Points Spanning the Envelope . . . . .	120
5.13 Comparison of Idle to Military Power Step Simulated using Linear Model Derived at Intermediate Power, the Nonlinear Model Derived from Linear Matrices and a Model using Linearizations at Each Point along the Trajectory . . . . .	121
5.14 Failed-Fixed Servo Valve Characteristic . . . . .	123
5.15 Revised Failed-Fixed Servo Valve Characteristic . . .	123
5.16 Block Diagram of Actuator Valve Servo Loop . . . . .	125
5.17 Modulation Interval, Sample Interval and Computation Interval . . . . .	127
5.18 Flowchart of Actuator Valve Servo Loop Simulation	128
5.19 Nonlinear Compensation for Actuator Servo Valve (FADEC 1) . . . . .	130
5.20 Step Response of FADEC Valve #1 to a 10% of Full Scale Step in Commanded Stroke . . . . .	131
5.21 Step Response of FADEC Valve #2 to a 10% of Full Scale Step in Commanded Stroke . . . . .	133

LIST OF FIGURES (Concluded)

	Page
5.22 Comparison of Step Response and Linear Servomechanism Response for a 10% Acceleration to SLS . .	135
5.23 Demonstration Trajectory Generator for VCE Linear Simulation Using a Fuel Flow Actuator and Two Nonlinear, Variable Rate Feedbacks . . . . .	136
5.24 Demonstration of Temperature and Surge Limiting Acceleration Trajectory Using Nonlinear, Variable Rate Feedback . . . . .	137

# LIST OF TABLES

		Page
2.1	Sensor Hardware . . . . .	13
2.2	Actuator Characteristics . . . . .	14
2.3	Flight Domain Related Control Criteria . . . . .	19
2.4	Engine Limits . . . . .	20
2.5	Error Tolerances on Set Points . . . . .	21
2.6	Failure Tolerance Specification . . . . .	22
3.1	Classical Control: Advantages and Disadvantages . . . . .	30
3.2	Modern Control: Advantages and Disadvantages . . . . .	32
4.1	Input/Output Signal Categories . . . . .	62
4.2	Preliminary Functional Description of Multivariable Control . . . . .	64
4.3	Mission/Aircraft Definition (Control Performance Criteria) . . . . .	71
4.4	Operating Constraints . . . . .	73
4.5	Modes of Operation . . . . .	74
5.1	Definition of Power Points . . . . .	98
5.2	Summary of Sixty Linearization Points . . . . .	99
5.3	Engine State Variables . . . . .	101
5.4	Engine Inputs . . . . .	101
5.5	Engine Output Variables . . . . .	102
5.6	Eigenvalues of VCE at SLS - Maximum Power . . . . .	106
5.7	Principal Dynamic Modes of VCE at SLS - Maximum Power . . . . .	106
5.8	State Variables for Reduced Order System . . . . .	110
5.9	Comparison of Eigenvalues* between F and $\hat{F}$ . . . . .	117
5.10	Preliminary Nonlinear Model Structure . . . . .	119

SECTION I  
EXECUTIVE SUMMARY

1.1 INTRODUCTION

Aircraft turbine engine propulsion control systems have been the focus of extensive development in recent years. Improvements in all types of engine components have been realized by optimized materials, and configuration, and the addition of variable geometry. Engine control hardware technology has accordingly progressed to utilize effectively the nearly unlimited capabilities of digital processing machines. This progress has occurred so rapidly that demonstrated theoretical synthesis techniques using the vastly increased performance potential have been few. Recently, programs sponsored by the Air Force Aero Propulsion Laboratory and NASA Lewis Research Center have begun to exploit this area [1,2]. The AFAPL/NASA LeRC-sponsored F100 multivariable controls program is an example of the successful demonstration of this emerging technology on a current production aircraft turbine [2,3].

Future engine cycles have been defined and include a significant variable geometry capability to the extent that the thermodynamic engine cycle varies over wide limits. This new variable cycle engine (VCE) definition, for example, includes the latest engine technology. The number of actuated variables have been similarly expanded and resulting control strategies are sufficiently complex to require extension of the current advanced multivariable control methodologies.

Military aircraft missions of the 1980's and beyond are dictating the requirement for multimode integration of airframe and propulsion systems over a wide flight envelope. In most present designs, the multimode requirement is being met by varying aircraft configurations or relying on active controls technology to accommodate response changes to varying flight conditions. It is becoming evident that much of the multimode capability must

be met by the propulsion system itself. The apparent tactical effectiveness of vectored thrust further highlights the need for multimode performance capability to be at least partially satisfied by the propulsion system.

The provision of multimode propulsion response capability, without sacrificing efficiency or performance, is achievable by engines with variable cycles which are controlled by commanded internal geometrical changes in the engine itself. Such control capability is achieved at the expense of a significant increase in engine complexity, addition of actuators, and addition of sensors. The subsequent control system complexity to maintain strict transient and steady state performance specifications forces attention to more accurate and reliable controller implementations. The evaluation of engine control technology is showing that such complex engine control functions could be implemented with digital electronic techniques, relying on hydromechanical control hardware for backup, fail/operate functions [4]. Control synthesis techniques for such digital systems are now being developed and demonstrate multivariable design techniques can integrate adequately the complex coupling of the system, its functions, modes, and performance requirements.

The variable cycle turbine engine, GE23-JTDE, represents a prototype of future multimode propulsion plants. It is a sophisticated design of highly variable geometry and multiple control inputs. To control such an engine, a large number of engine variables must be sensed including engine pressures, temperatures, rotor speeds, and airframe and inlet commands. A controller for this engine must therefore be delineated as multivariable (i.e., manipulating large numbers of input and output variables) and multifunctional (i.e., perform, in addition to control logic, also data conditioning and fault diagnosis). The development of such a full authority digital electronic controller must therefore utilize demonstrated multivariable design techniques to integrate adequately these complex system functions.

## 1.2 MULTIVARIABLE CONTROL DESIGN PROGRAM FOR THE GE-23 VARIABLE CYCLE ENGINE

Systems Control, Inc. (Vt) is conducting an advanced development program for the Air Force Aero Propulsion Laboratory to design a multivariable controller for an advanced variable cycle engine. An associated contractor, the General Electric Co., Aircraft Engine Group, is providing modeling and simulation data describing the Joint Technology Demonstrator Engine, the GE-23.

The GE-23 was selected as the test bed for advanced VCE multivariable control design because of the availability of digital hardware capability for direct application of digital control logic. An engine cross section is shown in Figure 1.1 [5]. The engine actuated variables include two variable fuel flows and eight variable geometries. It is a double-bypass, single nozzle, mixed-flow, augmented variable-cycle turbofan with forward and aft variable-bypass injectors. Both fan blocks and turbines are single stage. There are variable inlet guide vanes and variable-area turbine nozzles.

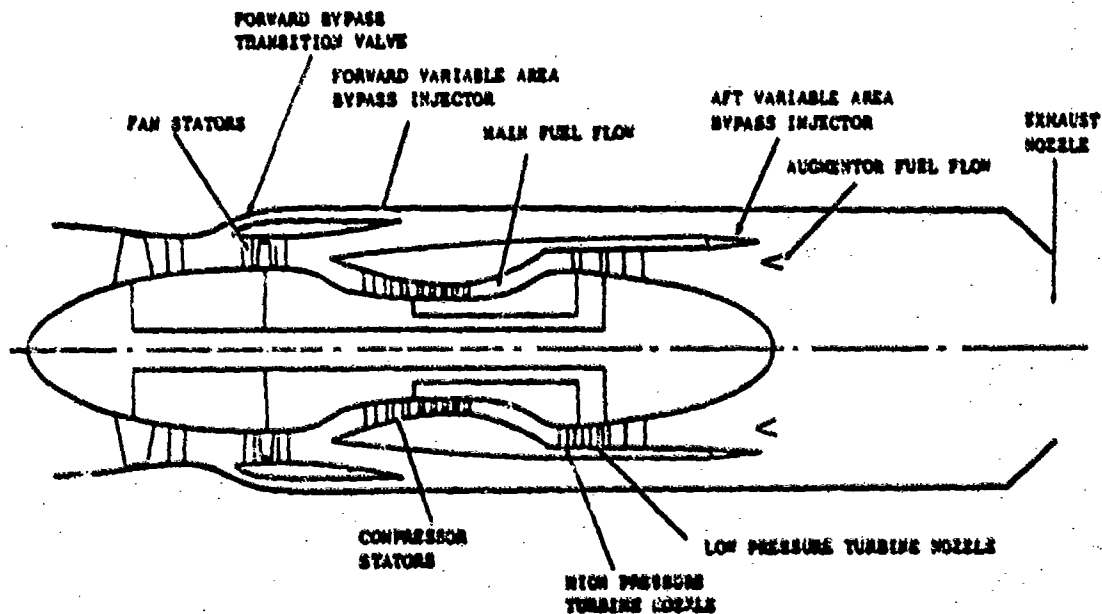


Figure 1. Variable Cycle Engine

The development program (Figure 1.2) consists of a Phase I control definition activity and a Phase II design demonstration. This report details the results of the Phase I control structure definition and presents selected examples of the application of the multivariable control design methodology. The development of a demonstrator MVC for the GE-23 engine will be accomplished in Phase II. Validation of the logic will be undertaken on a detailed nonlinear digital simulation of the engine. The controller will then be implemented on a hybrid simulation facility at General Electric, Evandale, Ohio, for detailed evaluation and validation of the performance throughout the flight envelope.

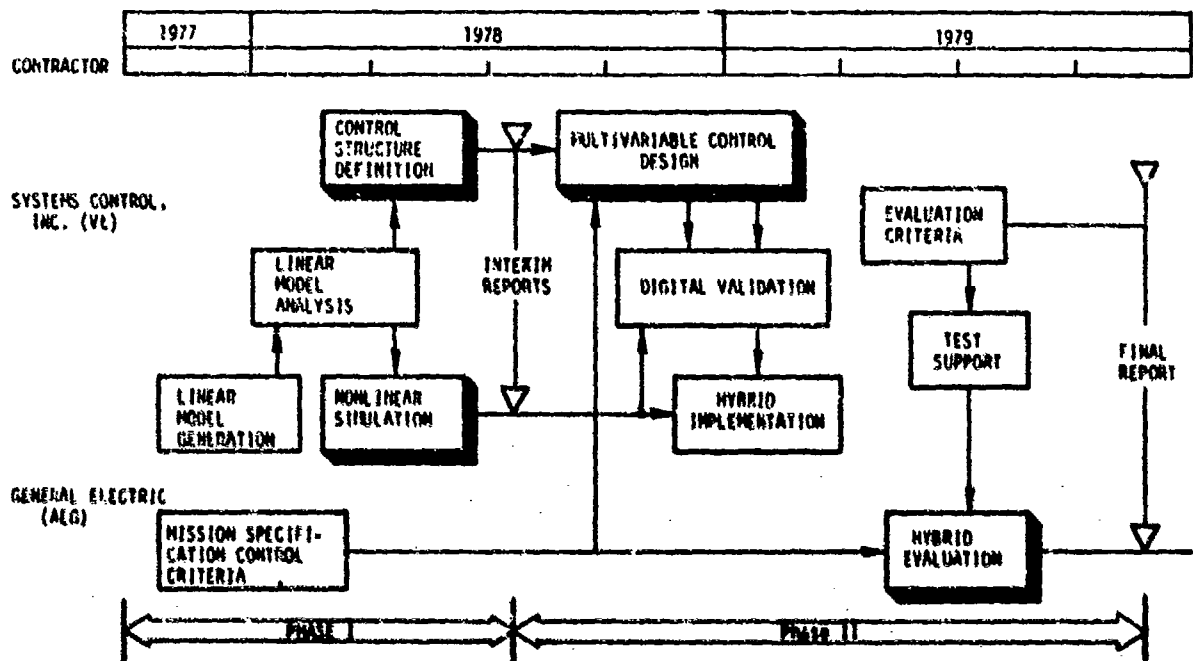


Figure 1.2 Multivariable Control Design Program for the GE-23 Variable Cycle Engine

The successful completion of these activities will represent a major accomplishment in the application of modern control technology to advanced cycle turbine propulsion systems. The realization of improved engine performance and reliability relies heavily

on the control algorithm which effectively operates the engine to satisfy the stringent limiting criteria and performance requirements in the presence of failures and degradation. It is the goal of this program to demonstrate the flexibility and effectiveness of modern, digital control design methodology in solving the difficult problems associated with the turbine engine application and prototype a system for installation in the future engine implementation.

### 1.3 SUMMARY

This report details the specification of a multivariable control structure for the GE-23 variable cycle engine. This report represents a self-contained document which describes the design methodology which has been developed to address the controls criteria, mission specification and hardware definition for operation of the engine within a typical installed envelope. The report is meant to provide a reference to the design process. The final report will describe the synthesis and evaluation of a control using the procedures presented below, for the GE-23. The anticipated computer storage requirement for this control is between 8K and 12K words of memory.

The report is organized as follows:

- Section II Control Requirements for the Variable Cycle Engine

This chapter presents the definition of the variable cycle engine (VCE) control problem for the GE-25. Engine hardware and interfaces are described. The installed mission definition is presented and the control design criteria are established. Each of these elements is considered during the formulation of the control structure and the underlying synthesis methodology.

- Section III Multivariable Control Design Methodology

This chapter details the synthesis procedures which are required for development of the multimode controller. The calculation of the control law, generation of trajectories and provision for failure tolerance and accommodation are treated from a theoretical viewpoint.

- Section IV Control Structure Definition

The functional definition of the control logic is presented in Chapter IV. The reference schedules, trajectory generator, multivariable control law, engine protection and fault tolerant filter modules are described. The synthesis of these blocks is related to the theoretical procedures presented in Chapter III and a detailed specification of the prototype system and alternatives is delineated.

- Section V Preliminary Design Results

Several procedures which will be utilized in the final control design have been exercised on preliminary data supplied by the engine manufacturer. Results concerning linear model analysis, nonlinear model development, control design methods and actuator compensation are presented and evaluated relative to the theoretical goals and ultimate design applications.

- Section VI Summary and Conclusions

Chapter VI summarizes the control structure and describes the design and synthesis activities being undertaken in Phase II.

This report represents interim progress in a major design effort. At this point in time, it appears that the control design process which will be a product of this study can have major and lasting impact on the production of the next generation high performance aircraft propulsion plants.

## SECTION II

### CONTROL REQUIREMENTS FOR A VARIABLE CYCLE ENGINE

#### 2.1 INTRODUCTION

The next generation aircraft weapon system will achieve higher levels of performance, versatility and effectiveness than its predecessors at the cost of increased complexity. The variable cycle engine incorporates larger numbers of actuated and sensed variables to meet these advanced mission requirements. This chapter describes a prototype variable cycle engine which will constitute the test bed for demonstration of the multivariable control design methodology.

The General Electric GE23-JTDE engine is described. This engine will be controlled by an engine-mounted microelectronic digital computer being developed under the Full Authority Digital Electronic Control (FADEC) program by the General Electric Company.

Mission definition and installation requirements are specified for an advanced, VSTOL-B military fighter concept, the Grumman 623. Control requirements are described for performance, response, limit protection and failure accommodation within the framework of the above control hardware and installed environment. This chapter describes the control criteria being addressed by the multivariable control design. Further information concerning the design data can be found in Ref. 6.

#### 2.2 THE GE23-JTDE VARIABLE CYCLE ENGINE

The GE23 is a twin-spool turbofan engine (see Figure 2.1). The compressor and high pressure turbine form the core assembly. Variable compressor stators (STP25) and turbine area (STP49) can be used to modulate the core operating characteristics. The low



The JTDE's variable geometry gives it the ability to operate over a significant power range at constant airflow. Cycle pressure and temperature ratio is varied to produce this operation. Conventional turbojets or turbofans modulate thrust by reducing airflow along with pressure and temperature ratio.

At intermediate power setting the JTDE operates as a low bypass ratio mixed flow augmented turbofan. The forward bypass transfer valve is closed, the forward bypass injector is open and the engine is operating at its maximum pressure ratio. All air flow is compressed by both blocks of the fan. As power is reduced, pressure ratio can be lowered by opening the nozzle or by bypassing air around the second block of the fan. Using control of the forward injector and the fan variable geometry, the second block can be unloaded without changing airflow or the operating conditions of the front block of the fan. Fan turbine nozzle area can be increased to reduce its power to match the reduced power required to drive the fan in the double bypass mode. The engine now operates like a higher bypass ratio turbofan for subsonic cruise power conditions. The aft bypass injector adjusts to accommodate the increased ratio of bypass air to core air. The engine also retains the ability to operate at high specific thrust where high power operation is necessary, i.e., takeoff and high Mach number operation.

The installation definition chosen for this study is the Grumman design 623 advanced VSTOL-B fighter. The aircraft (Figure 2.2) uses two GE23 engines to operate from vertical take-off to altitudes in excess of 50,000 feet and speeds in excess of Mach 2. The 623 is an advanced multimission fighter aircraft having both air-to-air and air-to-ground missions requiring the multimode capability of the variable cycle engine.

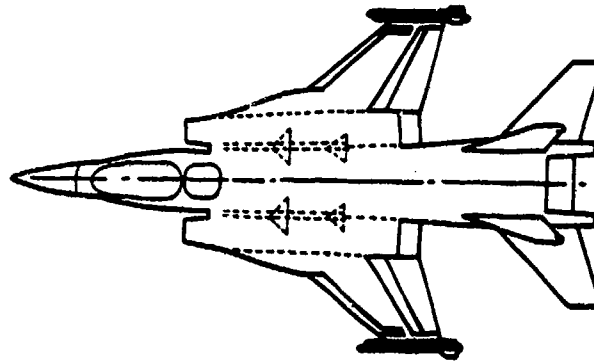


Figure 2.2 Grumman Design 623 VSTOL-B Fighter

### 2.3 CONTROL HARDWARE CHARACTERISTICS

The on-engine control hardware consists of engine actuators, sensors, a microcomputer and power supply, hardware failure overrides and a hydromechanical backup control. The FADEC computer is a fuel-cooled LSI processor with specially designed interface hardware for the actuators and sensors. The functional interconnection of these hardware elements is shown in Figure 2.3.

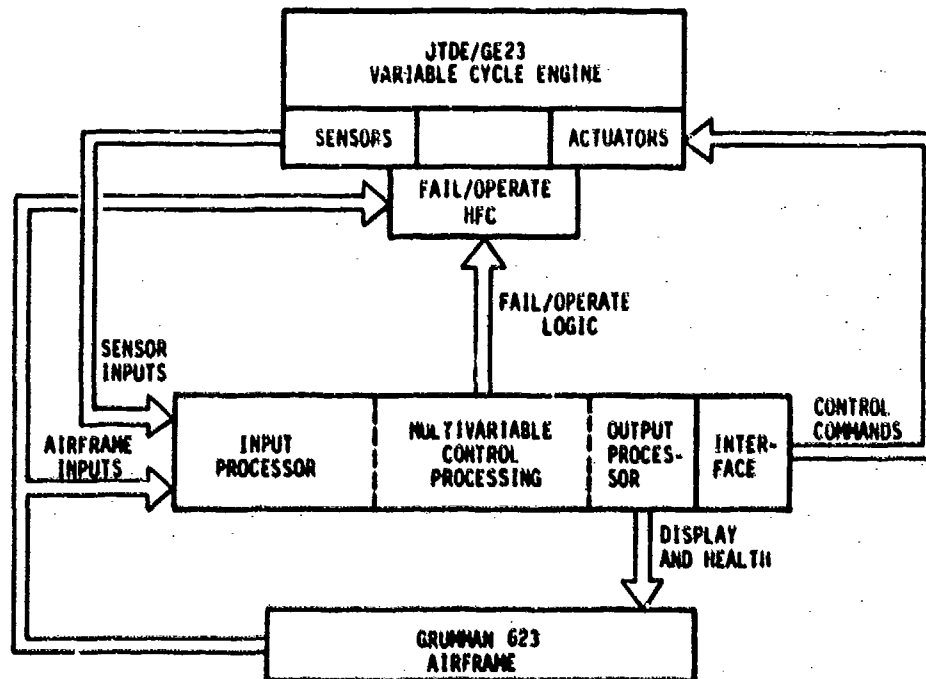


Figure 2.3 Functional Hardware Description

Inputs to the control computer are required from engine sensors, actuator position feedbacks and the airframe data bus (see Figure 2.4). Data from the airframe includes power level command, PLA, and aircraft sensor data-including Mach number, ambient temperature and pressure, thrust mode, wheels down and squat switch logic. Data can be received from the inlet control system on this communication link; however, the current Grumman design does not require this feature.

Actuator position feedback signals are provided by linear, variable phase transducers (LVPT) which measure stroke on the servo pistons. These instruments measure phase shift between excitation and return signals passing through a variable inductance device. A digital counter/threshold detector is used to time the phase difference and calculate the measured stroke. The phase converters are free running, and measured values are asynchronously loaded into the control processor. Error sources on these signals are due primarily to load deflection on the linkages and effective area changes in the variable geometry hardware. Ten actuator stroke positions are used.

The sensor inputs used by the control are listed in Table 2.1. Pressure measurements use vibrating crystal transducers. Frequency conversion of these signals provides asynchronous input to the computer memory. Static probes are located at the discharge stations of the two fan blocks and the high pressure compressor. Two differential probes are located behind each fan block. These probes produce high response signals. Error sources arise from rotating blade passage, stall pressure variations, hysteresis, temperature effects and distortion. Accuracy levels for these devices are in the 0.5% range (except near stall).

Accurate rotor speed measurements (<0.1%) are obtained from frequency conversion of an alternator output (high spool) and magnetic pickup (low spool). Converted measurements are asynchronously input. Time delays on these signals may exceed 25 ms

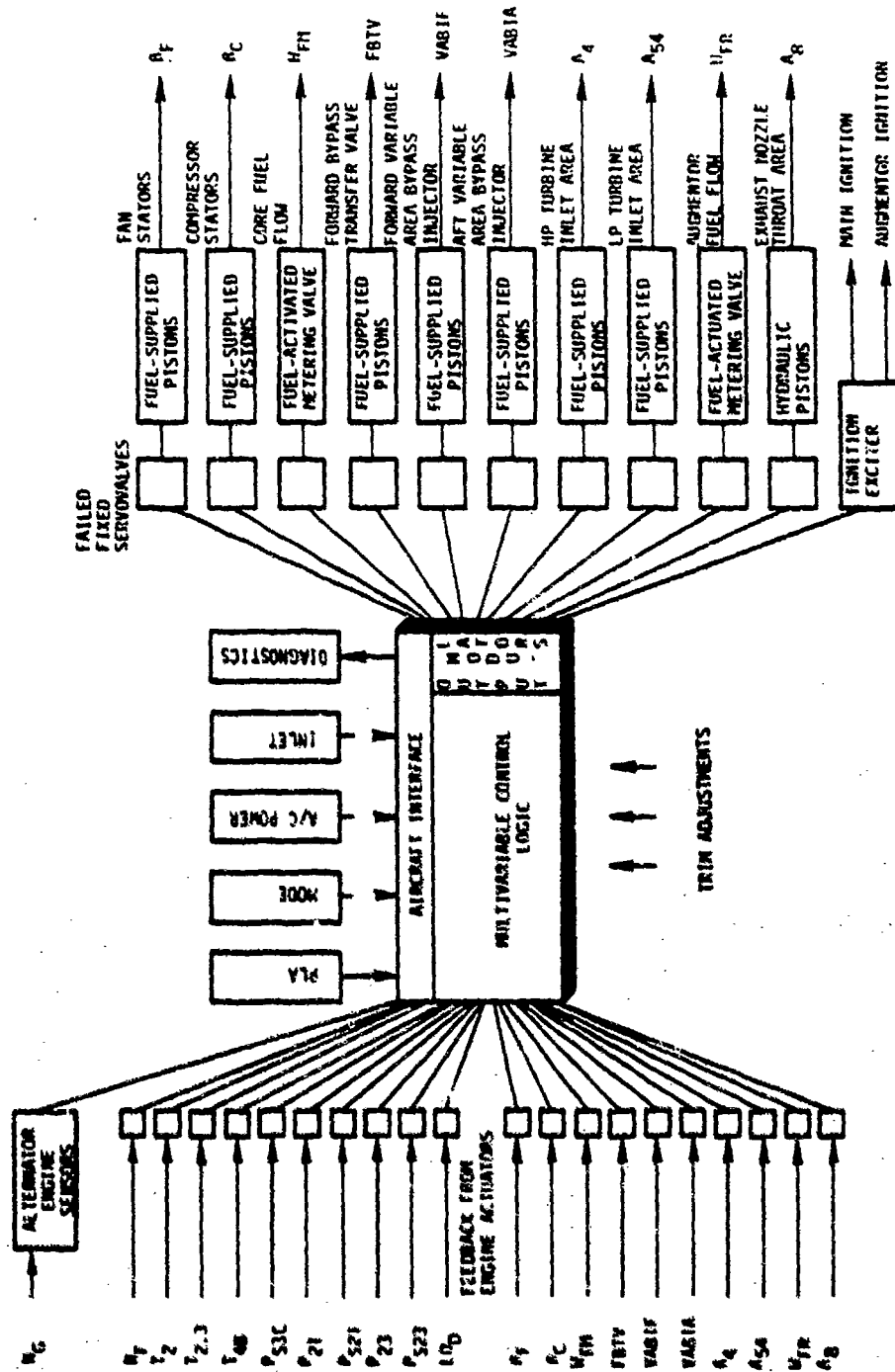


Figure 2.4 Control System Diagram

Table 2.1  
 SENSOR HARDWARE

PARAMETER	SENSOR TYPE	
$P_{S21}$ Absolute $\Delta P_{21}$ Differential	Quartz ↓	
$P_{S23}$ Absolute $\Delta P_{23}$ Differential		
$P_{S3}$ Absolute		
$T_{12}$ $T_{2.5}$		RTD ↓
$T_{48}$		I-R
Light-Off Detector	U-V	
$N_G$	Alternator	
$N_F$	Magnetic Pickup	

at low power. This effect is caused by counter delays at the low shaft frequencies.

Two analog signals measuring fan block discharge temperature are sensed through A-D converters. Platinum resistance thermometers (RTD) provide an accurate linear temperature/resistance relationship which is converted to an analog voltage and sampled by the computer. These devices have an airflow dependent time constant which can exceed eight (8) seconds at high altitude, low power conditions. An optical pyrometer measures high pressure turbine blade temperature. The device senses infrared emissions from the rotating elements. The response time of this probe is extremely fast; however, the blade temperature generally lags

the gas temperature at this station by several seconds due to mass effects in the rotor.

An augmentor light-off detector senses ultraviolet emissions from burning fuel in the tailpipe. This device produces a nearly instantaneous discrete indication of fuel ignition during augmented operation.

Ten actuators are used to modulate areas and flows in the GE23. These actuators are described in more detail in Chapter V and Ref. 6. A spool valve mechanism is used to modulate a fuel or hydraulically driven servo piston. The actuated elements are listed in Table 2.2. The spool valve control input is a pulse width modulated current from a FADEC output amplifier. The spool valve is designed to provide a fail/fixed operating characteristic as shown in Figure 2.5.

Table 2.2  
Actuator Characteristics

VARIABLE	TYPE	RATE LIMIT (% STROKE/SEC)
FSTV	Linear-Fuel	200
$\delta_f$	↓	100
VABI <sub>f</sub>		100
$\delta_c$		100
VABI <sub>A</sub>		100
A <sub>41</sub>		100
A <sub>58</sub>	↓	160
A <sub>8</sub>		Linear-Hydraulic
W <sub>f</sub>	Linear-Fuel	200
W <sub>ra</sub>	↓	100

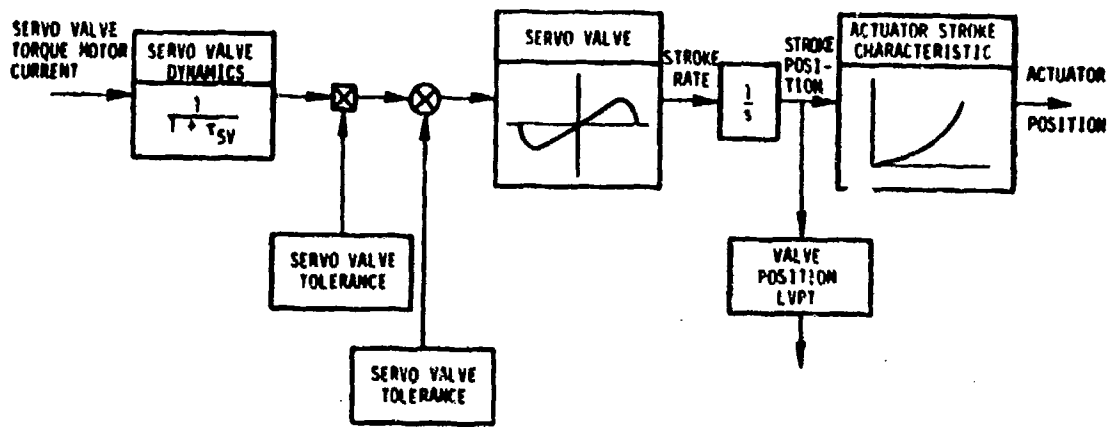


Figure 2.5 Fail-Fixed Servo Valve

If a modulator failure or internal mechanical failure drives the spool to one extreme or the other, the actuator is fixed in its last position. Leakage around the spool lands will cause the actuator to drift to a predetermined setting after a failure has occurred. This control actuator interface device provides an extremely useful tool for incorporating control logic to accommodate actuator failures since the necessity of compensating for fast, hardover response has been eliminated.

The hardware configuration of the GE23 incorporating control electronics, sensor, hydromechanical actuators and backup control provide the control designer with a flexible and powerful capability to control the engine reliably and efficiently throughout its envelope. This system represents a thoroughly integrated concept for failure compensation and fault tolerance which can, with proper control software, produce an overall design with hydromechanical reliability and digital electronic capability.

## 2.4 MISSION DEFINITION

The aircraft mission requirements are an important factor in determining the functional structure of the controller and the complexity of the implementation. The Grumman 623 is an advanced VSTOL-B fighter. The aircraft flight envelope is shown in Figure 2.6. The aircraft has both air-to-air and air-to-ground missions, three of which have been chosen for consideration during the study. The primary mission is fighter escort-air combat. The flight profile is shown in Figure 2.7. In addition, a surface surveillance and VTOL intercept mission were considered. These profiles are also shown in Figure 2.7.

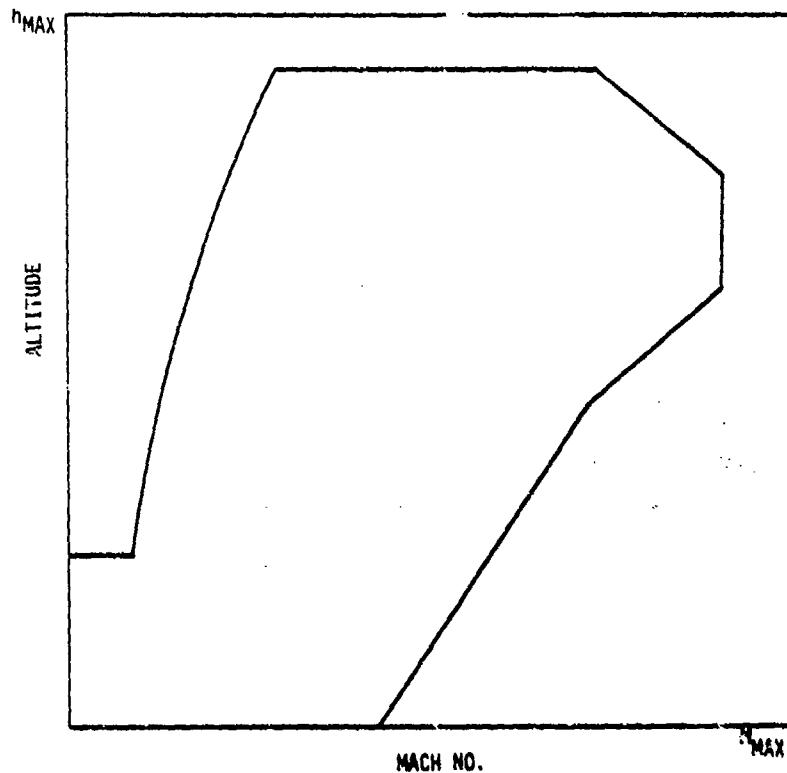


Figure 2.6 Grumman 623 Envelope

The mission definitions determine the type of engine performance which is important and the region of the power and

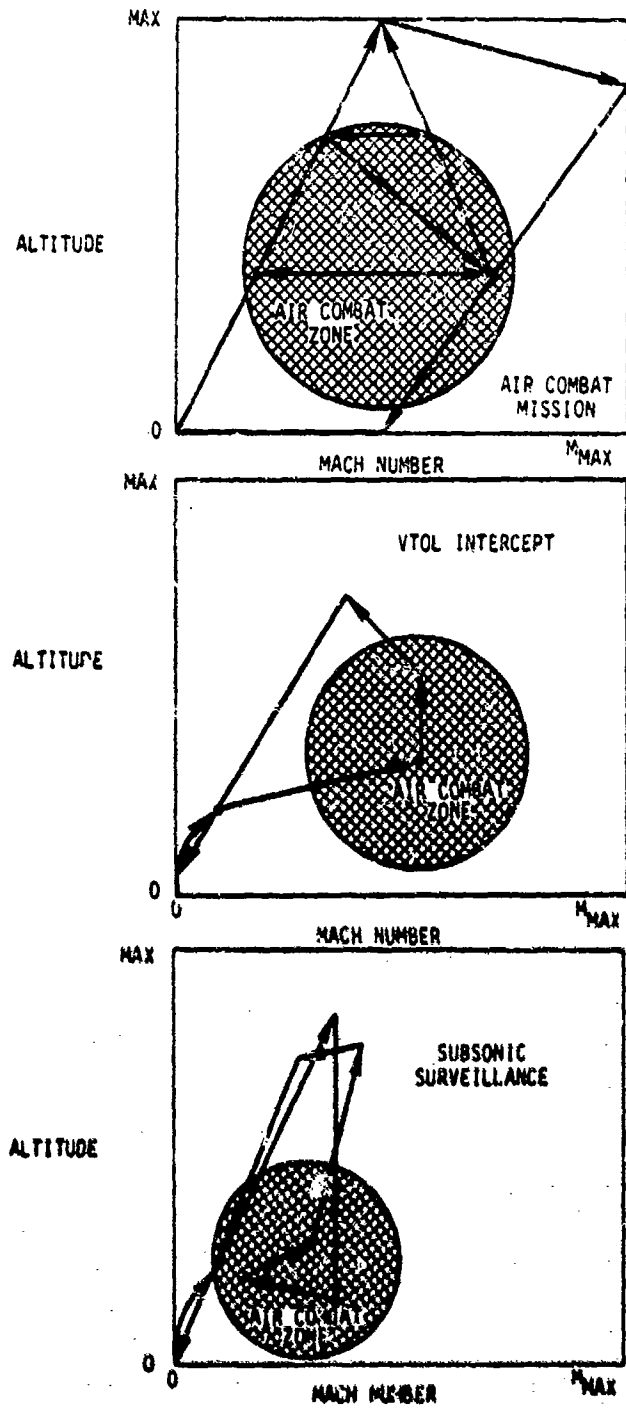


Figure 2.7 Three Typical Mission Profiles for the GE25/623 Involving Air Combat, VTOL Intercept and Subsonic Surveillance

flight domain in which this performance is required. The flight envelope can be partitioned into regions corresponding to each of the mission modes. These regions are shown in Figure 2.8. By considering the important operational characteristics of each domain, a definition of control design criteria can be developed. Table 2.3 lists the control criteria which are associated with each flight domain. The translation of these performance criteria into operating point specifications, reference point values and mode definitions is presented in Chapter IV.

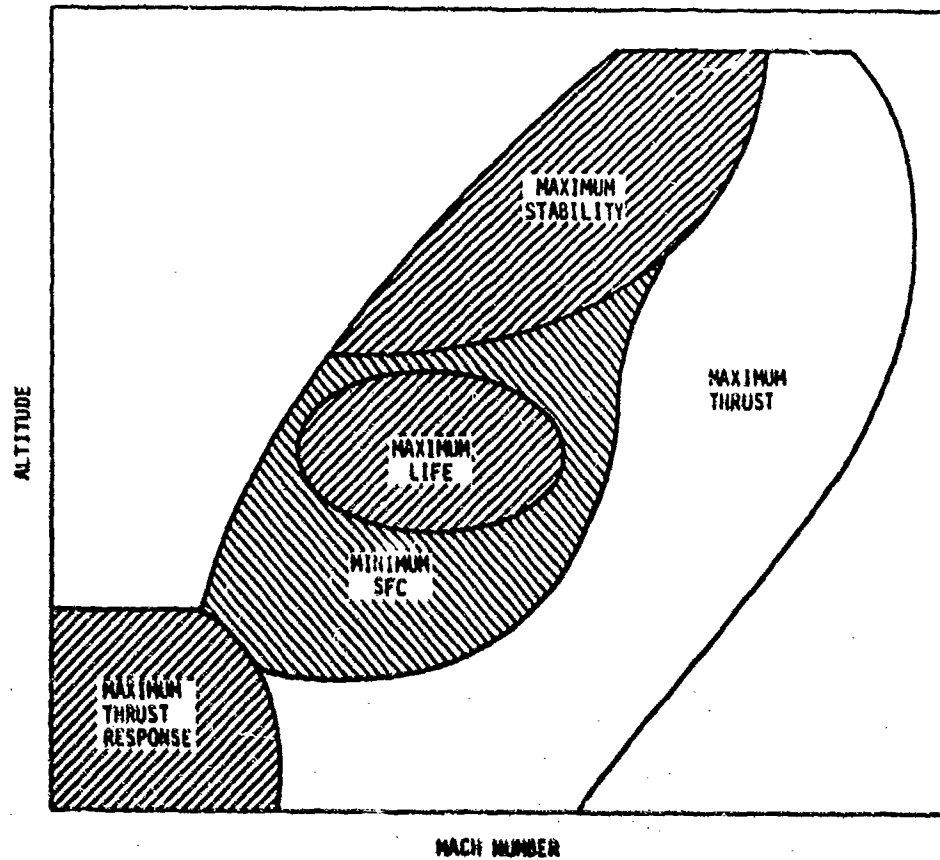


Figure 2.8 Partition of Operating Envelope into Mission Domains

Table 2.3  
Flight Domain Related Control Criteria

DOMAIN	CONTROL CRITERIA
Maximum Thrust	Maximize augmented and dry thrust at design points with minimum SFC between points
Cruise/Loiter	Minimum SFC at design thrust
Maximum Stability	Maximum augmented and dry thrust at design points with increased component stability margins
Maximum Response	Maximum thrust response at part power
Maximum Life	Rated thrust with minimum temperature/speed variation

## 2.5 CONTROL REQUIREMENTS

In addition to the performance definition discussed in Section 2.4, the controller must protect the engine from limit exceedances, accurately specify the set points and accommodate failures. These design specifications are presented below.

### 2.5.1 Engine Limit Protection

Engine limits arise in components operating in a high pressure, high temperature environment (see Table 2.4). Structural considerations of fatigue, creep and strength dictate temperature and rotational speed limits for the high pressure turbine entrance and the compressor discharge stations. In addition, life limits are imposed on turbine blade temperature rates during power changes. Structural limits are approached for combustor pressures also. Combustion stability must be maintained by limiting fuel-to-air

Table 2.4  
Engine Limits

● <u>FANS AND COMPRESSOR LIMITS</u>
Maximum Discharge Pressure
Maximum RPM
Maximum Corrected RPM
Minimum Surge Margin
Maximum Closure of Stators from Basic Schedule
Maximum Opening of Stators from Basic Schedule
● <u>COMBUSTOR AND AFTERBURNER LIMITS</u>
Rich Burner Blowout Limit
Lean Burner Blowout Limit
Minimum Pressure
Lightoff Limits
● <u>TURBINE LIMITS</u>
Maximum RPM
Maximum Inlet Gas Temperature
Maximum Turbine Blade Temperature
Maximum Rate of Change of Turbine Blade Temperature
● <u>BYPASS DUCT</u>
Maximum Airflow or Velocity
Minimum Airflow or Velocity

ratios between lean and rich limits and maintaining main and augmentor combustion pressures above a minimum value. Flow stability in the fan blocks and compressor is maintained by assuring surge margin limits [6] are maintained. Duct airflow must be maintained between Mach number limits to ensure stable, unchoked flow.

Each of the engine limits described above is approached during transient or steady state operation. For example, the engine will most efficiently operate at many intermediate power conditions at the maximum turbine temperature limits. The limiting values of the variables represent desired goals; however, to ensure maximum performance and response, these limits may be exceeded temporarily during transients. This limit philosophy is

incorporated into the control logic to provide the best overall system performance.

### 2.5.2 Steady State Accuracy Requirements

Control accuracy is defined as the difference between a desired operating point and the actual running condition in the presence of actuator uncertainties, disturbances, engine variations and degradation. Many control system designs use lag networks or integral logic to achieve a high d.c. gain to meet the specified accuracy levels. Thus, quantified error tolerances can be used during the design process to evaluate the regulator design and synthesize appropriate compensation. Table 2.5 lists the nominal error tolerances allowed at all flight and power conditions for the GE-23.

Table 2.5  
Error Tolerances on Set Points

SCHEDULED VARIABLE	TOLERANCE
Fan RPM (Military to Maximum)	$\pm 0.4\%$
Fan RPM (Submilitary)	$\pm 1.0\%$
Core RPM (Military to Maximum)	$\pm 0.2\%$
Core RPM (Submilitary)	$\pm 0.5\%$
$\Delta P/P$	$\pm 4.0\%$
Turbine Blade Temperature	$\pm 30^{\circ}R$
Fan and Compressor Geometry	$\pm 3\%$ to $\pm 5\%$ F.S.
Jet and Turbine Nozzles	$\pm 1\%$ to $\pm 2\%$ F.S.
Variable Bypass Geometries	$\pm 1\%$ to $\pm 2\%$ F.S.
Augmentor Fuel Flow	$\pm 4\%$

### 2.5.3 Failure Tolerance

The control hardware described in Section 2.3 is designed to produce a high level of failure tolerance by integrating hardware and software capabilities. The control requirements

for failure tolerance can be formalized for sensor, actuator, and electronics hardware. Table 2.6 summarizes the detection, isolation, and accommodation criteria specified. These criteria represent major considerations in the development of the controller structure described in Chapter IV.

Table 2.6  
Failure Tolerance Specification

FAILURE MODE	PRIMARY REQUIREMENTS	ADDITIONAL GOODNESS CRITERIA
<ul style="list-style-type: none"> <li>● Single Sensor Channel (all types)</li> </ul>	<ul style="list-style-type: none"> <li>● Detect, isolate, and indicate</li> <li>● No effect on performance</li> <li>● Real time, no hardware</li> <li>● Allow intermittants</li> </ul>	<ul style="list-style-type: none"> <li>● Satisfy all requirements</li> </ul>
<ul style="list-style-type: none"> <li>● Multiple Sensor Channels</li> </ul>	<ul style="list-style-type: none"> <li>● Detect, isolate, indicate</li> <li>● Allow intermittants</li> </ul>	<ul style="list-style-type: none"> <li>● Maximum insensitivity</li> <li>● Conservative control action</li> </ul>
<ul style="list-style-type: none"> <li>● Actuator Failures (single/multiple)</li> </ul>	<ul style="list-style-type: none"> <li>● Protect Engine</li> <li>● Smooth transfer to backup</li> </ul>	<ul style="list-style-type: none"> <li>● Maximum insensitivity</li> <li>● Detect, isolate, indicate</li> <li>● Exceed backup control capability</li> </ul>
<ul style="list-style-type: none"> <li>● Processor Hardware</li> </ul>	<ul style="list-style-type: none"> <li>● Detect</li> <li>● Transfer to backup</li> </ul>	<ul style="list-style-type: none"> <li>● Isolation, indication</li> <li>● Reinitialization</li> </ul>

## 2.6 SUMMARY

The requirements governing the development of a multivariable controller for the GE-23 engine are summarized in the following:

The general function of the digital electronic controller is to provide acceptable modulation of the actuators to operate the engine safely and efficiently. Specific functional requirements include:

- (1) Sensor signal conditioning to eliminate noise and provide reconstruction of failed channels.

- (2) Command input interfacing to provide external access to power level inputs, inlet commands, and direct digital access for executive integrated airframe commands.
- (3) Regulation of outputs to operate servo actuators smoothly and stably.
- (4) Failure detection and accommodation logic to provide fail operate and fail safe outputs.
- (5) Condition indication inputs to maintenance, diagnostics, and display processors via direct digital links.

All of these must support the primary controller functions providing smooth engine operation in transient and steady state regimes without exceeding engine operating restrictions.

This section has quantified the hardware specifications, mission definition and performance requirements for the controller. In Chapter III, design procedures for multivariable control synthesis are presented. Chapter IV then integrates the design problem and theoretical techniques to form a control structure definition for the GE-23 MVC.

SECTION III  
MULTIVARIABLE CONTROL DESIGN METHODOLOGY

3.1 INTRODUCTION

In this chapter, the methodology required for the design of a controller for the General Electric GE23-JTDE variable cycle engine is reviewed. Emphasis is on the design techniques which are available. This chapter forms the foundation for the control structure which is proposed in Chapter IV.

3.2 THE CONTROL DESIGN PROBLEM

The primary function of any controller is to maintain stable and smooth operation of the plant at acceptable levels of performance in both steady-state and transient regimes without exceeding specified operating restrictions. Acceptability is defined in terms of the specific application. Typical measures are:

- (1) Steady-state hangoff errors
- (2) Bandwidth
- (3) Rise time and overshoot
- (4) Mean square levels of control and state responses

In addition to the classical regulation criteria, modern controllers for complex dynamic systems must also include logic to provide sensor signal conditioning, command input processing, and failure detection and accommodation. These functional requirements are addressed by the synthesis procedures in the sections that follow.

The structure and type of the controller depends on the nature and complexity of the problem and on the design requirements. The controller may be open loop (feedforward) or closed

loop (feedback) or a combination of both. It may be based on the so-called classical and/or modern control design techniques.

Historically, feedback control (i.e., using plant outputs to effect compensating inputs) has been the foundation of control structures. Feedback control tends to require less detailed response models and is therefore particularly suited to simple implementations. In modern, digital control applications, the overhead associated with more detailed response models is not an important design factor. Thus, modern multivariable control designs are using more detailed open loop strategies in conjunction with feedback regulation. In this way, superior transient behavior is produced without many of the unfavorable stability and noise problems often associated with feedback computation alone. Feedforward design concepts are discussed below.

### 3.3 FEEDFORWARD AND TRANSITION CONTROL

If a perfect plant model was known, and if there were no unknown disturbances, then it would be possible to control the plant using only feedforward (open-loop) inputs. Furthermore, assuming the plant was stable, the feedforward could simply be a change in the control set point which would produce the desired steady-state condition. However, using this strategy, transition from the current state to that commanded would occur with the dynamics characteristic of the open-loop plant. There would be no direct control over the maximum output excursions.

More control over the response dynamics and maximum excursions of plant variables is possible if the input is more sophisticated. One example is an input time history that requires the state variables to ramp (at specified rates) from their current values to those requested at the new steady state. Specifically,

if the system is linear and the vector of ramp rates is  $\dot{x} = R$ , then from the equations of motion

$$\dot{x} = Fx + Gu \quad (3.1)$$

one can find the control and state time histories during the transient. Defining an acceleration steady state as  $\ddot{x} = 0$  yields

$$\ddot{x} = 0 = F\dot{x} + G\dot{u} \quad (3.2)$$

$$\text{or } 0 = FR + G\dot{u} \quad (3.3)$$

If the number of controls ( $m$ ) equals the number of states ( $n$ ), then  $G^{-1}$  exists and

$$\dot{u} = -G^{-1}FR. \quad (3.4)$$

If  $m > n$ , then  $m-n$  additional constraints must be imposed on the controls to yield a unique solution for  $\dot{u}$ . If  $m < n$ , then  $m-n$  constraints must be removed from the state vector. Using the example with  $m=n$  yields

$$u(t) = u(o) + \int_0^t \dot{u} dt = u(o) - G^{-1}FR t \quad (3.5)$$

and

$$x(t) = x(o) + \int_0^t \dot{x} dt = x(o) + Rt. \quad (3.6)$$

Another more sophisticated approach calculates an input time history that is optimal with respect to a specified performance index. Current techniques for trajectory optimization [7] utilize an engine simulation of varying complexity. A cost functional is derived which represents desirable trajectory attributes (e.g. maximum thrust reponse or minimum turbine inlet temperature rates), and a group of constraints in the trajectory are formulated to respect stability limits and other physical operating constraints. A trial trajectory is calculated which may or may not satisfy the constraints. Standard function

optimization procedures can be used to derive feasible and optimal paths.

The problems with this type of procedure are threefold. First, engine transient simulations, especially for gross transitions, may poorly represent engine behavior; second, implementation of exact trajectories is inevitably impractical; and third, there is no convenient control law formulation of the optimal solution.

An interesting technique [8] has been proposed which could yield substantially improved implementation properties which make the scheme compatible with real-time, on-board application.

A fairly general dynamic optimization problem can be formulated where the performance index, system equations, and path constraints are modeled as linear functions of the control. The solution is a bang-bang control law. The vector control history  $u(t)$  which minimizes the performance functional

$$J = \phi(x(t_f), t_f) + \int_{t_0}^{t_f} (a(x, t) + b^T(x, t)u(t))dt \quad (3.7)$$

subject to the vector system differential equations

$$\dot{x} = f(x, t) + g(x, t)u(t) \quad (3.8)$$

and of path inequality constraints

$$c_i(x, t) + d_i^T(x, t)u(t) \leq 0 \quad i = 1, 2, \dots, q \quad (3.9)$$

must be calculated.

The initial state and time are assumed to be specified, i.e.,

$$x(t_0) = x_0 \quad (3.10)$$

while the terminal state and time are subject to the  $p$  terminal constraints ( $p \leq n + 1$ )

$$\psi_i(x(t_f), t_f) = 0 \quad i = 1, 2, \dots, p \quad (3.11)$$

The functions  $\phi$ ,  $a$  and  $c_i$  are scalar functions of  $x$  and  $t$ , while  $b$  and  $d_i$  are vector functions of dimension  $(r \times 1)$ . The terminal time  $t_f$  may be either fixed or free.

The necessary conditions [8] for the optimal solution can be derived as follows:

$$\begin{aligned} \dot{\lambda}^T &= \frac{\partial a}{\partial x} - \frac{\partial b^T}{\partial x} u(t) - \lambda^T \frac{\partial f}{\partial x} - \lambda^T \frac{\partial g}{\partial x} u(t) \\ &\quad - \sum_{i=1}^q \left[ \mu_i \frac{\partial c_i}{\partial x} + \mu_i \frac{\partial d_i^T}{\partial x} \right] u(t) \end{aligned} \quad (3.12)$$

$$b^T + \lambda^T g + \sum_{i=1}^q \mu_i d_i^T = 0 \quad (3.13)$$

$$\mu_i \geq 0; \mu_i = 0 \quad \text{if} \quad c_i + d_i^T j < 0 \quad (3.14)$$

The switching function in Eq. (3.13) can be calculated and perhaps stored as a feedback control law in a modified bang-bang form. Another approach which mimics the character of the above optimal trajectory, while avoiding the required computation is discussed in Section 4.1.5.

As indicated in the beginning of this section, a feedforward strategy alone (even "optimal") may not be adequate to control a plant due to modeling errors and unknown disturbances. Regulator logic is usually required. In general terms, the objective of regulator design is to determine a set of feedback gains which provide a system with desired response characteristics. Such desired characteristics include stability, frequency, damping, decoupling, and minimum error in following a specific command. Classical and modern control techniques for designing regulators are discussed below.

### 3.4 CLASSICAL CONTROL SYNTHESIS

Classical design techniques are well known and will not be reviewed in detail here. When applicable, these techniques are very powerful and can lead to easily designed and effective regulators. In fact, over 40 years of successful control system designs have been achieved by what is now called classical synthesis. This approach is based on analysis of the transfer function representation of the system (e.g., the frequency domain relationship between input and output).

Examples of design techniques which have been used are the root locus method, the Nyquist method, and the Bode method (a derivative of the Nyquist method). The basic design approach is to analyze the transfer function with respect to desired system characteristics (e.g., gain and phase margin, transient response) and introduce compensating lead or lag filters to modify the response to that desired.

The compensators can provide lead or lag and may introduce a pure integral effect to eliminate steady-state errors from step inputs. Sufficient stability margin is provided such that small errors in the design parameter values do not affect the stability of the system. All modes can be made adequately fast and well damped within design requirements. These methods were originally devised for single-input, single-output systems and are difficult to use with multi-input, multi-output systems. A summary of the advantages and disadvantages of these techniques is given in Table 5.1.

### 3.5 MODERN CONTROL SYNTHESIS METHODS

Modern control design methods have their basis in the state space representation of dynamic systems. The state space approach leads naturally to the description of both linear and nonlinear

Table 3.1

## Classical Control: Advantages and Disadvantages

	ADVANTAGES	DISADVANTAGES
CLASSICAL CONTROL	(1) Provides basis for engineering design decisions and evaluation (for low-order systems). (2) Inherent use of stability margin (e.g., gain and phase margins) to reduce controlled sensitivity to uncertainties in system parameters. (3) Best for single-input/single-output systems.	(1) Much trial-and-error in design, particularly for large systems such as engines. (2) Frequently leads to controls fighting each other. (3) Difficult to apply to multi-input/multi-output systems.

systems in time domain. The control inputs may be chosen to minimize a certain criterion function which is a quantitative measure of the penalty for undesired state response and the control input effort required (quadratic synthesis methods). Alternately, the control may be selected by specifying the desired transient response characteristics of a system, and using algebraic synthesis techniques to solve for the required gains (e.g., pole placement methods, modal control methods, etc.).

A major control theory development occurred during the late 1950's which was fostered by high-speed computers and an advanced technology space program. Now known under various names (quadratic synthesis, linear-quadratic Gaussian synthesis, modern optimal control theory, linear quadratic regulator theory), this development has been the subject of intensive theoretical research. It is known that optimal control has great potential since it is inherently a multi-input/multi-output linear system control design method also applicable to nonlinear systems. Much of the demonstration of the versatility of the method, however, has been limited to simulation studies, and the applications through actual implementation are not nearly as extensive. Characteristics of quadratic synthesis are:

- (1) Quadratic synthesis techniques design on a different objective than classical techniques. Instead of attempting to obtain a specific transient response (as do classical methods), LQR methods minimize the control energy required to keep the mean square response of the system as small as possible. The design parameters are weightings or penalties on deviations of states and controls as well as the choice of augmented states and controls). Desirable transient response is obtained indirectly.
- (2) Quadratic synthesis techniques are highly automatic once the performance index and the design model have been selected.
- (3) Quadratic controls can produce simple control systems if the design process is conducted with an integrated understanding of the system physics. This is because many of the simplifications to an "optimal controller" can be based on certain types of analysis of the feedback structure and relating this structure to its actual effect on the system.

Modern optimal control theory can accommodate nonlinear systems and criterion functions. However, the control laws thus generated may be very complicated (e.g., non-state-variable feedback). An alternate method is to schedule a set of linear (state variable feedback) control laws throughout the operating region of the system. Each control law is designed using a linearized model of the system in its region of effectiveness. The piecewise linear control law formed in this fashion is generally simpler to calculate and easier to implement than the corresponding nonlinear control law; yet it sacrifices little performance.

The advantages and disadvantages of modern control synthesis methods are summarized in Table 3.2.

### 3.5.1 State Variable Feedback

Most common applications of LQR theory involve calculation of a feedback gain matrix on the system state variables. These gains minimize a criterion function (or performance index),  $J$ , of the form

$$J = \phi[x(t_f), t_f] + \int_{t_0}^{t_f} L[x(t), u(t), t] dt \quad (3.15)$$

Table 3.2  
Modern Control: Advantages and Disadvantages

	ADVANTAGES	DISADVANTAGES
MODERN CONTROL	(1) Leads to automatic synthesis of controls once performance index and model have been determined. (2) Designs are inherently minimally sensitive if proper P.I. is chosen. (3) Automatically includes optimum control and state cross-coupling.	(1) Places more emphasis on correctness of model used for design (e.g., if model is in error, controlled system could be unstable) and relevance of performance index. (2) Most applications tend to be naive because too much confidence placed on automatic LQR methods to replace knowledge of system and modeling accuracy.

where  $\phi$  represents a penalty on the terminal error and  $L$  represents a penalty on trajectory errors. Several choices of  $\phi$  and  $L$  are possible. A common choice is state and control weighting of the form

$$J = \int_{t_0}^{t_f} [x^T(t)A(t)x(t) + u^T(t)B(t)u(t)] dt \quad (3.16)$$

where  $A(t)$  is a weighting matrix on state errors and  $B(t)$  is a weighting on control effort.

Assuming the state equations are in matrix form

$$\dot{x} = Fx + Gu \quad (3.17)$$

$$y = Hx + Du \quad (3.18)$$

the control law which minimizes Equation (3.16) is given by

$$u(t) = -C(t)x(t) \quad (3.19)$$

where

$$C(t) = [B(t)]^{-1} G^T(t)S(t) \quad (3.20)$$

and  $\dot{S}(t)$  is the solution of a matrix Riccati equation

$$\dot{S} = -SF - F^T S + SGB^{-1}G^T S - A \quad (3.21)$$

A constant feedback gain matrix that yields "nearly optimal" control is given by the steady state solution to Equation (3.21) (setting  $\dot{S} = 0$ ). Computationally efficient algorithms exist for solving this problem. An eigenvector decomposition technique is described in Ref. 9. The result is a control law of the form

$$u(t) = -C x(t) \quad (3.22)$$

### 3.5.2 State Estimation and Sensor Compensation

In the preceding discussion it was assumed that the controller had perfect knowledge of the state. A model reduction procedure can be used to allow the control designer some freedom to choose conveniently measurable quantities as state variables. However, this is not always possible. Models containing unmeasured states must sometimes be formulated to describe system response accurately. Measurement errors, model errors and sensor dynamics all tend to make the knowledge of the state only approximate. The dependence of the regulator control law on measurement uncertainties must be analyzed so that the impact on performance can be evaluated.

The regulator gains are assumed independent of the uncertainty in the knowledge of the state. This assumption allows the synthesis procedure to maintain its systematic simplicity and separates the compensation of the transduced signals from the control design. The justification of this assumption is discussed below.

For the general, linear stochastic control problem, the system follows:

$$\dot{x} = Fx + Gu + w \quad (3.23)$$

$$y = Hx + v \quad (3.24)$$

In this case,  $w$  and  $v$  are zero mean, Gaussian random processes with covariances defined below:

$$E[w(\tau)w^T(t)] = Q\delta(t-\tau) \quad (3.25)$$

$$E[v(\tau)v^T(t)] = R\delta(t-\tau) \quad (3.26)$$

The performance index for the problem remains unchanged except that the mean value of the cost is minimized.

The solution to the problem follows directly from a change of coordinates. The maximum likelihood estimate of the state given all the measurements to time  $t$  is the function  $\hat{x}(t)$  that makes the residual process white, i.e.,

$$v(t) = y(t) - H\hat{x}(t) \quad (3.27)$$

$$E[v(t)v^T(t)] = M\delta(t-\tau) \quad (3.28)$$

It can be shown that there is an  $(n \times p)$  matrix function of time,  $K(t)$ , which will produce the maximum likelihood estimate as follows:

$$\dot{\hat{x}} = Fx + Gu + K(t)v(t) \quad (3.29)$$

Now, the problem can be rewritten with new variables as follows:

$$e = \hat{x} - x \quad (3.30)$$

$$J = \frac{1}{2} E \left\{ \begin{bmatrix} \hat{x}^T \\ u^T \end{bmatrix} \begin{bmatrix} A & N \\ N^T & B \end{bmatrix} \begin{bmatrix} \hat{x} \\ u \end{bmatrix} \right\} + E[e^T A e] \quad (3.31)$$

The error term,  $e$ , follows the linear system relationship,

$$\dot{e} = (F - KH)e + Kv + w \quad (3.32)$$

and is independent of the control. The regulator problem minimizes the first term of Eq. (3.31). The solution is derived [10] as follows:

$$u(t) = - C\hat{x}(t) \quad (3.33)$$

where the matrix  $C$  is determined under the assumptions of perfect state knowledge.

For nonlinear systems and for systems without white Gaussian disturbances, this separation principle may not hold. However, it is often approximately true and utilization of separate design procedures for control and estimation yields satisfactory closed-loop systems.

This philosophy has been used for many years in classical design. The goal of sensor compensation is to remove the random error from the signal and produce the best estimate of the measured quantity for control.

There are two criteria used in sensor compensation. If a sensor has a very high bandwidth, spurious, high frequency input may enter the feedback loop and cause unacceptable behavior. The standard remedy is a low pass filter at a bandwidth higher than the closed-loop frequency.

For most digital control systems, it is standard practice to filter all input signals to eliminate aliasing. Each transduced input will have an ample amount of noise at all frequencies due to line pickup, power supply fluctuation, EMI, etc. Sampling into this noise can often lead to difficult problems. Higher order filters with steeper attenuation characteristics are sometimes necessary.

Sensor compensation must also improve poor dynamic response relative to the closed-loop dynamics. Many transducers can be modeled by first order lags. If the bandwidth of these sensors is

significantly lower than the desired closed-loop bandwidth, poor transient behavior can be anticipated due to the phase lag introduced by the instrument.

Classical compensation philosophy can also be applied [2] to multivariable systems. With many measurements, it is possible to choose the high bandwidth variables to regulate the transient response of the system. Slower, high accuracy sensors can be utilized for trim or bias control. The design proceeds by the appropriate choice of model, quadratic weights and, finally, filter compensation.

It is possible to implement a full order filter directly. This increases the complexity of the control law from simple proportional feedback to an nth order dynamic compensation. An examination of the optimal filter roots for a group of measurements typically shows that some filter time constants will be well above the closed-loop bandwidth. Single-loop prefiltering can be used to limit noise transmittance in these inputs. The measured variables will naturally decompose into a set of high bandwidth signals which are necessary to the control function but which do not have sufficient response for use directly in the control law [2].

### 3.5.3 Output Feedback

In many applications, the quantities that are to be regulated are system output variables and not system state variables. Using state variable feedback in these applications (outputs weighted in the performance index) generally involves estimation of unmeasured states (e.g., the Kalman filter) and mathematical modeling of the system's output equations (e.g.,  $y = Hx + Du$ ). If the mathematical model of the plant were known exactly, this procedure would produce an acceptable control law. However, modeling errors are generally present. Consequently, additional integral or trim control is often necessary to insure satisfaction of performance requirements.

These difficulties may often be avoided by designing a controller that feeds back output errors directly [11]. One disadvantage to this, however, is that the resulting gain matrices cannot be found as solutions to a matrix Riccati equation. They must be found by solving a set of nonlinear equations.

The output feedback problem can be formulated as follows. Given the set of plant equations

$$\dot{x} = Fx + Gu \quad (3.34)$$

$$y = Hx + Du \quad (3.35)$$

find the matrix  $C$  of the form

$$u = Cy \quad (3.36)$$

which minimizes the performance index

$$J = 1/2 \int_0^{\infty} [x^T A_x x + u^T B_u u + y^T A_y y] dt \quad (3.37)$$

or equivalently

$$J = 1/2 \int_0^{\infty} \begin{bmatrix} x^T & u^T \end{bmatrix} \begin{bmatrix} A & N \\ N^T & B \end{bmatrix} \begin{bmatrix} x \\ u \end{bmatrix} dt \quad (3.38)$$

This performance index is clearly a function of the gain matrix,  $C$ . One technique of finding its minimum (with respect to  $C$ ) involves the use of a gradient search procedure. One efficient procedure is the modified Newton Raphson with derivative technique [12]. It requires the gradient of  $J$  with respect to  $C$ .

The gradient of  $J$  with respect to  $C$  is developed in part in Ref. 13. Summarizing briefly, let

$$y^* = Hx = y - Du \quad (3.39)$$

and

$$u = \bar{C} y^* \quad (3.40)$$

with

$$\bar{C} = C(I-DC)^{-1} \quad (3.41)$$

Then, from Refs. 13 and 14

$$\frac{dJ}{d\bar{C}} = (B\bar{C}H + N^T) LH^T + G^T K LH^T \quad (3.42)$$

where

$$F^* = F + G\bar{C}H \quad (3.43)$$

$$0 = LF^{*T} + F^*L + X_0 \quad (3.44)$$

$$0 = KF^* + F^{*T}K + A + H^T\bar{C}^T B\bar{C}H + N\bar{C}H + H^T\bar{C}^T N^T \quad (3.45)$$

and

$$X_0 = E[x(0) x^T(0)] \quad (3.46)$$

Note that, in this formulation

$$J = 1/2 \text{ trace } (K X) \quad (3.47)$$

Thus, the gradient of J with respect to  $\bar{C}$  is provided.

The gradient search may therefore be used to find a matrix  $\bar{C}$  ( $u = \bar{C} y^*$ ) which minimizes J. The resulting  $\bar{C}$  may be transformed to C ( $u = C y$ ) using Equation (3.41).

One difficulty remains. The resulting feedback gain matrix, C, is, in general, full. That is, there is a feedback path from every output to every control. Often, unimportant or ineffective error to actuator paths can be identified and eliminated - yielding significant reduction in the number of feedback paths which must be implemented. Optimization of this resulting fixed-structure gain matrix requires an extension to existing theory, however.

Specifically, the gradient of J with respect to C (instead of  $\bar{C}$ ) must be found.

The derivation of  $\frac{dJ}{dC}$  is provided in Appendix A. The result is

$$\frac{dJ}{dC} = (I + CBD)^T \frac{dJ}{d\bar{C}} \beta^T \quad (3.48)$$

where

$$\beta = (I - DC)^{-1} \quad (3.49)$$

With  $\frac{dJ}{d\bar{C}}$  available, the gradient search procedure can be used to optimize specific elements in the C matrix with the remaining elements fixed (e.g., at zero). A block diagram of the procedure is presented in Figure 3.1.

### 3.6 MODEL GENERATION

The design procedures discussed above rely heavily on an accurate mathematical model of the system. Consequently, a critical step in the control design procedure is the generation of tractable design models. Linear models are one class of such design models, and as will be shown, can be effectively integrated to provide a nonlinear control function.

A dynamic description of the response of important variables near a trim condition is the goal of linear model generation. From these, closed-loop controls can be developed. Typically, complex simulations are developed before the actual system is built. The linear models used in control design can be produced from these large simulations. Alternately, data from prototype tests can be processed to develop models which are accurate representations of the behavior useful in control design and validation of the nonlinear simulation.

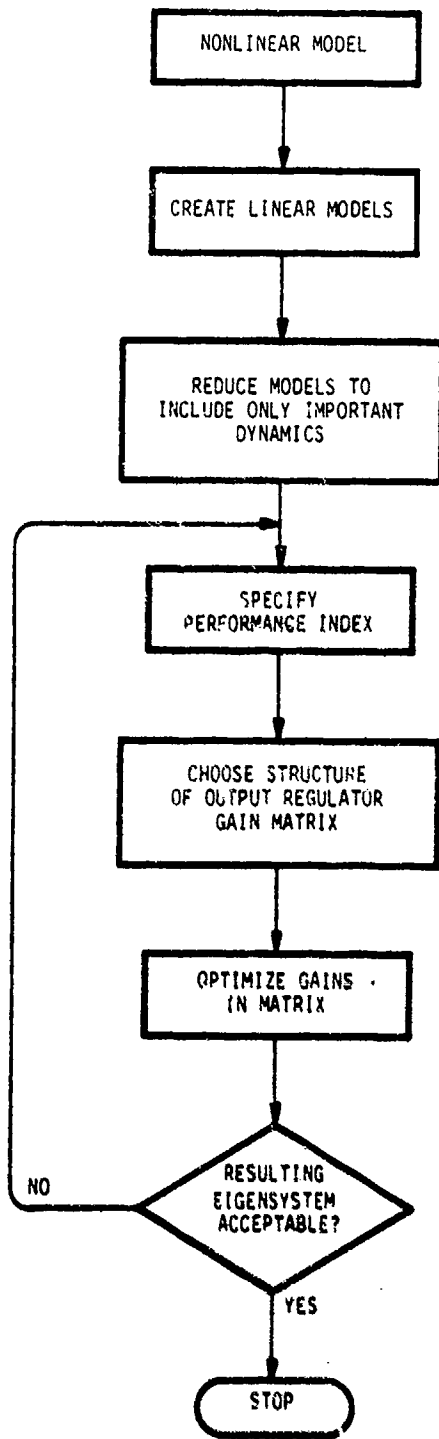


Figure 3.1 Block Diagram of Output Regulator Design

An equilibrium point is determined for a given set of control inputs, which can be written as follows:

$$0 = f(x, u, \theta) \quad (3.50)$$

where  $f(x, u, \theta)$  are the detailed nonlinear equations governing system operation. The states,  $\delta x$ , are a group of independent dynamic variables. The controls,  $\delta u$ , determine the inputs. The linearization point is determined by the ambient conditions,  $\theta$ .

Expanding Eq. (3.50) about trim yields the following:

$$\delta \dot{x} = f_x \delta x + f_u \delta u + g(\delta x, \delta u) \quad (3.51)$$

where  $\delta \dot{x}$  are the perturbation state rates, and  $g$  is at least second-order small in the perturbations.

Standard offset derivative generation procedures use Eq. (3.51) directly. The selected control and ambient inputs are applied and an equilibrium point is reached. All dynamic integrations are then held. States and controls are perturbed in order and the inputs to the integrators calculated. The calculation is written as follows:

$$(f_x)_{ij} = (\delta \dot{x}_i / \delta x_j) \left| \begin{array}{l} i, j, k=1, \dots, n \\ \delta x_k=0 \\ k \neq j \end{array} \right. \quad (3.52)$$

$$(f_u)_{il} = (\delta \dot{x}_i / \delta u_l) \left| \begin{array}{l} l=1, \dots, m \\ \delta x_i=0 \end{array} \right. \quad (3.53)$$

A modification to this method can be used to improve the low frequency accuracy of the models [15]. First, the simulation is trimmed at the selected flight condition. States are perturbed in order and the dynamics matrix calculated as in Eq. (3.52). Controls are perturbed in order and the resulting steady-state trim point calculated. The models are formed as follows:

$$(f_x)_{ij} = (\delta \dot{x}_i / \delta x_j) \left| \begin{array}{l} i, j, k=1, \dots, n \\ \delta x_k=0 \\ k \neq j \end{array} \right. \quad (3.54)$$

$$(\bar{f}_u)_{i\ell} = (\delta \dot{x}_i / \delta u_\ell) \Big|_{f=0} \quad \ell=1, \dots, m \quad (3.55)$$

The two methods produce different steady-state gains as shown below: For the standard method:

$$(\delta x_i)_{ss} = - (f_x^{-1} f_u)_{ij} \delta u_j \quad (3.56)$$

and for the forced match method:

$$(\delta x_i)_{ss} = - [\delta x_i / \delta u_j] \Big|_{f=0} \delta u_j \quad (3.57)$$

In the standard method, the steady-state response gain from the control to the state perturbations is given by Eq. (3.56) [derived from Eqs. (3.52) and (3.53)]. This gain matrix depends on the independently calculated quantities  $(f_x)$  and  $(f_u)$ . In practice, these independent calculations are susceptible to numerical inaccuracies which degrade the low frequency response of the associated linear models. However, the accuracy at all frequencies in modeling control inputs is presumably good. The forced match procedure uses the steady response as the defining relationship [Eq. (3.57)] in the calculation of the control distribution matrix. This forces the steady-state response of the nonlinear simulation and the linear model to coincide for at least one set of inputs. In general, the low frequency response of these models is quite accurate.

Both procedures are computationally efficient and yield models suitable for closed-loop control design. Also, both yield linear models of the form

$$\dot{x} = Fx + Gu \quad (3.58)$$

$$y = Hx + Du \quad (3.59)$$

directly. Specifically, the elements in F, G, H and D are

$$F(i,j) = (f_x)_{ij} \quad (3.60)$$

$$G(i, \ell) = \begin{cases} (f_u)_{i\ell} \\ \text{or} \\ (\bar{f}_u)_{i\ell} \end{cases} \quad (3.61)$$

and, though not discussed, but derived by similar means

$$H(k, i) = (g_x)_{ki} \quad (3.62)$$

$$D(k, \ell) = (g_u)_{k\ell} \quad (3.63)$$

where there are  $p$  measurements given by

$$y = g(x, u, \theta)$$

and

$$(g_x)_{ki} = \left. \left( \frac{\partial y_k}{\partial x_i} \right) \right|_{\delta x_j = 0} \quad \begin{array}{l} k=1, \dots, p \\ i, j=1, \dots, n \\ j \neq i \end{array} \quad (3.64)$$

$$(g_u)_{k\ell} = \left. \left( \frac{\partial y_k}{\partial u_\ell} \right) \right|_{\delta x_i = 0} \quad \begin{array}{l} k=1, \dots, p \\ \ell=1, \dots, m \\ i=1, \dots, n \end{array} \quad (3.65)$$

An alternate strategy is possible in which  $F$ ,  $G$ ,  $H$  and  $D$  are determined indirectly. This technique requires the solution of a set of linear equations (and the associated numerical difficulties), but may be more convenient for some forms of simulation programs. Specifically, the incremental changes in the states and the outputs are found due to perturbations in the state derivatives and controls. Hence the following matrix is identified:

$$\begin{bmatrix} x \\ \vdots \\ y \end{bmatrix} = \begin{bmatrix} A_{11} & \vdots & A_{12} \\ \vdots & \vdots & \vdots \\ A_{21} & \vdots & A_{22} \end{bmatrix} \begin{bmatrix} \dot{x} \\ \vdots \\ u \end{bmatrix} \quad (3.66)$$

where

$$A_{11}(i,j) = \left( \frac{\partial x_i}{\partial \dot{x}_j} \right) \Big|_{\delta \dot{x}_k=0} \quad \begin{array}{l} i=1,\dots,n \\ j=1,\dots,n \end{array} \quad (3.67)$$

$$A_{12}(i,j) = \left( \frac{\partial x_i}{\partial u_j} \right) \Big|_{\delta \dot{x}_k=0} \quad (3.68)$$

$$A_{21}(i,j) = \left( \frac{\partial y_i}{\partial \dot{x}_j} \right) \Big|_{\delta \dot{x}_k=0} \quad k \neq j \quad (3.69)$$

$$A_{22}(i,j) = \left( \frac{\partial y_i}{\partial u_j} \right) \Big|_{\delta \dot{x}_k=0} \quad (3.70)$$

F, G, H and D may then be found as

$$F = A_{11}^{-1} \quad (3.71)$$

$$G = - A_{11}^{-1} A_{12} \quad (3.72)$$

$$H = A_{21} A_{11}^{-1} \quad (3.73)$$

$$D = A_{22} - A_{21} A_{11}^{-1} A_{12} \quad (3.74)$$

Generating perturbation size is important in all techniques because of inherent nonlinearities in the behavior and numerical accuracy in both the hybrid and digital environment.

Often, linear models generated numerically do not contain the most convenient parameterization of the dynamics and, indeed, contain far too complex a description to be practically utilized for design. Some method is required to analyze the dynamical models and establish simpler systems which include only elements important to the desired control function. Without such simplification, application of design procedures can result in highly complex and parameter sensitive controlled systems. Utilizing the reduced order

models, regulator synthesis procedures become physically intuitive and far less sensitive to parameter variation.

### 3.6.1 Modal Decomposition

A modal decomposition provides the framework for reducing arbitrary linear models to design models containing the appropriate parameterization for the control function. The procedures are well known [2] and their application to model reduction is described below.

The linear Eqs. (3.58) and (3.59) can be transformed to block diagonal form assuming the  $n \times n$  dynamics matrix,  $F$ , has no repeated eigenvalues:

$$x = Tz \quad (3.75)$$

$$\dot{z} = \Lambda z + \Xi u \quad (3.76)$$

$$y = HTz + Du \quad (3.77)$$

where  $\Lambda$  is an  $n \times n$  block diagonal matrix,  $T$  is an  $n \times n$  matrix composed of the column eigenvectors of  $F$ ,  $Z$  is an  $n \times 1$  modal coordinate vector, and  $\Xi$  is the  $n \times m$  modal control distribution matrix. Also,

$$FT = T\Lambda \quad (3.78)$$

The system of Eqs. (3.75) through (3.77) can be partitioned into a set of  $q$  states and  $q$  eigenvalues (time constants) and  $n-q$  states and eigenvalues as follows:

$$\begin{bmatrix} x_1 \\ x_2 \end{bmatrix} = \begin{bmatrix} T_{11} & T_{12} \\ T_{21} & T_{22} \end{bmatrix} \begin{bmatrix} z_1 \\ z_2 \end{bmatrix} \quad (3.79)$$

$$\begin{bmatrix} \dot{z}_1 \\ \dot{z}_2 \end{bmatrix} = \begin{bmatrix} \Lambda_1 & 0 \\ 0 & \Lambda_2 \end{bmatrix} \begin{bmatrix} z_1 \\ z_2 \end{bmatrix} + \begin{bmatrix} \Xi_1 \\ \Xi_2 \end{bmatrix} u \quad (3.80)$$

where  $x_1$  and  $z_1$  are  $q \times 1$  vectors partitioning the states and modes and  $x_2$  and  $z_2$  are  $(n-q) \times 1$  vectors partitioning the remaining states and modes.

If the following equilibrium relationship is approximately true (within the time frame of control interest),

$$\dot{z}_2 \approx 0 \quad (3.81)$$

then the following reduction can be made

$$\dot{x}_1 = F_r x_1 + G_r u \quad (3.82)$$

where  $x_1$  is now the  $q \times 1$  state vector,  $F_r$  is the  $q \times q$  dynamics matrix, and  $G_r$  is the  $q \times m$  control distribution matrix. Also,

$$\begin{bmatrix} x_2 \\ y \end{bmatrix} = \begin{bmatrix} H^* \\ H_r \end{bmatrix} x_1 + \begin{bmatrix} D^* \\ r \end{bmatrix} u \quad (3.83)$$

where  $x_2$  is treated as an additional  $(n-q) \times 1$  output vector with a  $(n-q) \times q$  state distribution matrix  $H^*$  and a  $(n-q) \times m$  control distribution matrix  $D^*$ . The original output distribution matrices,  $H$  and  $D$ , are modified to  $H_r$  and  $D_r$ , respectively. The formulas for these matrices are shown below in terms of the partitioned modal decomposition:

$$F_r = T_{11} \Lambda_1 T_{11}^{-1} \quad (3.84)$$

$$G_r = T_{11} (\Lambda_1 T_{11}^{-1} T_{12} \Lambda_2^{-1} \Xi_2 + \Xi_1) \quad (3.85)$$

$$H^* = T_{21} T_{11}^{-1} \quad (3.86)$$

$$D^* = (T_{21} T_{11}^{-1} T_{12} - T_{22}) \Lambda_2^{-1} \Xi_2 \quad (3.87)$$

$$H_T = H_1 + H_2 H^* \quad (3.88)$$

$$D_T = D + H_2 D^* \quad (3.89)$$

Care must be exercised in the partitioning of the system to assure that states retained span the space of the reduced modal system. In other words,  $T_{11}$  must be invertible.

### 3.6.2 Second Stage Reduction

The control structure proposed in Chapter IV requires an accurate mathematical model of the engine throughout its operating flight envelope. It is highly desirable to provide this model in a simple form to minimize computer storage and computation requirements. A first step in a model reduction procedure has been described above. It involves the reduction in order of the system equations to include only those modes which are important for control purposes. Outlined below is a procedure for further simplifying the reduced order system (system order remains unchanged). The procedure is based on eliminating (setting to zero) those elements in the system dynamics matrix,  $F$ , which have "little" effect on the system's state dynamic response. The result is a "simplified" system dynamics matrix,  $\hat{F}$ . Note that concentrating on system dynamics is justifiable if the equations are implemented in the form

$$\begin{aligned} \dot{x} &= F(x - g(x, u, \theta)) \\ \text{or} \quad \dot{\hat{x}} &= \hat{F}(\hat{x} - g(\hat{x}, u, \theta)) \end{aligned}$$

since the correct steady state is guaranteed by the steady state schedules.

The procedure is comprised of three steps:

Step 1: Identify those elements in  $F$  which have little effect on the engine's dynamic response. Specifically, let  $J_0$  represent a measure of the total system state response.

$$J_0 = \frac{1}{2} \int_0^{\infty} x^T A x dt \quad (3.90)$$

with

$$\dot{x} = Fx$$

and  $E[x(0)x(0)^T] = X_0$ . (= I if random initial conditions are assumed).

"Unimportant" elements,  $F_{ij}$ , are those for which

$$\frac{\partial J_0 / J_0}{\partial F_{ij} / F_{ij}} \ll 1 \quad (3.91)$$

or

$$\frac{\Delta J_0 / J_0}{\Delta F_{ij} / F_{ij}} \ll 1. \quad (3.92)$$

That is,  $F_{ij}$  is unimportant if a 100% change in  $F_{ij}$  produces a small percentage change in  $J_0$ . Define all of these elements as  $F_{ij}^*$ .

Step 2: Set all the  $F_{ij}^* = 0$ , and define the resultant system dynamics matrix as  $\bar{F}$ . That is

$$\bar{F} = F \Big|_{F_{ij}^* = 0} \quad (3.93)$$

Step 3: Modify the non-zero elements in  $\bar{F}$  to minimize the mean square difference between the initial condition responses of the reduced system ( $\dot{\hat{x}} = F\hat{x}$ ) and the original ( $\dot{x} = Fx$ ). Specifically, find

$$\hat{F} = \min_{\bar{F}} \left\{ J = \frac{1}{2} \int_0^{\infty} (x - \hat{x})^T A_2 (x - \hat{x}) dt \right\} \quad (3.94)$$

where

$$\dot{x} = Fx$$

$$\dot{\hat{x}} = \bar{F}\hat{x}$$

and

$$E \begin{bmatrix} x(0) & x(0)^T \end{bmatrix} = X.$$

with

$$\hat{x}(0) = x(0).$$

$\hat{F}$  is the optimum reduced F matrix.

A procedure for solving Step 3 is presented in Appendix B. A block diagram of the overall model reduction procedure is presented in Figure 3.2.

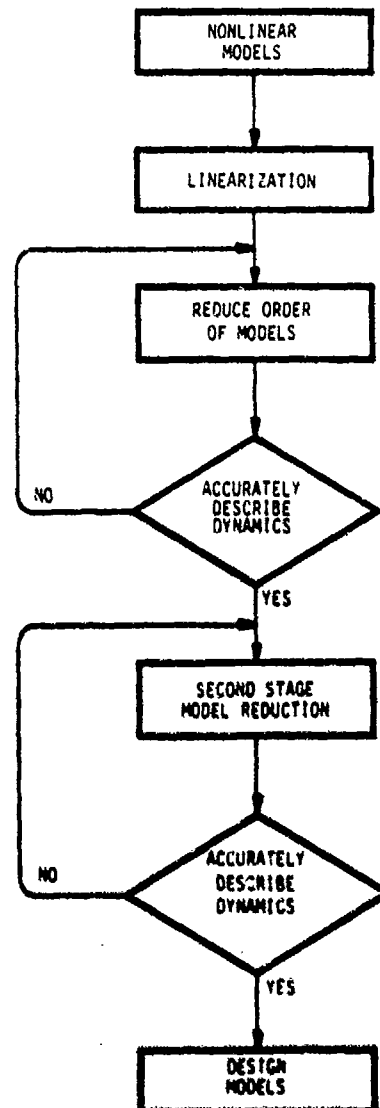


Figure 3.2 Generation of Design Models

Example:

A simple second order example is presented to clarify the procedure. Consider the system

$$\dot{x} = \begin{bmatrix} -10 & 1 \\ 0 & -20 \end{bmatrix} x .$$

Clearly, the diagonal elements will dominate this response. Hence, it is desired to find an  $\hat{F}$  matrix of the form

$$\hat{\dot{x}} = \begin{bmatrix} a & 0 \\ 0 & b \end{bmatrix} \hat{x}$$

which most nearly matches the initial condition's response of the original system. That is,  $J$  is minimized where

$$J = \frac{1}{2} \int_0^{\infty} (x - \hat{x})^T (x - \hat{x}) dt$$

and

$$x(t) = e^{Ft} x(0)$$

$$\hat{x}(t) = e^{\hat{F}(t)} \hat{x}(0). \quad \hat{x}(0) = x(0)$$

If specific initial conditions are chosen, the problem is easily solved in closed form. That is,  $x(t)$  and  $\hat{x}(t)$  may be found; then, from these,  $J$  may be computed. The parameters  $a$  and  $b$  can then be chosen to minimize  $J$ .

For the case

$$x(0) = \begin{bmatrix} 1 \\ 10 \end{bmatrix} \text{ and } \hat{x}(0) = \begin{bmatrix} 1 \\ 10 \end{bmatrix}$$

The solution is

$$\hat{F} = \begin{bmatrix} -6.495 & 0 \\ 0 & -20 \end{bmatrix}.$$

Note that due to the one-way coupling in the system, the  $F_{22}$  element was not affected; only the  $F_{11}$  element was altered.

These results are plotted in Figure 3.3;  $x_1(t)$  is the original response,  $\hat{x}_1(t)$  is the response of the reduced system, and  $\tilde{x}_1(t)$  is the response of the system obtained by setting  $F_{12} = 0$  without altering  $F_{11}$  (i.e.,  $\dot{\tilde{x}}_1 = -10 \tilde{x}_1$ ). These results show that by increasing the system time constant, the reduced system can be made to duplicate more closely the original.

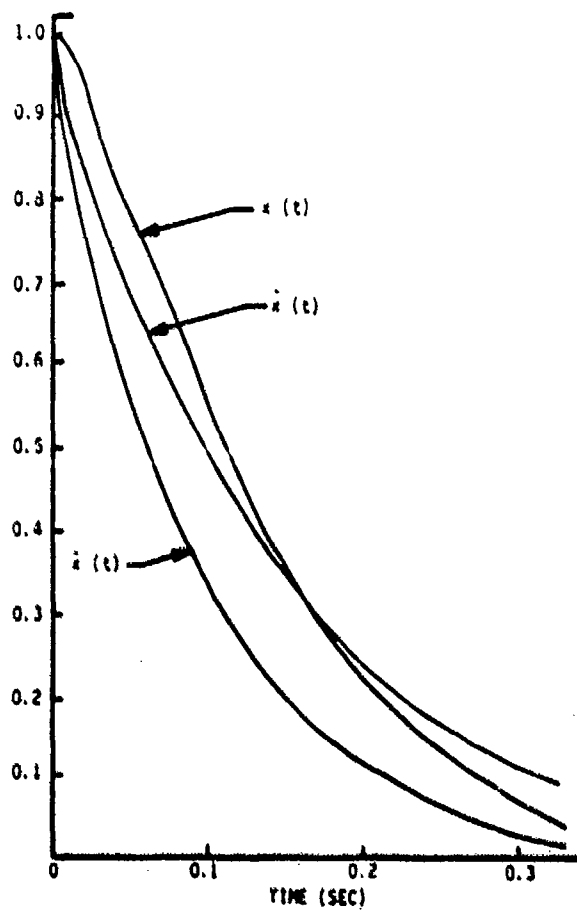


Figure 3.3 Comparison of Time Histories for Second Stage Reduction Example

### 3.7 NONLINEAR MODEL DEVELOPMENT

The procedures used to derive linearizations of a complex nonlinear simulation at selected flight points is discussed in Section 3.6. These linearizations are the basis for point design of control regulation logic discussed above. The simplified dynamic models can also be used in the controller to implement transition logic, filter update equations, and fault tolerant strategies. The primary requirement for a simple model equation arises from the real time, microprocessor implementation. For example, a typical nonlinear digital design simulation of an advanced engine requires 64-128 thousand words of memory and uses several thousand multiplication operations for each integration step. These programs describe each component using empirical operating maps and detailed aerothermodynamic equations to derive the cycle balances existing during engine operation. Clearly, this type of implementation is far too complex to use in a real time microprocessor environment. However, the program derived linear models can be used as a starting point for development of real-time, simplified nonlinear equations which closely match the full engine simulation program. This method is described below. Engine dynamics can be represented by the  $n^{\text{th}}$  order set of nonlinear equations:

$$\dot{x} = f(x, u, \theta) \quad (3.95)$$

$$y = h(x, u, \theta) \quad (3.96)$$

where  $m$  quantities,  $u$ , (controls) and  $q$  inputs,  $\theta$ , (ambients) determine the  $n$  states and state rates,  $x$  and  $\dot{x}$  respectively. These variables appear as nonlinear algebraic functions in the output equations for  $p$  quantities,  $y$  of interest. Much is known about the steady state engine response. This can be written:

$$0 = f(x_{ss}, u, \theta) \quad (3.97)$$

$$y = h(x_{ss}, u, \theta) \quad (3.98)$$

Most of the modeling effort should go into matching steady state response since it is at these points that engine performance is usually evaluated. Dynamical response is also important to the overall description of the behavior since these dynamical properties determine stability.

A linear approximation to equation (3.95) can be evaluated if derivative matrices of  $f$  are available as described in Section 3.6. The function,  $f$ , in Eq. (3.95) can be expanded about an equilibrium point  $(x_0, u_0)$  as follows:

$$\begin{aligned}\dot{\delta x} &= f_x(x_0, u_0)\delta x + f_u(x_0, u_0)\delta u \\ \delta x &= x - x_0 \\ \delta u &= u - u_0\end{aligned}\tag{3.99}$$

If it is assumed that  $u(t)$  is piecewise constant on an interval  $[nT, (n+1)T]$ , equation (3.95) can be rewritten relative to the constant value of  $u$  and the value of  $x$  which would be reached if  $u$  remained at that value, or,

$$\dot{x} = F_x(x_{ss}, u(n)) [x(t) - x_{ss}]\tag{3.100}$$

where  $x_{ss}$  must satisfy the nonlinear equilibrium relationship

$$0 = f(x_{ss}, u(n), \theta)\tag{3.101}$$

or, equivalently,

$$x_{ss} = g(u(n), \theta)\tag{3.102}$$

where  $g(u(n), \theta)$  is defined as the reference schedule of the states given the control input levels.

The time interval,  $T$ , can be made small relative to the dynamics so that the constant control assumption is valid for any  $u(t)$ .

Equation (3.100) is the linear simulation of the nonlinear dynamics in Eq. (3.95). It is an accurate model only when  $\delta x$  and  $\delta u$  remain within a suitable region of linearity. Unfortunately, the controls in complex engines often change quickly and the engine operates away from the equilibrium points during most large power level changes. The concept of the linear simulation of the form in Eq. (3.99) can be expanded to produce a more accurate representation of the true nonlinear dynamics.

The model reduction procedure described in Section 3.6 produces low order linear models parameterized with terms which are important to the response. These models represent the important dynamic behavior of the engine throughout its flight envelope. The first step in the nonlinear model development procedure produces polynomial functions which fit the dynamic parameters with engine operating variables. This is a curve-fitting problem which can be stated as follows. For a set of operating variables,  $z$ , e.g., rotor speeds, ambient conditions, and control inputs, terms of the following form are created at each model generation point:

$$t_j(z) = \prod_{i=1}^q z_i \quad (3.103)$$

The set of coefficients,  $a_j$ , which minimize the following cost function are found:

$$J^* = \min_{a_j, r, q} \left\{ \sum_{k=1}^N \left[ p(k) - \sum_{j=1}^r a_j t(z(k)) \right]^2 \right\} \quad (3.104)$$

where the non-zero elements of the reduced dynamics matrix,  $p(k)$  at each of  $N$  flight points are fit with a set of polynomial functions of the operating variables  $t(z(k))$ . (Note that the set of variables,  $z$ , may contain other  $p$ 's). The minimization is carried over the constant coefficients,  $a_j$ , the number of terms used,  $r$ , and the highest powers represented in each term,  $q$ . This

procedure is known as optimal subset selection in a ridge regression problem [18]. In Section 5.2, this procedure is illustrated for the GE 23.

The resulting dynamic matrix can be written as follows:

$$\left. \frac{\partial f}{\partial x} \right|_{\dot{x}=0} = F(x) \quad (3.105)$$

i.e., the matrix  $F$  represents the gradient of the nonlinear function,  $f(x,u)$  along the steady state operating line. A Taylor series expansion of  $f(x,u)$  matches the function at an arbitrary  $(x,u)$  to the gradient at the static operating line,  $F(x)$ . This development is shown in Appendix C. The results indicate that to match the nonlinear dynamics at arbitrary point to order  $||\delta x||^5$ , the following form can be used:

$$f(x,u) = \frac{1}{2} [F(x_1) + F(x_2)] + 0((x-x_0)^5) \quad (3.106a)$$

$$\Delta \tilde{F}(x, x_{SS}) \quad (3.106b)$$

where

$$x_1 = x_0 + \frac{x-x_0}{q_1} \quad (3.107)$$

$$x_2 = x_0 + \frac{x-x_0}{q_2} \quad (3.108)$$

$$q_1 = 3 + \sqrt{3} \quad (3.109)$$

$$q_2 = 3 - \sqrt{3} \quad (3.110)$$

$$x_0 = g(u) \quad (3.111)$$

The implication of Eqs. (3.106) through (3.111) is that the linear simulation in Eq. (3.100) can be replaced by a far more accurate ( $||\delta x||$  vs.  $||\delta x||^5$ ) nonlinear simulation as follows:

$$\begin{aligned}\dot{x} &= \tilde{F}(x, x_{ss})(x - x_{ss}) \\ x_{ss} &= g(u(n), \theta)\end{aligned}\tag{3.112}$$

This method can be illustrated with the following simple example. Suppose the nonlinear model is the following scalar equation (which is assumed unknown):

$$\dot{x} = x^4 - 2x^3 u^2 + u^3\tag{3.113}$$

Gradients of this function were available and the linearized models were fit to form fitted dynamics matrix:

$$F(x, u) = (4x^3 - 6x^2 u^2)\tag{3.114}$$

The reference point schedule indicates that  $u_{ss} = 1$ ,  $x_{ss} = 1$ , is a static equilibrium. The "engine simulation" for a step input to

$$\dot{x} = \frac{1}{2} \left( F\left(1 + \frac{x-1}{3+\sqrt{3}}, 1\right) + F\left(1 + \frac{x-1}{3-\sqrt{3}}, 1\right) \right) (x-1)\tag{3.115}$$

The model in (3.94) can be compared to the actual equation in (3.92) as follows:

$$\begin{aligned}\dot{x} &= \frac{1}{2} \left\{ \left[ \left(1 + \frac{x-1}{3+\sqrt{3}}\right)^3 + \left(1 + \frac{x-1}{3-\sqrt{3}}\right)^3 \right] \right. \\ &\quad \left. - 6 \left[ \left(1 + \frac{x-1}{3+\sqrt{3}}\right)^2 + \left(1 + \frac{x-1}{3-\sqrt{3}}\right)^2 \right] \right\} (x-1) \\ &= \left\{ x^3 + x^2 + x + 1 - 2(x^2 + x + 1) \right\} (x-1) \\ &= x^4 - 1 - 2(x^3 - 1) \\ &= x^4 - 2x^3 + 1\end{aligned}\tag{3.116}$$

i.e., the procedure creating Eq. (3.115) from the gradients produces the exact representation of Eq. (3.113) since the original dynamics function is a polynomial of order less than  $x^5$ .

### 3.8 SUMMARY

Several procedures for developing important components of the multivariable controller have been presented. Trajectory generation methods have been discussed which produce feedforward commands to the plant. Output regulator design methods have been derived which result in simplified regulator gains for the perturbation logic. Finally, a model analysis methodology has been explained which uses a complex nonlinear engine simulation to produce low order, linear design models, reduced-parameter linearizations and, finally, simplified nonlinear equations for the plant.

In Chapter IV, the structure of a multivariable controller for the GE 23 is presented which addresses the control requirements discussed in Chapter III and uses procedures presented in Chapter III to produce a reliable and efficient full envelope control law for the GE 23 variable cycle engine.

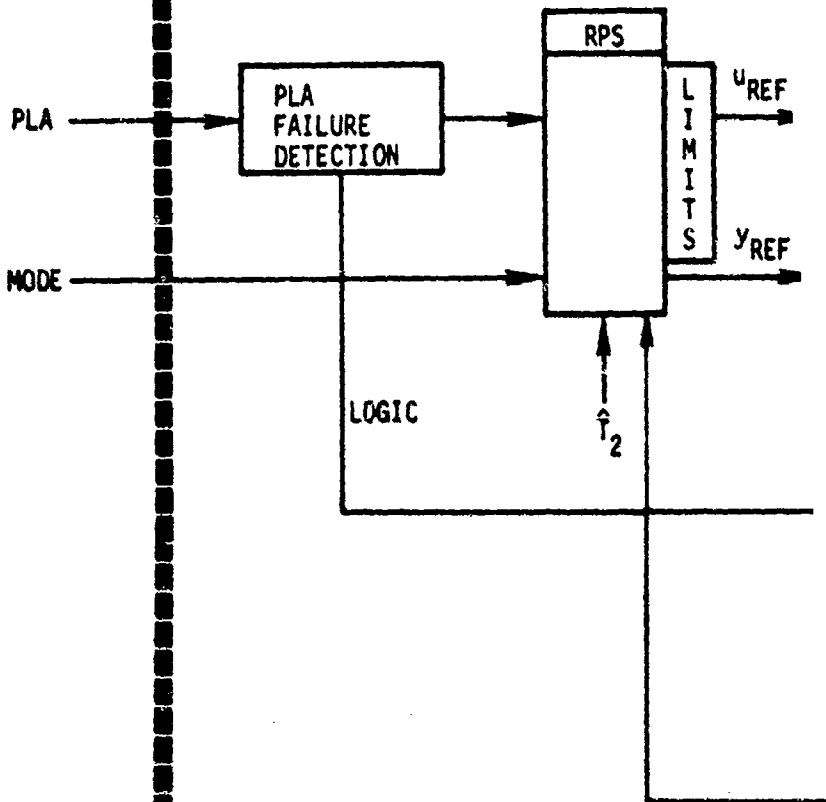
SECTION IV  
CONTROL STRUCTURE DEFINITION

4.1 INTRODUCTION

The design requirements for a controller for the General Electric GE23-JTDE variable cycle engine were developed in Chapter II. The purpose of this chapter is to describe a control structure and design methodology proposed by SCI (Vt) which satisfies these requirements.

The proposed controller is diagramed in Figure 4.1. It utilizes a model following structure for the control law, and incorporates a nonlinear engine model that is common to several of the functional blocks. Transient regulation, steady-state performance and failure accommodation criteria can be met with this technique. The primary purpose of this controller is to operate the engine at desired levels of thrust and airflow in the presence of disturbances, failures, and plant variations without violating constraints on component stability and physical limits. Any flexibility available after these primary goals have been attained is used to maximize secondary goodness criteria such as response time, fuel consumption, and life.

The hardware environment in which the control logic will be implemented is defined in terms of the FADEC microprocessor configuration (Figure 4.2). The signals entering and leaving the controller are defined in the figure. They are listed and categorized in Table 4.1. These signals can be grouped into gas path sensor outputs, actuator stroke feedbacks, logic inputs, operating point inputs, actuator commands and logic outputs. A precise definition of these quantities is important to initial structure definition.



PILOT COMMAND

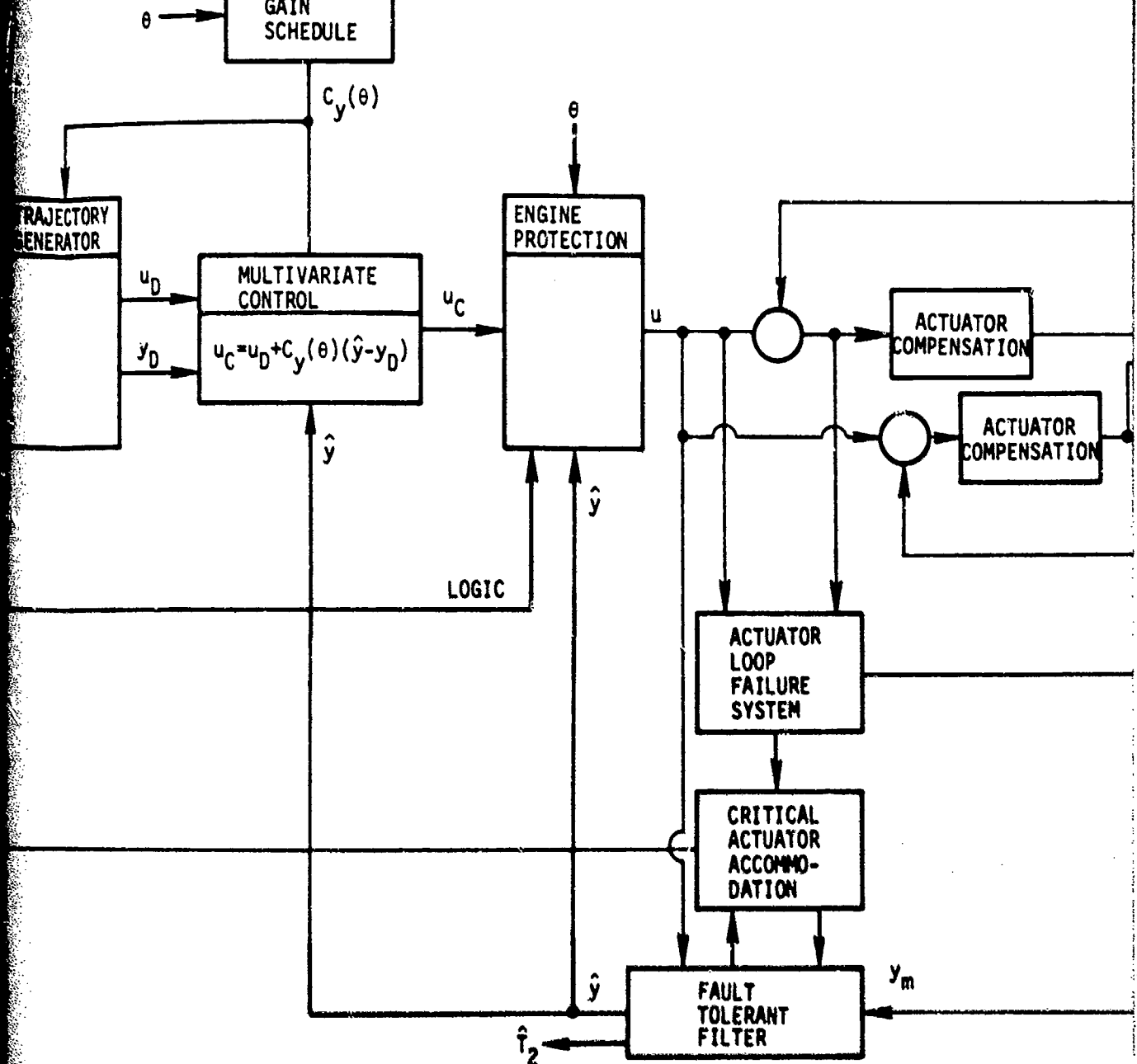
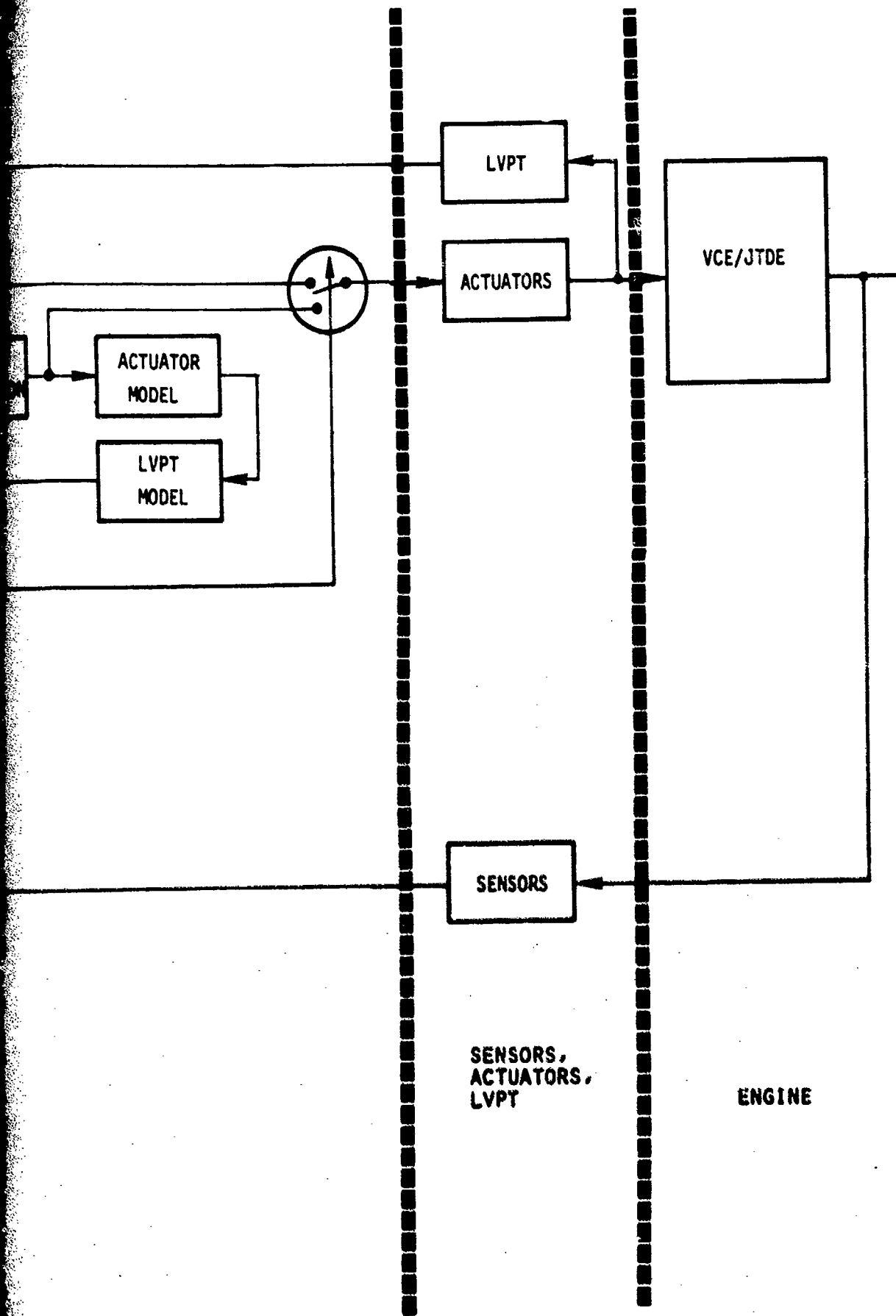


FIGURE 4.1 CONTROL LOGIC/COMPUTER



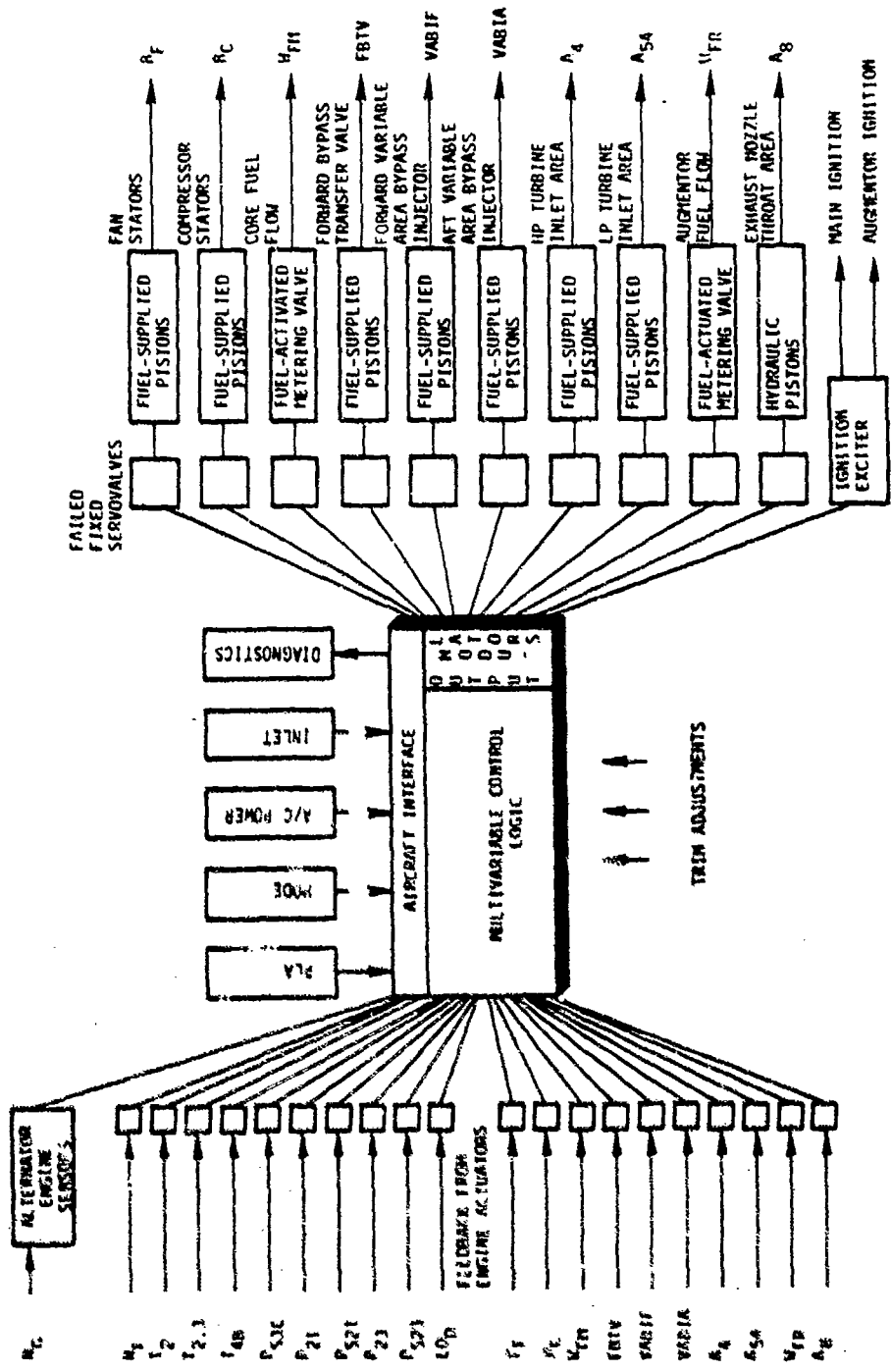


Figure 4.2 FADEC Hardware

Table 4.1  
Input/Output Signal Categories

SIGNAL	SOURCE	CONVERSION	TYPE
NG	Sensor	F/D	Sensor Input
NF	Sensor	F/D	Sensor Input
T <sub>2</sub>	Sensor	A/D	Sensor Input
T <sub>2.5</sub>	Sensor	A/D	Sensor Input
T <sub>4B</sub>	Sensor	A/D	Sensor Input
P <sub>s3</sub>	Sensor	F/D	Sensor Input
ΔP <sub>21</sub>	Sensor	F/D	Sensor Input
P <sub>s21</sub>	Sensor	F/D	Sensor Input
ΔP <sub>23</sub>	Sensor	F/D	Sensor Input
P <sub>s23</sub>	Sensor	F/D	Sensor Input
LOD	Sensor	Switch	Logic Input
B <sub>F</sub> (FB)	Sensor	P/D	Sensor Input
B <sub>C</sub> (FB)	Sensor	P/D	Sensor Input
WFM (FB)	Sensor	P/D	Sensor Input
FBTV (FB)	Sensor	P/D	Sensor Input
VABIF (FB)	Sensor	P/D	Sensor Input
VABIA (FB)	Sensor	P/D	Sensor Input
A54 (FB)	Sensor	P/D	Sensor Input
WFR (FB)	Sensor	P/D	Sensor Input
AB (FB)	Sensor	P/D	Sensor Input
PLA	Data Bus		Thrust Request
MODE	Data Bus		Mode Select
POWER	Data Bus		On/Off
INLET	Data Bus		
FAIL	Data Bus		Logic Output
STATUS	Data Bus		Binary Output
B <sub>F</sub>	Modulator	PWM	Actuator Command
B <sub>C</sub>	Modulator	PWM	Actuator Command
WFM	Modulator	PWM	Actuator Command
FBTV	Modulator	PWM	Actuator Command
VABIF	Modulator	PWM	Actuator Command
VABIA	Modulator	PWM	Actuator Command
A54	Modulator	PWM	Actuator Command
WFR	Modulator	PWM	Actuator Command
AB	Modulator	PWM	Actuator Command
MAIN IGNITION	Driver	Switch	Output Logic
AUGMENTOR IGNITION	Driver	Switch	Output Logic

A functional description of the controller is presented in Table 4.2. Described in the sections below are the functional blocks of logic which accomplish these indicated tasks as well as the signal flow paths between the blocks.

Note that the control logic is discussed from a continuous time viewpoint since this approach tends to be more clear. Actual implementation of the logic, however, will be through full discretization of the equations. Program structure will be a multirate/multiloop design. Depending on the availability of loop clocks, the controller may operate in a free-running mode where actual loop times are variable. Synthesis techniques are available to accommodate this mode of operation.

#### 4.2 OVERVIEW OF SYSTEM

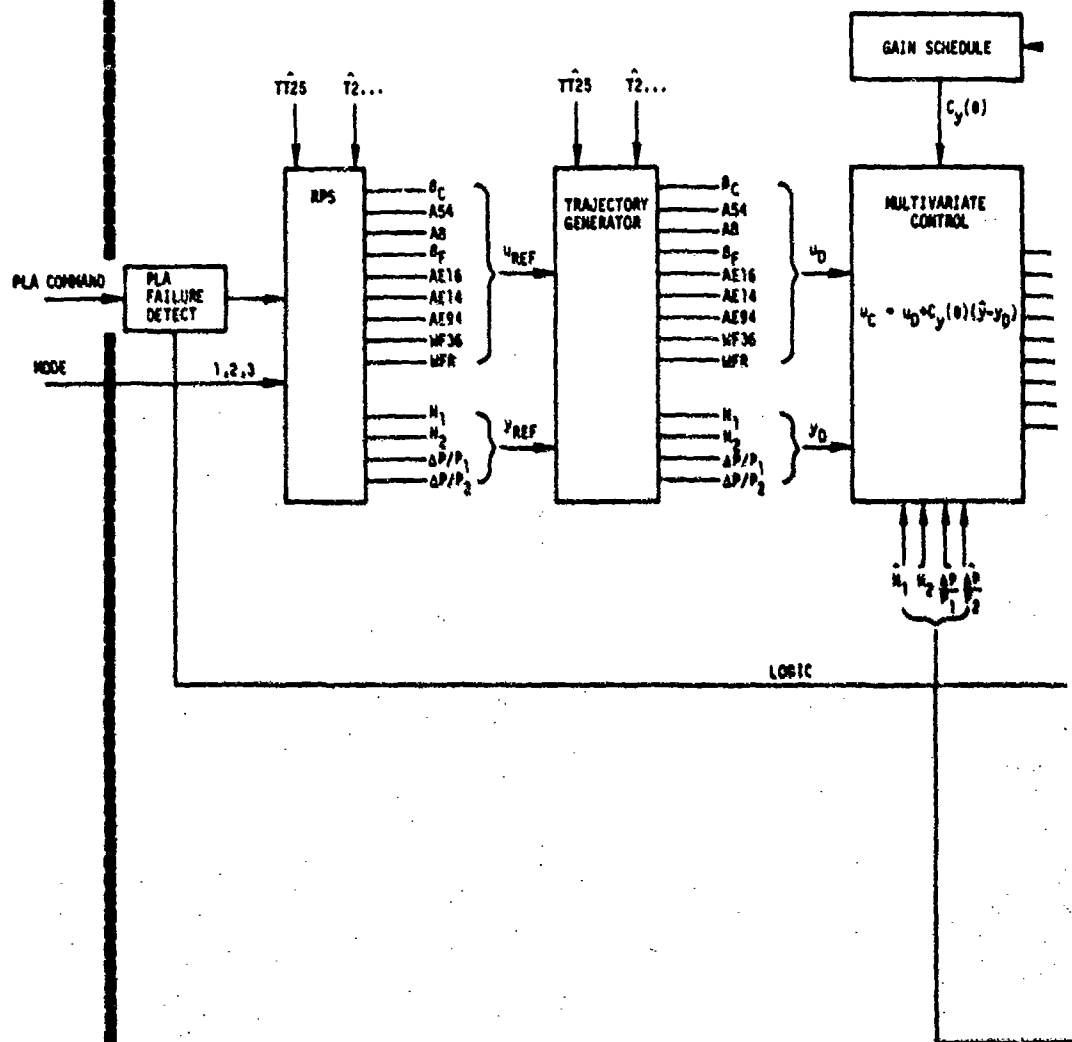
The operation of the interconnected system is described below. Figure 4.3 shows a detailed diagram of the signal connections defined at this time. Details of each block are presented in the following section.

Pilot and inlet commands are the primary performance setting variables. The pilot input is treated as a thrust request and an inlet input as an airflow request. In addition to these two continuous inputs, a digital mode input is provided to define the engine performance and operating line behavior at various mission-oriented flight conditions. The modes are discussed in the description of the reference point schedules. These input quantities are used to set the desired operating point. Ambient pressure and temperature signals are synthesized in the fault tolerant filter for the remaining degrees of freedom in specifying the desired performance.

Reference point schedules produce an estimate of the equilibrium point quantities at the requested operating points. These

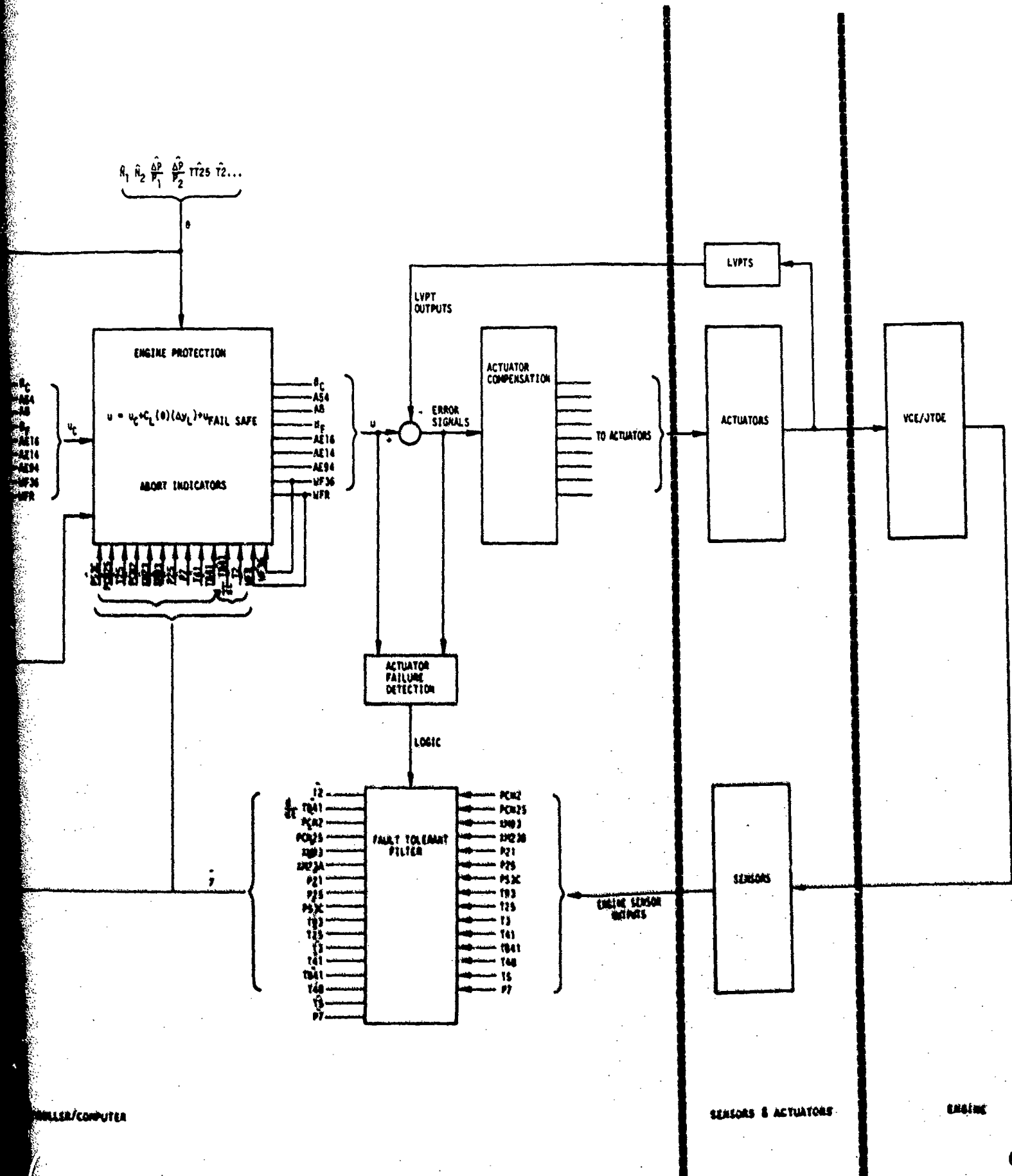
Table 4.2  
 Preliminary Functional Description of Multivariable Control

FUNCTION	DESCRIPTION OF REQUIREMENT	INPUTS	SYNTHESIS METHOD
TRANSIENT REGULATION	ACCURATE REFERENCE POINT TRACKING	REFERENCE POINT PERTURBATIONS DISTURBANCES	LINEAR OPTIMAL CONTROL THEORY
STEADY STATE REGULATION	ACCURATE INSTALLED PERFORMANCE WITH MODE CHANGES, BUILD DIFFERENCES, INSTRUMENT ERRORS	PLA AMBIENT CONDITIONS	NONDIMENSIONAL EXPANSION WITH TRIM PROCEDURE AS REQUIRED
TRANSIENT CONTROL	SUITABLE TRANSITION FROM ONE CONDITION TO ANOTHER RESPECTING LIMITS	LARGE REFERENCE CHANGES	OPTIMAL THEORY OR LINEAR APPROXIMATE DESIGN
SIGNAL PROCESSING	CONDITION INPUTS ON NOISE ESTIMATES AND OTHER VARIABLES	SENSED INPUTS	MODERN ESTIMATION THEORY
FAILURE DETECTION AND ACCOMMODATION	DETECTION OF FAILED ACTUATORS AND SENSORS AND LOGIC FOR BACKUP INITIATION	PROCESSED SIGNALS AND COMMANDS	ADVANCED STATISTICAL TECHNIQUES



PILOT

FIGURE 4.3 C1



schedules represent the static portion of the nonlinear engine model.

The estimated equilibrium values generated by the reference point schedules are passed to the trajectory generator. This block uses the dynamic engine model to form compatible, nominal trajectories in the engine variables and controls to move from the present point to the desired point in an optimal fashion without limit exceedances.

The nominal path specifications for the regulator are the trajectory generator outputs. The regulator uses sensed engine state information compared to these nominal values to form an actuator command. The regulator has no time varying components. The d.c. gains from set point quantities to controls will be designed so that acceptable static performance can be achieved without the integral trim or d.c. gain enhancing compensation.

Outputs from the regulator are actuator commands. These are processed through output failure detection and accommodation logic to prevent abnormal actuator inputs to the engine. Limit protection overrides appear in this block. Also, sensed gas path and actuator stroke inputs are processed through a fault-tolerant filter which is designed to produce the best estimate of the required regulator inputs, given a set of noisy and failed sensors. Passive adaptation of logic to ambient and power conditions is accomplished with a centralized gain schedule.

Failure accommodation is provided throughout the logic. Thrust, airflow, and mode inputs are monitored according to slew rate and allowable range; sensor inputs have full analytical redundancy in the fault-tolerant filter; control commands are monitored for abnormal conditions; and, servo error signal response is monitored to detect failed output servos. The procedures proposed are discussed in a later section.

Section 4.3 describes the engine model setup. The function of the reference point schedules is developed in Section 4.4.

Several approaches to the trajectory generator are described in Section 4.5. Section 4.6 describes the format of the regulator and the procedure for deriving feedback gains. Fault tolerant filtering and the engine protection blocks are described in Sections 4.7 and 4.8. Finally, failure detection and accommodation protocols are discussed in Section 4.9.

#### 4.3 NONLINEAR MODEL

A simple, accurate description of the dynamic and static behavior of the engine is required. The model structure should allow separate programming of steady state and dynamic response. The implementation of the model will be in a subroutine format so that various control blocks can utilize the same code with slightly different inputs and outputs.

The initial approach is described in Chapter III and is summarized below. The engine operating point is derived as a function of the inputs. Thus, PLA, mode, TT2 and PT2 (derived) represent a complete set. Set point schedules currently used will be incorporated so that engine set point performance will meet specification. Peripheral variables such as sensor output and non-scheduled actuator deflections are also predicted in this portion of the model. Nonmeasured outputs such as thrust, stability, margin and airflows can also be approximated. The general form is:

$$y = h(x,u) \quad (4.1)$$

where  $u$  is a group of terms that specify the set point uniquely and  $y$  is the estimate of all other states, outputs, measurements, and controls of interest at this set point. The functions,  $h(x,u)$ , will consist of tables or polynomial fits depending on the most efficient implementation.

The dynamics of the model will be constructed from reduced order linear models produced at various points in the flight.

envelope and mapped by a group of low order functions of auxiliary variables. These functions will most likely be implemented as polynomials of low order. Sensitivity methods will be used to reduce the problem to a tractable form. The model for the linear dynamics is:

$$F(x,u) = \frac{\partial f}{\partial x}(x,u) \quad (4.2)$$

where  $f(x,u)$  are the nonlinear plant equations.

$$\dot{x} = f(x,u) \quad (4.3)$$

The advantage of using the gradients rather than  $f$  directly lies in the independent calculation of the reference point. The dynamic model has the following form:

$$\dot{x} = \mathcal{L}(F(x,u)) (x - x_{ss}) \quad (4.4)$$

where  $\mathcal{L}(\cdot)$  is a linear functional described in Appendix C.

#### 4.4 REFERENCE POINT SCHEDULES

The reference point schedules are basically given in Equation (4.1) with  $x = x_{ss}$ . Figure 4.4 shows the reference point schedules in more detail. A procedure for generating logic is discussed below.

The inputs to the schedules are PLA, mode, inlet commands and derived ambient variables TT2, PT2. PLA requests thrust continuously and freely from idle to maximum power. Inlet inputs are also available. Ambient variables determine the gas state at the engine face. The mode command is a means of moving the operating point to a region near the nominal point in order to satisfy specific operating constraints. These mode criteria are shown in Table 4.3, where the aircraft envelope is divided as shown in Figure 4.5.

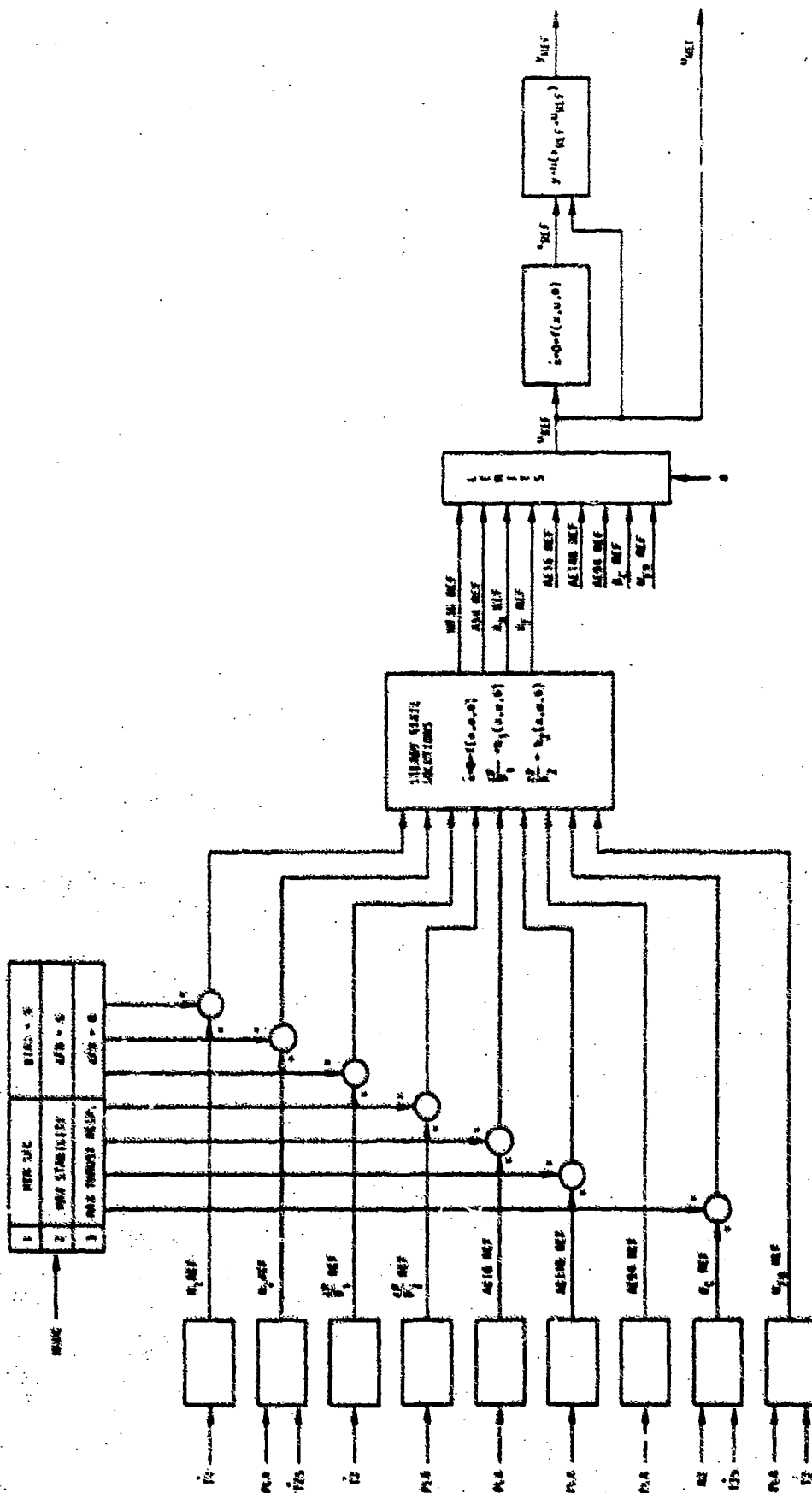


Figure 4.4 Reference Point Schedule Generator

Table 4.3  
Mission/Aircraft Definition  
(Control Performance Criteria)

CONTROL CRITERIA DOMAINS	COMMANDED THRUST	COMMANDED MODE	OPTIMAL CONTROL CRITERIA
MAXIMUM THRUST DOMAIN	MAXIMUM	INLET INTEGRATION WEAPONS MANEUVER	MAX. THRUST TO INLET LIMITS MAXIMIZE SURGE MARGIN
	INTERMEDIATE TO MAX.	INLET INTEGRATION WEAPONS MANEUVER	MIN. INSTALLED SFC AT INLET LIMITS MAXIMIZE SURGE MARGIN
	INTERMEDIATE	INLET INTEGRATION WEAPONS MANEUVER	MAX. DRY THRUST TO INLET LIMITS MAXIMIZE SURGE MARGIN
	BELOW INTERMEDIATE	INLET INTEGRATION WEAPONS/MANEUVER	MIN. INSTALLED SFC - THRUST RANGE LIMITED BY INLET AIRFLOW MATCHING MAXIMIZE SURGE MARGIN
MINIMUM SFC DOMAIN	MAXIMUM	CRUISE/ACCELERATE WEAPONS/MANEUVER	MAX. THRUST TO ENGINE LIMITS MAXIMIZE SURGE MARGIN
	INTERMEDIATE TO MAX.	CRUISE WEAPONS/MANEUVER	MIN. INSTALLED SFC MAXIMIZE SURGE MARGIN
	INTERMEDIATE	CRUISE WEAPONS/MANEUVER	MAX. DRY THRUST TO ENGINE LIMITS MAXIMIZE SURGE MARGIN
	BELOW INTERMEDIATE	CRUISE/LOITER WEAPONS/MANEUVER	MIN. INSTALLED SFC MAXIMIZE SURGE MARGIN
MAXIMUM STABILITY DOMAIN	MAXIMUM	MAX. STABILITY	MAX. THRUST WITH HIGH SURGE MARGIN
	INTERMEDIATE TO MAX.	MAX. STABILITY	MIN. INSTALLED SFC WITH HIGH SURGE MARGIN
	INTERMEDIATE	MAX. STABILITY	MAX. DRY THRUST WITH HIGH SURGE MARGIN
	BELOW INTERMEDIATE	MAX. STABILITY	MIN. INSTALLED SFC WITH HIGH SURGE MARGIN THRUST RANGE LIMITED BY BURNER P AND AT
MAXIMUM THRUST RESPONSE DOMAIN	MAXIMUM	APPROACH VSTOL	MAX. THRUST TO ENGINE LIMITS MAX. THRUST WITH HIGH SURGE MARGIN
	INTERMEDIATE TO MAX.	APPROACH VSTOL	MAX. THRUST RESPONSE UPWARD MAX. THRUST RESPONSE UP AND DOWN WITH HIGH SURGE MARGIN
	INTERMEDIATE	APPROACH VSTOL	MAX. DRY THRUST TO ENGINE LIMITS REQUIRES CONTROL ACTION TO AVOID A B LIGHTOFF DISCONTINUITY
	BELOW INTERMEDIATE	APPROACH VSTOL	MAX. THRUST RESPONSE UPWARD MAX. THRUST RESPONSE UP AND DOWN WITH HIGH SURGE MARGIN

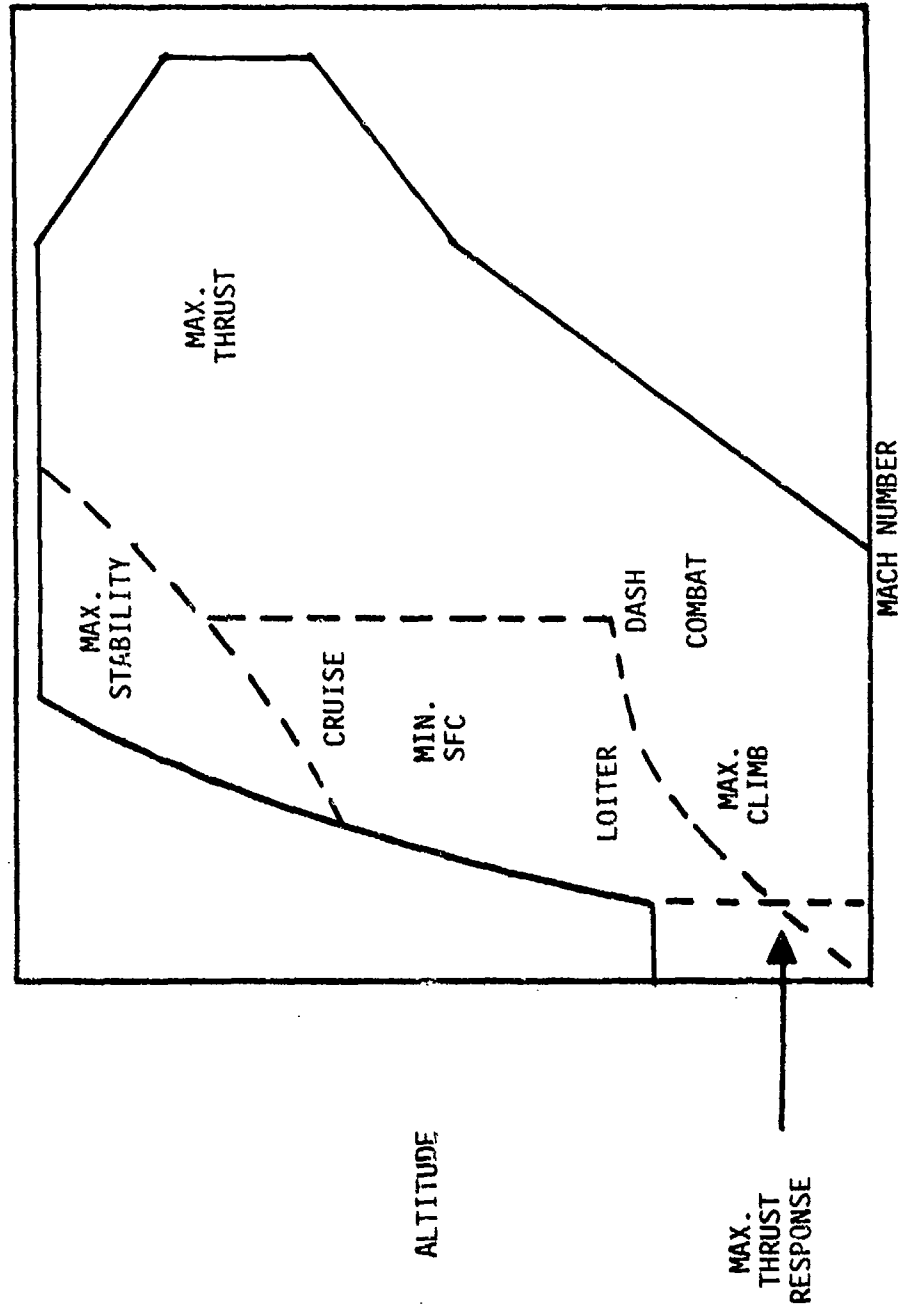


Figure 4.5 Control Criteria Within Flight Envelope

The data have been used to define three modes of operation which will be developed to satisfy a group of flight-dependent constraints. Each control criterion in Table 4.3 can be grouped within one of four constraints shown in Table 4.4. The first constraint is satisfied by the engine manufacturer's operating point design as supplied by the control schedules. Further optimization in this mode could be achieved by outer loop adjustment of the operating point to minimize TSFC. This portion of the logic will be optional until later in the development effort. The second constraint is based upon inlet limits and matching. The details of these interactions have not been identified at this point. The third constraint involves increasing component stability margins to accommodate distortion, weapons' discharge and low ambient pressure effects. The increased stability will be produced at constant thrust and increased fuel consumption. The final constraint is a high response match point which will provide continuous thrust modulation at increased response rates.

Table 4.4  
Operating Constraints

Constraint	Definition
C <sub>1</sub>	Within engine limits, run to maximum augmented and dry thrust points with minimum TSFC modulation continuously between them.
C <sub>2</sub>	Inlet airflow compatibility
C <sub>3</sub>	Increase stability margins at constant thrust.
C <sub>4</sub>	Maximize thrust response rates w/o discontinuities.

Three modes are defined and regions of the envelope where these modes are operative are shown (Table 4.5). The normal operating mode is shown to be active in all parts of the envelope except

Table 4.5  
Modes of Operation

MODE	SYMBOL	DESIGN CONSTRAINT	ACTIVE REGION*
Normal	$M_0$	$C_2, C_1$	I, II, IV
Increased Stability	$M_1$	$C_3, C_2, C_1$	I, II, III
High Response	$M_2$	$C_4, C_1$	IV

\*REGIONS:      I Supersonic                      III Left-Hand Corner  
                   II Cruise                              IV Approach

Region III (left-hand corner). In this region, selection of mode 0 or 1 or 2 will have the same result. Similarly,  $M_3$  is not distinguishable from mode  $M_0$  anywhere except approach.

The initial calculation of  $M_0$  (baseline) reference schedules will be accomplished as follows. Steady state control and outputs will be derived from the linear model base points and the nonlinear simulation when available. The engine set point quantities will be determined from the control schedules and output schedules provided by the manufacturer. It is anticipated that the output schedules will have to be modified to incorporate control saturations which are only implicitly handled in the schedules. This effect is shown in Figure 4.6 for the  $N_F$  schedule. At low PLA settings, the variable low turbine area saturates and the rotor speed falls off. For the reference point logic, a more feasible schedule is shown in the figure. Steady state data is schematically represented. Predicted values of  $N_F$  will be closer to actual running values and control action will not tend to compensate inappropriately for large offsets. A flow chart of the reference point calculation is shown in Figure 4.7. The PLA and mode inputs form the initial set point command. Mode biasing will be discussed below. The first

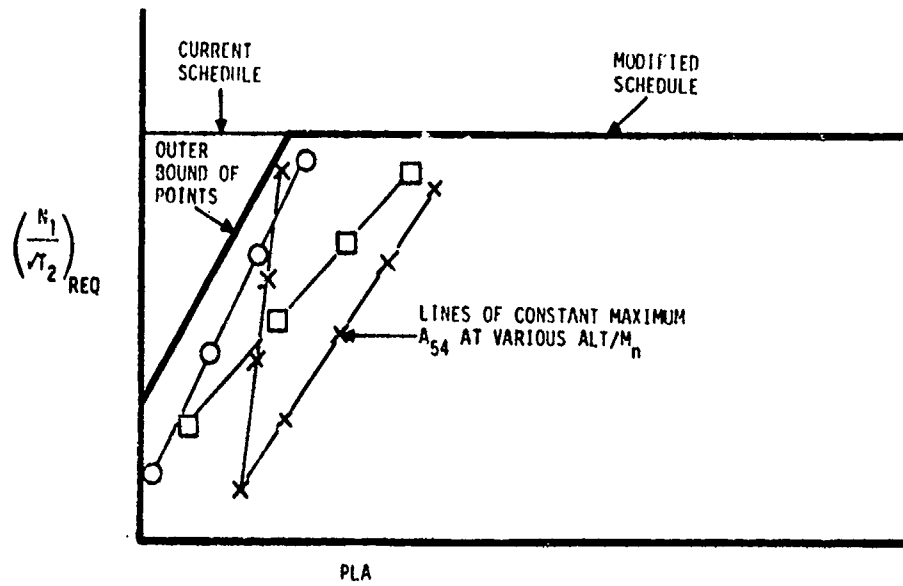


Figure 4.6 Control Saturation Effects on  $N_F$  Schedule

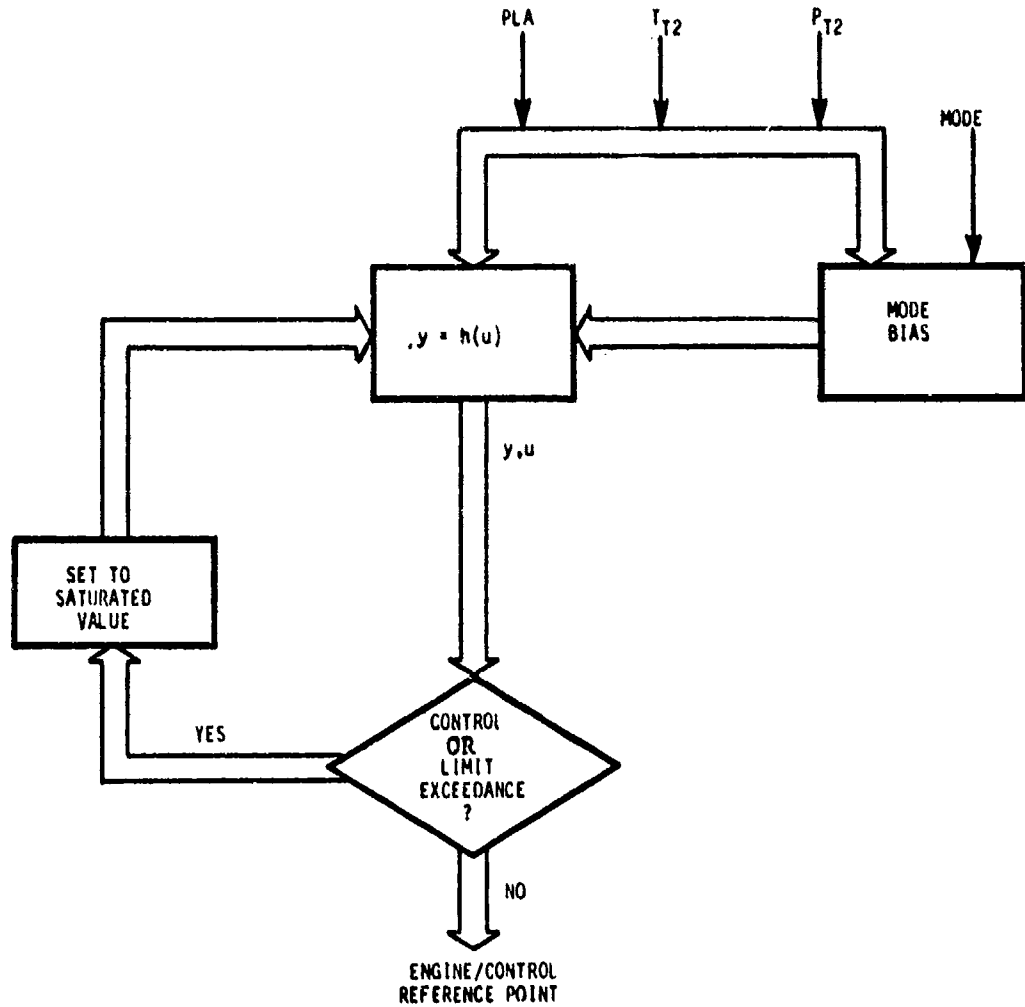


Figure 4.7 Reference Point Calculation Flowchart

calculation uses the set points as inputs. Control actuator saturations on output are reset to their maximum or minimum value and the routine is entered with these new inputs. The resulting reference point is an estimate of the desired equilibrium within operating limits and without actuator limit saturation. Set point schedules and actuator limits will be constructed with a small "overlap" so that operating points with predicted control saturations will actually cause the engine to operate with its controls limited. This outer bound is illustrated in Figure 4.6.

Mode switching will be handled by alteration of the reference point. Transition and regulation will be accommodated as in any other operating point shift. This procedure simplifies the logic significantly.

The procedure for generating control mode shifts involves generating a group of trial biases from the linear models. These biases will be evaluated on the nonlinear simulation to determine actual performance level shifts. Final schedules will be determined from these results. In general, the simplest structure will be sought.

This procedure is described for the increased stability mode. In this case, the fan and compressor stabilities will be increased at constant thrust and airflow. A direction in state space for this effect can be deduced from the linear models in steady state. The general motion of the operating point for changes in control can be written as follows:

$$\delta y = H \delta u$$

where H is steady state performance sensitivity matrix derived from the models. By choosing appropriate values of  $\delta y$  to be zero (e.g.,  $\delta F_n$  and  $\delta W_{fan}$ ) and regarding others to be positive ( $\delta SMF$ ,  $\delta SMC$ ),

appropriate linear combinations of the  $\delta u$ 's can be calculated. Reasonable values for these can be used to generate a perturbed operating point. Actual performance shifts must then be evaluated in the nonlinear deck.

#### 4.5 TRAJECTORY GENERATOR

The outputs from the reference point schedules represent a group of engine variables and controls which satisfy equilibrium conditions and which are within physical and operating limits. These quantities are based on the values of PLA, mode, and inlet conditions. These may instantaneously change from sample to sample because of pilot inputs. The actual reference outputs could be discontinuous over a large range. If these reference values were linked directly to the regulator, moderate engine transitions would saturate the actuators. To rate limit the reference points or the PLA commands would seriously degrade small signal response. Also, since the system response to very large inputs is nonlinear, the response achieved without some input compensation would be suboptimal (and most likely, catastrophic). The transition generator is designed to produce an ideal reference between the present engine state and the state most recently requested by the reference values.

The nominal reference trajectory should have the following attributes:

- (1) it should be nearly compatible with actual engine response, i.e., the reference input trajectory should nearly produce the reference output trajectories,
- (2) it should nearly track all engine and actuator limits, and
- (3) it should exhibit optimized response for both large and small inputs.

The approach chosen for this function is to utilize the dynamic model of the engine compensated with a nonlinear feedback law and

driven by the reference point schedule as the generator of this nominal path.

Several issues can be addressed at this point. A common question that arises concerns the requirement for a trajectory generator. Since the model is compensated by a feedback law, a similar control strategy could be used on the actual engine without the need for a complex software block. As the control strategy is simplified, this argument becomes more viable. However, the internal model can exhibit the response of the engine without actuator and sensor dynamics. The frequency response of the model can be made quite high in order to produce responsive, limit accommodating paths. These paths can be used at the regulator inputs. Stiff regulator compensation can be designed to assure accuracy of the actual engine in the presence of plant variation and disturbances. Small and large signal responses are optimized in this process. In a more complex strategy, the model can be used iteratively to calculate on-line optimized trajectories relative to nonlinear cost functions including minimum time. Thus, advanced control strategies can be applied to the system with the model without a large impact on the control structure. Since this is a viable option in the design, SCI has chosen to maintain an accurate dynamic model in the control and use the model reference structure as the design basis.

The preliminary trajectory generation logic is shown in Figure 4.8. A nonlinear, proportional override logic is used as the compensation. The critical element in the design is that the model compensation gains are generated directly from the regulator gain schedules. This procedure uses an asymptotic assumption on the optimal response. The procedure results in a 50 percent reduction of the gain schedule storage requirement. Operation of the trajectory generator and the initial design approach is discussed below.

For small transients, reference inputs are used as direct commands to the engine model. The mode response is further compensated

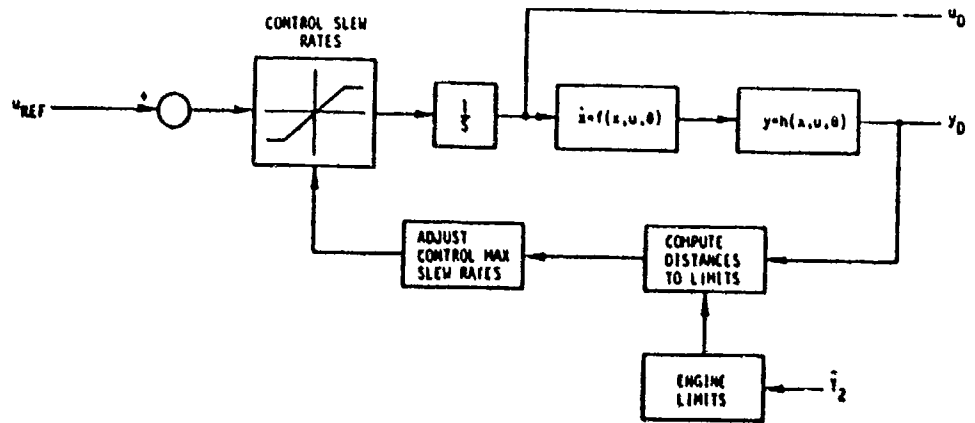


Figure 4.8a Trajectory Generator Logic - Large Transient Control Loop

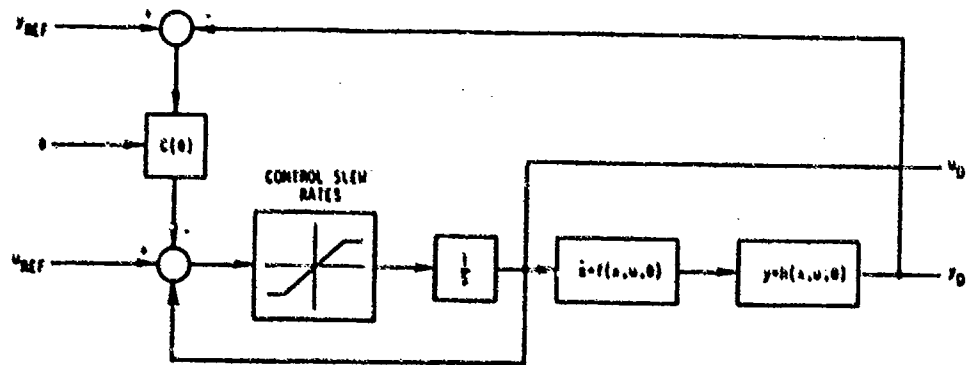


Figure 4.8b Trajectory Generator Logic - Small Transient Loop

with output gains which are proportional to the optimal regulator gains. When no limits are exceeded by the model, the response of the model is controlled by the locally linear gains. When a model output approaches a limit, the servo rate limits are proportionally reduced. This has the effect of transferring the control law from the unlimited regulator to one of several specifically designed multivariable limit loops. The rate limit is proportional to the error signal from the limiting blocks. This feedback in one or more of the control channels will tend to cause the model to move smoothly onto a limit. If the proportional error signal indicates that the system can move away from the boundary, the limit is smoothly removed. The feedback gains for the limit loops are designed using output weightings on the specific engine constraints. This yields a feedback vector for the limit loop. This vector will be simplified using sensitivity calculation and scheduled as a function of ambient conditions.

The large input performance of the system will tend to behave in a time optimal fashion. This assertion is justified from optimal solution to the minimum time problem for a linear system. Here, optimal trajectories consist of a minimum time (corresponding to a bang-bang control) trajectory to a limit, tracking the limit, and moving off the limit to the final point. The character of the trajectories generated in this method will be very similar to this type of motion without the requirement of explicit solution of non-linear optimization problems.

A second, higher risk option, will be investigated during the second phase of the program. Using the system model and auxiliary differential equations, solutions to optimal trajectories can be calculated in real time. Trajectories of this type will be generated off-line and used to tune the trajectory generation implemented above. Specific performance tradeoffs will be investigated. If warranted, further development of on-line optimization will then be incorporated into the transition logic.

It is also possible to modify the trajectory generator logic to include a variable transient response mode for increasing engine life.

Two possible strategies are proposed. Both require specification of a "transient life function" (TLF) in the form

$$TLF = \int_0^T f(T_4, \dot{T}B_4, N_{25} \dots) dt$$

Technique 1:

The current philosophy behind the trajectory generator is to produce a feedforward control which takes an engine to, and holds it on, its operating limits ( $T_4$ ,  $\dot{T}B_4$ ,  $N_{25}$ , etc.). These limit schedules are the same as those employed in the engine protection block of the controller logic. By modifying the limit schedules, the engine could be made to track a less "severe" limit. The transient response would be degraded, but the engine life would be increased. A simple example would be to require a lower  $\dot{T}B_4$  at higher values of  $T_4$  as indicated in Figure 4.9. Specification of the actual schedules requires knowledge of the TLF function.

Technique 2:

A full nonlinear, optimal life, trajectory generation procedure is possible. This is a higher risk approach than that proposed as Technique 1, but it may provide a corresponding payoff. The calculation could be performed on-line replacing the present Trajectory Generator, or it could be performed off-line and the results (trends, etc.) incorporated into the current trajectory generator. These calculations would be impossible without the TLF.

#### 4.6 MULTIVARIABLE REGULATOR LOGIC

The outputs of the trajectory generator are continuous control commands and engine variable references which predict the transition

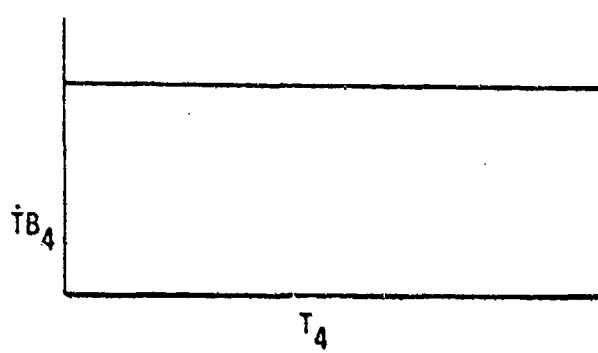


Figure 4.9a  $\dot{T}_4$  Limit Schedule

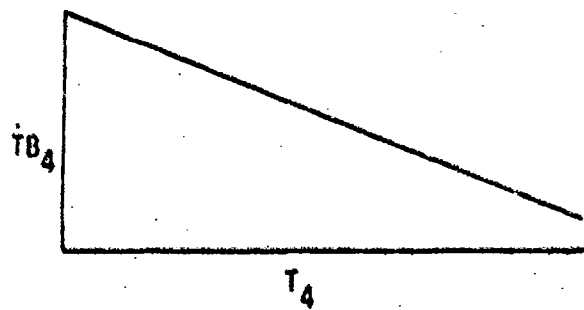


Figure 4.9b  $\dot{T}_4$  Limit Schedule for  
Increased Engine Life

of the engine from one point to another without exceeding physical or operational limits. If this prediction were exact or, alternately, if the mathematical model matched the engine exactly, there would be no reason to include the regulator. The regulator is designed to cause the engine to track small perturbations from a nominal trajectory. Further, it attempts to cause the engine to track the reference in steady state. As the model accuracy gets better, a higher bandwidth can be sustained by the regulator logic and the d.c. accuracy will be proportionally improved. The regulator model is proportional-only control with the set point accuracy and stability characteristics designed using linear optimal theory.

Two procedures will be used to calculate the optimal regulator gains. The first procedure will use a reduced order state model produced from the linearized engine model. Linear optimal control laws will be designed using output weighting. The state feedback laws will be converted to output feedback laws using the invertibility of the output distribution matrix partitioned as follows:

$$\begin{array}{ll}
 \text{Model:} & \dot{x} = Fx + Gu \\
 \text{Control Law:} & u = Cx \\
 \text{Output Partition:} & y = Hx + Du \\
 \text{Output Control Law:} & u = (I + CH^{-1}D)^{-1}CH^{-1}y
 \end{array}$$

An alternate procedure is preferred over this method. The models are reduced to include the important engine dynamics and then augmented by important sensor and actuator time constants. The output feedback matrix is then directly calculated by minimizing quadratic cost function weighting the response. This procedure is more complex than the LQG approach; however, it offers several advantages. In particular, sensitivity calculations can be used to reduce the number of feedback gains and the system can be reoptimized for the fixed structure response. Thus, a single synthesis algorithm will yield the optimized control law. The procedure offers a large flexibility in model and feedback components which is more difficult to realize in the LQG approach.

The accommodation of variation in flight conditions and the development of the gain schedule algorithm will be accomplished using several procedures. In addition to the ad hoc methods of gain fitting, several systematic approaches will be explored. An attractive approach involves using the output regulator design routine to optimize a fixed structure control law for a group of operating points. Additional operating points are incorporated into the design group until a performance degradation threshold is exceeded. Gains are then held at the optimal value within the design envelope and scheduled in regions between the envelopes. A variation in this procedure is to assume a functional relationship in the gain law which is derived from point designs. The parameters of gain relationship are then optimized to produce a point-wise optimal/nonlinear control law or schedule. The procedures will be investigated.

The gain schedule algorithm will be used by the regulator and the transition logic for gain inputs. Transition generator will use a proportional gain constant to vary the gain values to achieve the desired model response.

#### 4.7 FAULT TOLERANT FILTER

The signals entering the controller represent various types of discretized information. These signals provide many orders of redundancy concerning the actual measured quantities. The filter block functions to provide the best available estimate of required information to the control law. The fault tolerant filter must operate on all analog sensor channels except PLA and inlet commands to provide:

- (1) noise attenuation,
- (2) dynamic compensation,
- (3) error correction, and
- (4) fault insensitivity.

The filter uses the dynamic model of the engine as the primary means for providing analytical redundancy necessary.

The most important function of the filter is to provide attenuation of errors due to various sensor noise sources and compensate sensor dynamics which would otherwise compromise control performance. Accurate d.c. response must not be degraded by the filter. The form chosen will be a series of decoupled extended or nonlinear Kalman filters with reduced gain matrices. The gains may be a function of the flight condition. The filter update will be provided by the nonlinear dynamical engine model. The design goals of this block will be high frequency noise rejection and d.c. accuracy. Foldover and aliasing due to sampling high frequency noise will be addressed by the design. Analog/digital prefiltering requirements, random sampling time algorithms and adaptive noise rejection techniques will be investigated.

A sensor failure detection algorithm will be associated with the filter. The purpose of this block will be to correlate filter residuals, sensed levels and model outputs into inferences on soft and hard channel failures. Multiple failures will be detected. This block will examine all gas path variables (including TT2). In addition to the detection function, sensor failure accommodation will be provided. This will consist of manipulation of filter inputs to reduce the effects of bad sensor channels and optimize the integrity of the filter outputs. Also, logic indications will be passed to the central failure accommodation block discussed below for GO/NO-GO and secondary diagnostic processing.

#### 4.8 ENGINE LIMIT LOGIC

The outputs from the trajectory generator are measured against their limits and are used to produce nominal trajectories which track predicted engine response. Because of model inaccuracies, sensor and actuator lags and nonlinearities, build differences, etc., it is possible that actual engine limits may be exceeded

transiently or in steady state. It is currently planned that no integral control will be used to compensate these types of errors. The engine limit logic provides additional d.c. gain to the system when limits are approached or slightly exceeded. Also incorporated with this logic is a failure indication concerning the overall control operation.

The purpose of this logic is to produce control action which tends to keep the engine state under its limits. As thresholds are exceeded, this control action will have increasing authority. This initial design philosophy is sketched in Figure 4.10.

As a limit is approached, a nonlinear factor is provided to the output regulator gains specifically designed for this limit. (These gains are also used by the trajectory generator.) As the exceedance increases, larger control effort is commanded. Above a certain value, it is concluded that the control logic is unable to produce safe regulation. At this point, an integrated over-limit-flag is passed to the error accommodation logic. The failed condition represents a non-specific failure in the overall control function due to input failure, pilot error, actuator failure, engine component deterioration, engine auxiliary failure, or related causes. The control regards this as a NO-GO situation and appropriate backup sequences are initiated.

A preliminary diagram of the detailed logic is presented in Figure 4.11.

#### 4.9 FAILURE ACCOMMODATION LOGIC

Failure indications are monitored in a central location. Logic is provided to produce coordinated transfer to backup options. This logic integrates with the hardware BIT capabilities but provides a far more powerful tool in assessing the function of the overall control in running the engine. Emphasis is placed on fault detection. The important decision point is the transfer to the backup mode.

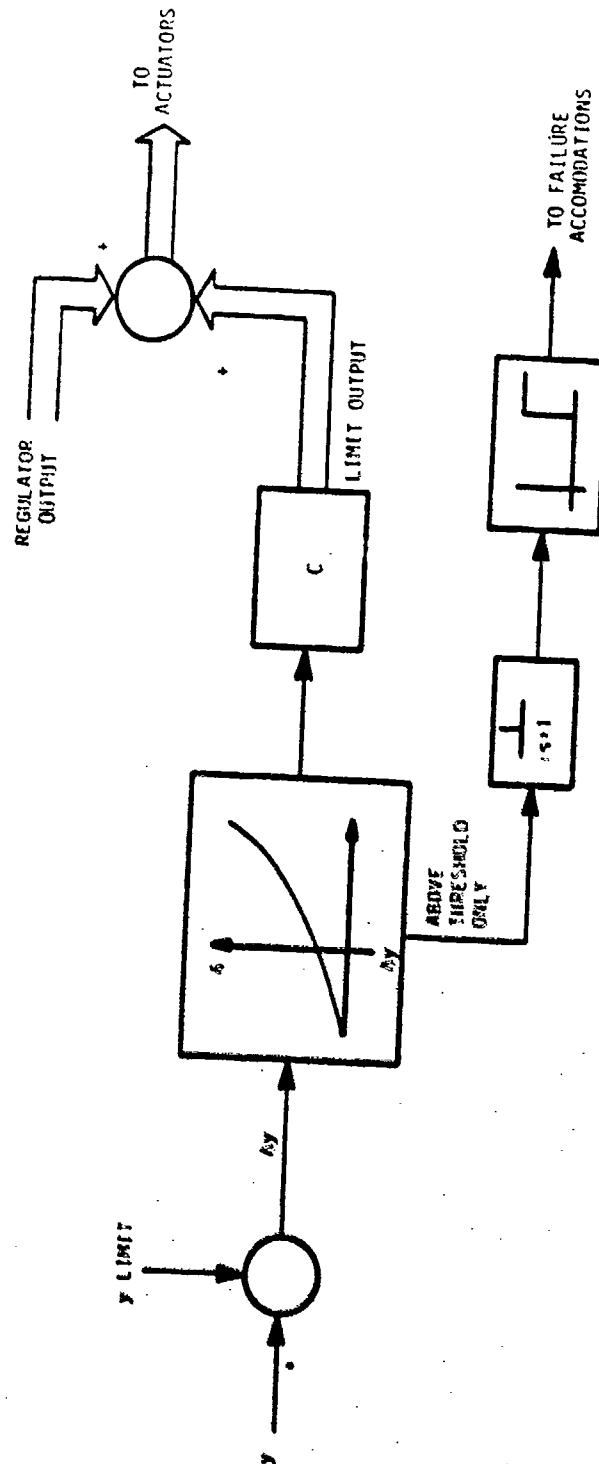
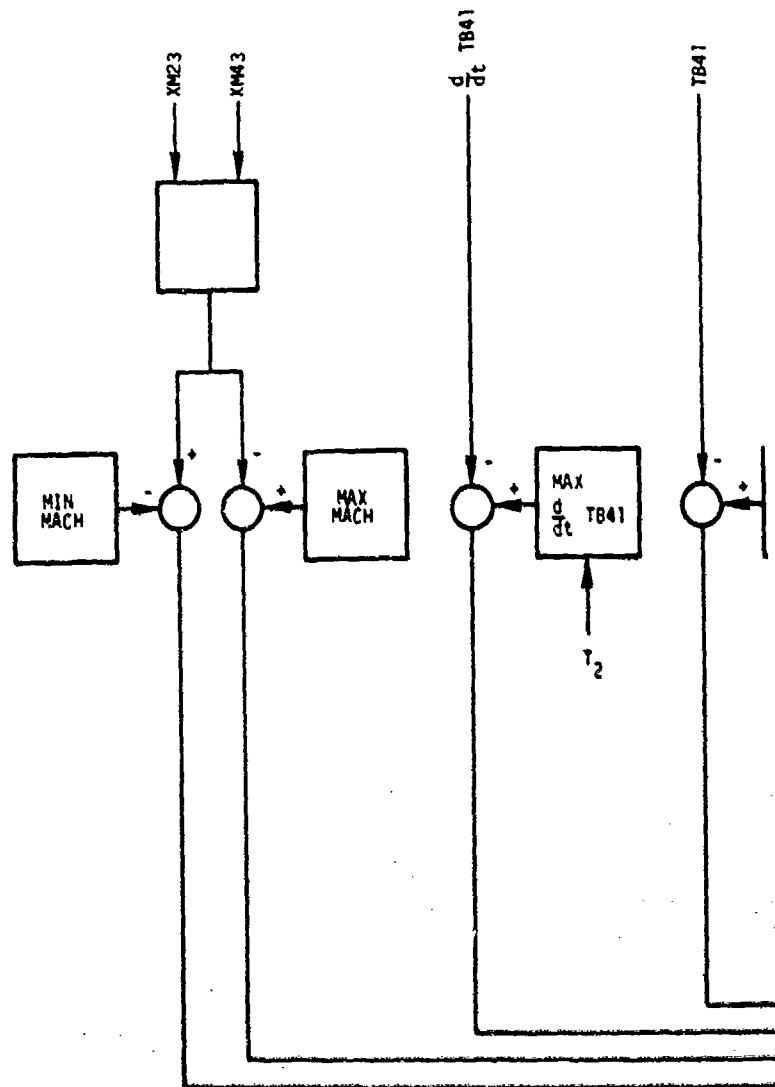


Figure 4.10 Engine Limit Logic

BYPASS DUCT AIRFLOW LIMITS



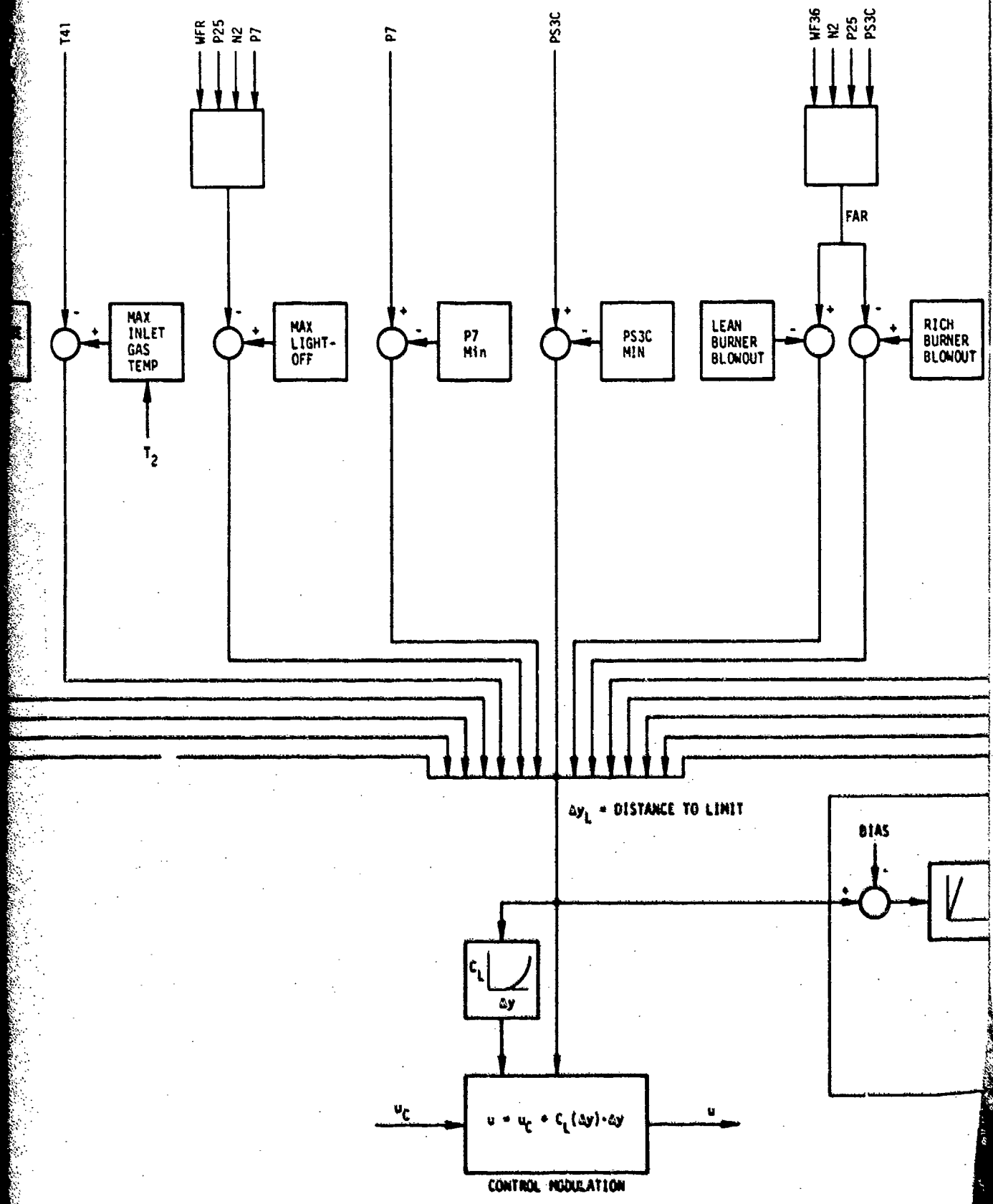
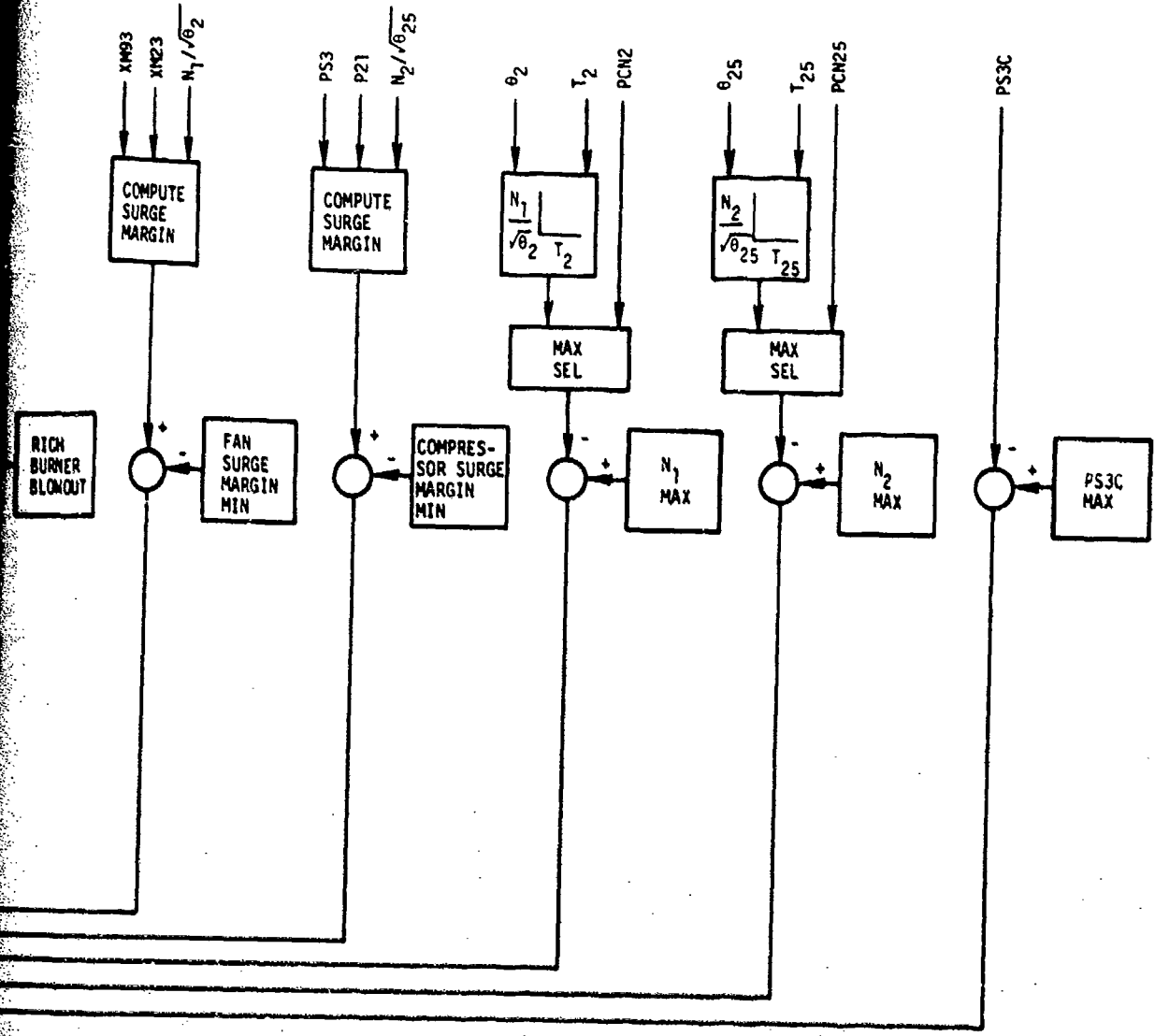
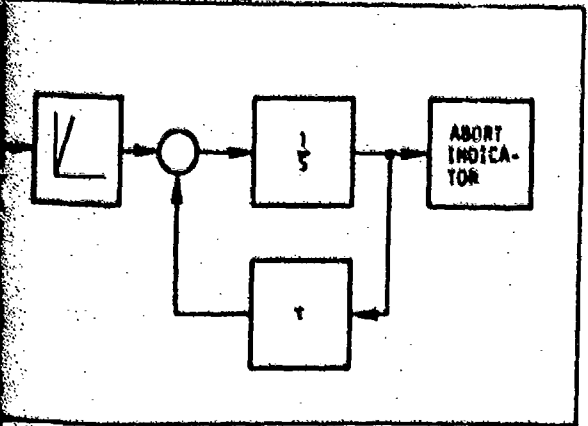


FIGURE 4.11 OVERVIEW OF ENGINE LIMIT LOGIC

FAN & COMPRESSOR LIMITS



FAILURE DETECTION



This decision is not made when a failure is detected, but rather when that failure has caused the engine to operate away from predicted nominal performance levels. In this situation, the controller has failed since it no longer can be used to satisfy its primary requirement.

Peripheral failure diagnostics are also generated for cockpit and flight line utilization. Failure accommodation is not stressed except in removing the effect of noncritical instrumentation and bringing the engine to a fail safe backup transition point after a critical failure has been detected.

Inputs are monitored by the logic. Redundant PLA channels may be monitored. Failed channel selection will be based on fail-safe operation. In addition, maximum slew rate limits will be detected. The action for PLA failures will be a NO-GO state and transition to the backup control mode.

Actuators are monitored for correct servo following. This system monitors error signal magnitudes compared to a threshold which is a function of the command level and changes in command levels. Threshold exceedance is considered as an actuator loop failure. The failure could be either the actuator or the LVPT, however. If the failure is in the LVPT, it is possible that the actuator could still be used to control the engine. Logic for accomplishing this is proposed in Figure 4.12 (detection of the failure is addressed below).

Normal operation is described in Figure 4.12a. Here the actuator is driven by an error signal (compensated) which is formed by comparing the actuator command to the LVPT output. In the event of a failed LVPT, the actuator can be driven by an estimate of the error signal as indicated in Figure 4.12b. Here the error signal estimate is provided by an internal mathematical model of the actuator in the form of a subroutine. It is further suggested that one common subroutine could be used to model all the servoloops in a computer storage efficient structure.

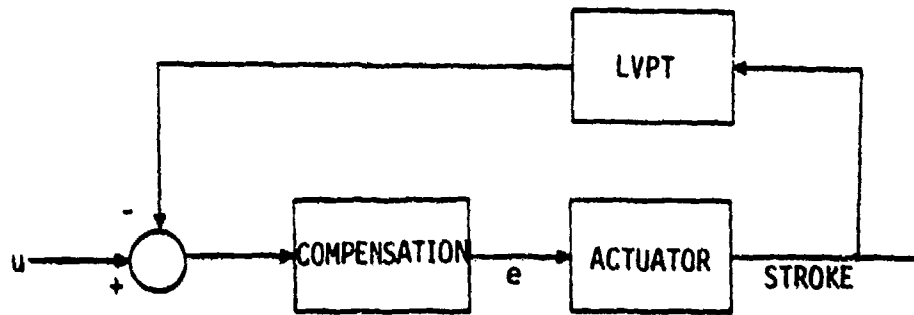


Figure 4.12a Normal Operation of Actuator Servo Loop

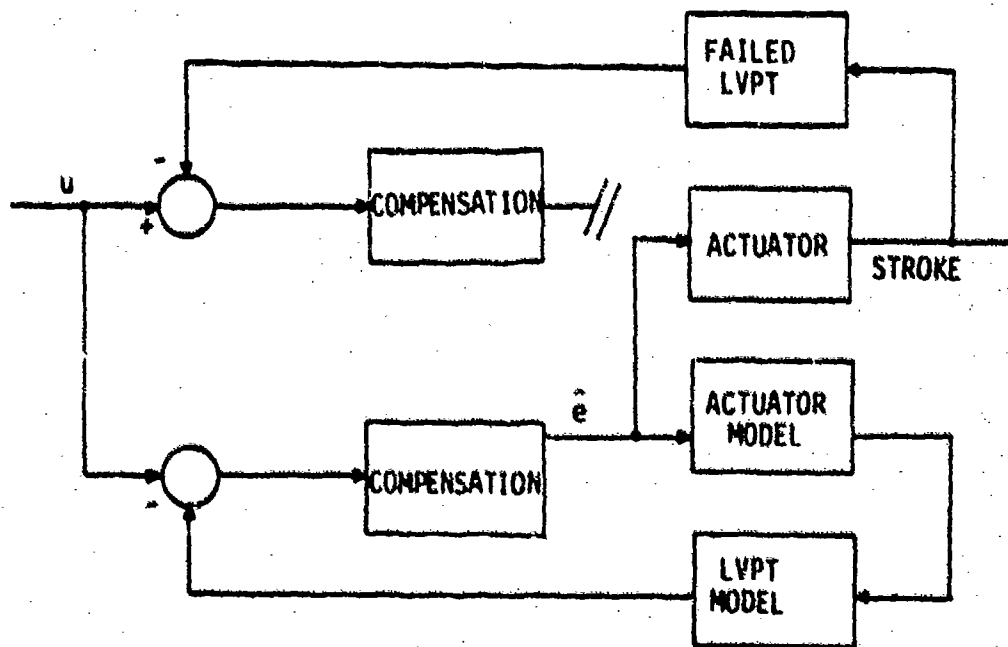


Figure 4.12b Operation of Actuator with Failed LVPT

Once the switch to this backup mode has been made, the bandwidth of the actuator "loop" will be reduced. Modeling errors combined with the loss of the feedback will result in hangoff and drift in the actuator's output. Outer loops in the regulator logic and engine protection logic will, however, act to reduce these effects.

Using this strategy, actuator effort is estimated without relying on information contained in the engine output variables (slow dynamic response) as would be the case if the actuator loop was included as part of the fault tolerant filter. Also, a switch to this backup mode will have negligible effect on any other component of the control logic.

It is anticipated that most actuators will be "non-critical." That is, the controller will be capable of running the engine within its constraints with one of these actuators failed. Consequently, reconfiguration of the control law will be unnecessary. The "disturbance" produced by a failed actuator will be compensated by action in the remaining healthy control loops - and an allowable (but degraded) engine response will be maintained. A failure in an actuator servoloop can now be accommodated by proceeding as if the feedback sensor (LVPT) was at fault, i.e. if corrective action is taken for a failed LVPT and the failure is in fact in the actuator, no accommodation incompatibility exists.

Some actuators may be "critical." That is, loss of one of these will result in the control structure being incapable of running the engine within its constraints. Consequently, a failure will require a switch to either hydromechanical backup or a reconfiguration of the control structure. Which actuators are critical is dependent on the logic that is implemented. Therefore, identification of critical actuators cannot be addressed until the control law is actually designed.

The failure diagnostic logic consists of a series of decision points to determine the ability of the control to safely operate the engine. When failure indications in a group of monitored points occur, transition to the backup mode is initiated. This procedure involves a pilot indication of control failure and simultaneous movement of the engine operating point to the nearest "fail safe region." No action is taken if the engine is operating in a safe region. The fail safe region will be defined in detail later. However, initially an operating point in the non-augmented power and away from temperature, pressure and rotor speed limits is desired. This transition is treated as an overriding mode switch to the reference point logic and normal control regulation to this point is attempted.

#### 4.10 SUMMARY

The passively adaptive control structure is defined for the VCE. Each block will be further refined. The results of the Phase I activity will be a more detailed definition of each block and a group of proposed design specifications and procedures for one or more synthesis method which will be undertaken in Phase II.

## SECTION V

### PRELIMINARY DESIGN RESULTS

This chapter is a compendium of design results generated during the Phase I study. These results serve two purposes. First, they form a base from which to build an innovative, practical controller in Phase II. Second, they both demonstrate and verify the design procedures presented in Chapters III and IV. This is important, since many of the proposed procedures have never been implemented in digital propulsion controls and represent extensions to the present levels of complexity in control law development.

Section 5.1 summarizes the results of the linear model analysis. A set of reduced order and reduced parameter models is generated. In Section 5.2, an accurate nonlinear model is developed using these reduced models. This nonlinear model is computer storage efficient and will become the base of the implemented controller. Section 5.3 discusses the design and simulation of compensation for the actuator servo valves. Finally, Section 5.4 presents preliminary simulation results of the trajectory generation logic of Section 4.1.5.

#### 5.1 LINEAR MODEL ANALYSIS

A mathematical model which characterizes accurately both static and dynamic operation of the GE23 throughout its flight envelope is highly nonlinear. However, there exist two major advantages to linearizing this model before attempting to design a controller. The first is that control logic design procedures for linear mathematical models are well developed and easy to use. The second is that, with a linear model, important dynamic interactions may be identified and analyzed using well known time domain, frequency domain and eigensystem analysis procedures; thus, physical insight may be gained which is necessary for the design of a practical controller.

There are dangers which must be avoided in the linearization process, however. First, the linear models may be inaccurate due to procedural errors. Choosing too large a linearization interval and ignoring numerical truncation are examples. Second, the set of linearization points chosen may ignore important couplings and/or dynamics which arise as a result of some nonlinearity. Consequently, an insufficient set of models may be in use. Care must therefore be exercised to validate the linear models before and during the design phase.

Described below are the results of an analysis of linear models supplied by the engine manufacturer. Section 5.1.1 describes how the linearization points were specified; Section 5.1.2 describes the form of the models; Section 5.1.3 justifies the reduction in order from eleventh to fifth; and Section 5.1.4 demonstrates the use of second-stage model reduction (see Section 3.6.2) to eliminate terms in the system dynamics matrix ( $F$  in  $\dot{x} = Fx + Gu$ ).

#### 5.1.1 Model Linearization Points

Model linearization points must be chosen to explore fully the envelope of engine operation (Section 2.9). Specifically, points must be chosen which span the inlet pressure, density and temperature ranges (e.g., altitude and Mach number) at all power levels. Sixty such points have been specified during Phase 1. They are detailed in Figures 5.1 and 5.2 and in Tables 5.1 and 5.2. The flight points are displayed against altitude and Mach number in Figure 5.1a and against inlet pressure and temperature in Figure 5.1b. The power levels examined at these flight points are pictured in Figure 5.2 and summarized in Table 5.1.

Table 5.2 presents a summary of the sixty combinations chosen. Included in this table are comments explaining why each flight point was selected.

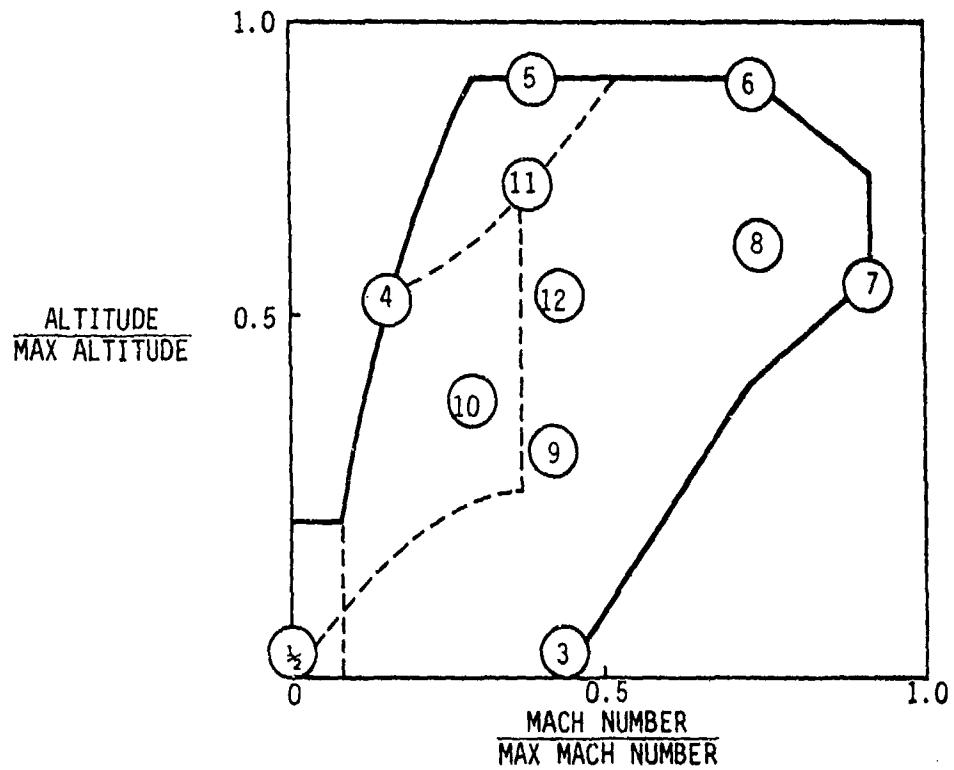


Figure 5.1a Definition of Flight Points Vs. Altitude and Mach Number

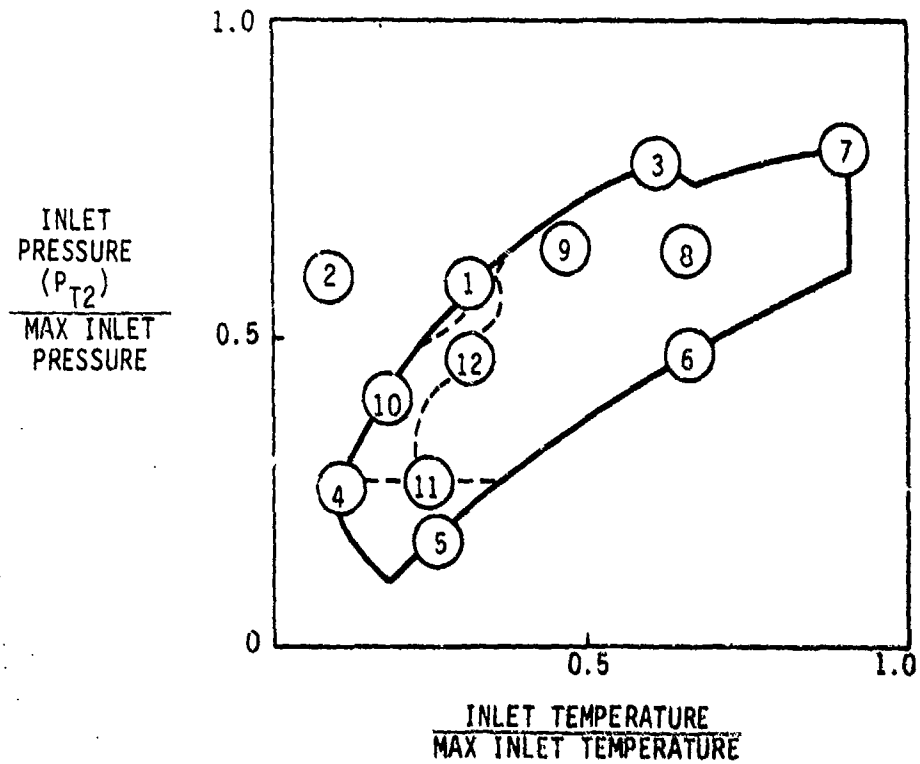


Figure 5.1b Definition of Flight Points Vs.  $P_{T2}$  and  $T_{T2}$

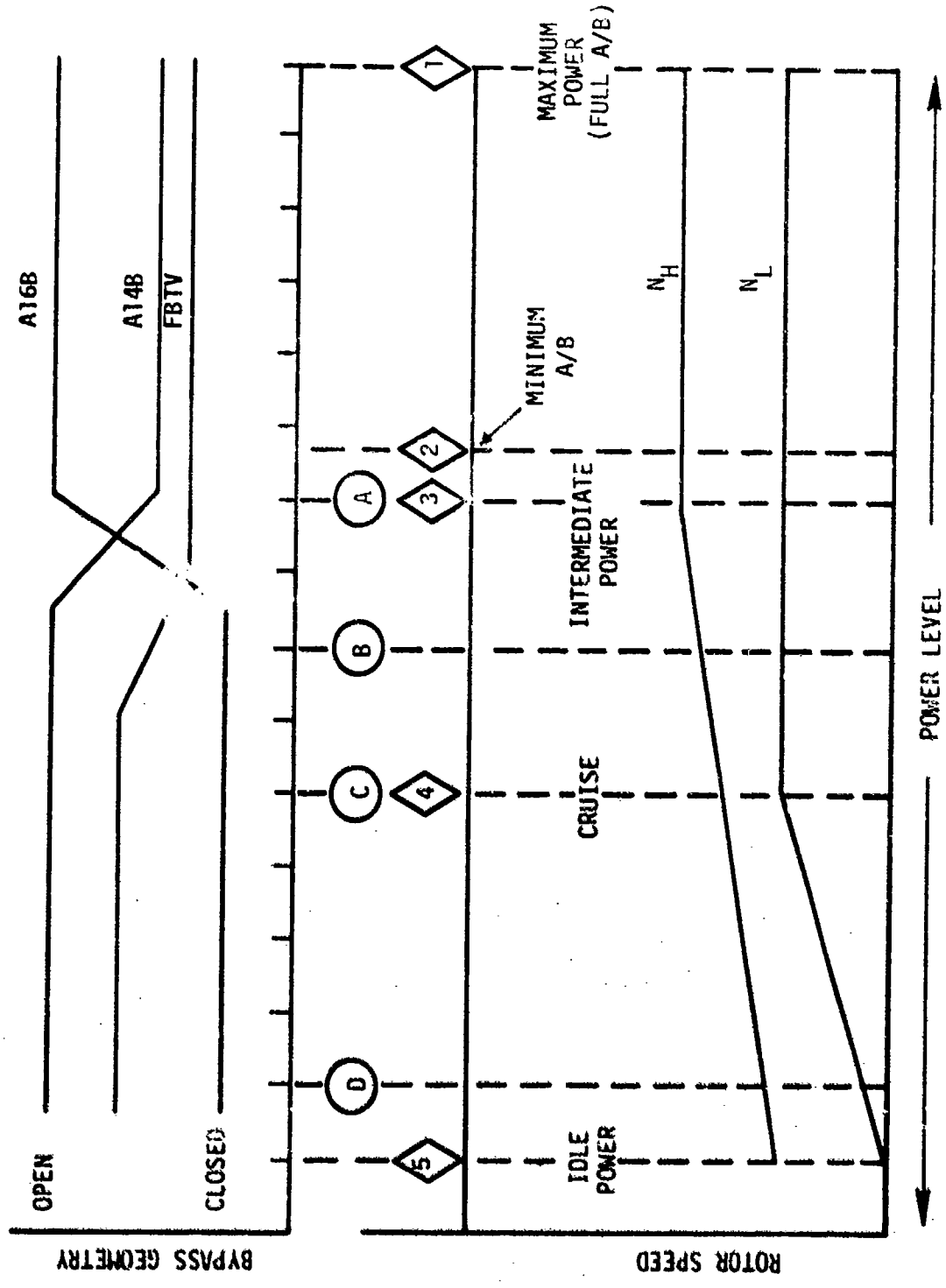


Figure 5.2 Definition of Power Points 1 through 5 and A through D

Table 5.1  
Definition of Power Points

POINT	DEFINITION
A and 3	Intermediate Power (Maximum Dry Power)
B	Bypass Transition <ul style="list-style-type: none"> <li>● A14B Open</li> <li>● A16B Closed</li> <li>● FBTV Scheduled</li> </ul>
C and 4	Power Break <ul style="list-style-type: none"> <li>● A54 Saturation Point</li> <li>● <math>N_L</math> Begins to Fall Off</li> </ul>
D	Off-Idle <ul style="list-style-type: none"> <li>● Point at 20% of Distance between Idle and C Measured in Thrust Change</li> </ul>
1	Maximum Power
2	Above Intermediate <ul style="list-style-type: none"> <li>● A16B Open</li> <li>● A14B Closed</li> <li>● FBTV Closed</li> </ul>
5	Idle

### 5.1.2 Form of the Linear Models

The linear models generated by the engine manufacturer are 11th order with 9 control inputs and 22 outputs. The state variables, controls and outputs used are listed in Tables 5.3, 5.4 and 5.5 respectively. In Figure 5.3, a schematic of the engine is presented showing the physical locations of the controls and output quantities.

Table 5.2  
Summary of Sixty Linearization Points

\*  $\eta_{RAM} = 1$

NO.	FLIGHT POINT	POWER POINT	ALT./Mn	PT2/TT2*	COMMENTS
1	1	1	0/0	14.7/518	SLS OP Line
2	1	2		↓	
3	1	3		↓	
4	1	4		↓	
5	1	5		↓	
6	2	1	0/0	14.7/395	SLS-Cold Day
7	2	2		↓	
8	2	3		↓	
9	2	4		↓	
10	2	5		↓	
11	3	1	0/1.2	35.4/668	Sea Level RAM
12	3	2		↓	
13	3	3		↓	
14	3	4		↓	
15	3	5		↓	
16	4	1	40K/0.47	3.1/407	Low T2
17	4	2		↓	
18	4	3		↓	
19	4	4		↓	
20	4	5		↓	
21	5	1	60K/1.1	2.2/485	Low P2
22	5	2		↓	
23	5	3		↓	
24	5	4		↓	
25	5	5		↓	
26	6	1	60K/2.0	7.5/702	Low Density
27	6	2		↓	
28	6	3		↓	
29	6	4		↓	
30	6	5		↓	

Table 5.2 (Concluded)

\*  $\eta_{RAM} = 1$

NO.	FLIGHT POINT	POWER POINT	ALT/Mn	PT2/TT2*	COMMENTS
31	1	B	0/0	14.7/518	Additional Operating Line Points
32	2	B	0/0	14.7/395	
33	3	B	0/1.2	35.4/668	
34	4	B	40K/0.47	3.1/407	
35	5	B	60K/1.1	2.2/485	Extreme TT2, PT2
36	6	B	60K/2.0	7.5/702	
37	7	A	40K/2.4	40/839	
38	7	B	↓	↓	
39	7	C	↓	↓	Coverage
40	7	D	43.5K/2.0	18/702	
41	8	A	↓	↓	
42	8	B	↓	↓	
43	8	C	↓	↓	Dash/Combat
44	8	D	22.5K/1.35	18/600	
45	9	A	↓	↓	
46	9	B	↓	↓	
47	9	C	↓	↓	Cruise Min SFC
48	9	D	30K/0.8	6.7/465	
49	10	A	↓	↓	
50	10	B	↓	↓	
51	10	C	↓	↓	High Cruise Low Stability Low PT2, TT2
52	10	D	53K/1.0	3.1/485	
53	11	A	↓	↓	
54	11	B	↓	↓	
55	11	C	↓	↓	Cruise/Combat Extreme
56	11	D	38K/1.28	8.0/518	
57	12	A	↓	↓	
58	12	B	↓	↓	
59	12	C	↓	↓	
60	12	D	↓	↓	

Table 5.3  
Engine State Variables

NUMBER	VARIABLE	SYMBOL
1	Front Fan Percent Corrected Speed	PCN2
2	HP Compressor Percent Corrected Speed	PCN25
3	HP Compressor Metal Temperature	TM3
4	HP Turbine Metal Temperature	TM41
5	HP Turbine Blade Temperature	TB41
6	Bypass Duct Gas Weight Per Unit Volume	RH15B
7	Bypass Duct Gas Entropy Per Unit Volume	SRH15B
8	Main Combustor Gas Weight Per Unit Volume	RH31
9	Main Combustor Gas Entropy Per Unit Volume	SRH31
10	Tailpipe Gas Weight Per Unit Volume	RH6
11	Tailpipe Gas Entropy Per Unit Volume	SRH6

Table 5.4  
Engine Inputs

NO.	VARIABLE	SYMBOL
1	Second Fan IGV Stator Angle	STP22
2	Exhaust Nozzle Throat Physical Area	A8
3	Main Combustor Effective Fuel Flow*	WF36
4	LP Turbine Nozzle Position	STP49
5	Inner Duct Mixer Exit Physical Area	A14B
6	Bypass Duct Mixer Effective Area	AE16
7	Augmentor Effective Fuel Flow	DWF6
8	High Compressor Stator Angle	STP25
9	Forward Blocker Door	AE94

Table 5.5  
Engine Output Variables

NUMBER	VARIABLE	SYMBOL
1	Front Fan Percent Corrected Speed	PCN2
2	HP Compressor Percent Corrected Speed	PCN25
3	Front Fan Exit Mach Number	XM93
4	Second Fan Exit Mach Number	XM23A
5	Front Fan Exit Total Pressure	P21
6	HP Compressor Inlet Total Pressure	P25
7	HP Compressor Discharge Static Pressure	PS3C
8	Front Fan Discharge Tip Total Temperature	T93
9	HP Compressor Inlet Total Temperature	T25
10	HP Compressor Discharge Total Temperature	T3
11	HP Turbine Rotor Inlet Total Temperature	T41
12	HP Turbine Blade Temperature	TB41
13	HP Turbine Discharge Total Temperature	T48
14	LP Turbine Discharge Total Temperature	T5
15	Exhaust Nozzle Inlet Total Pressure	P7
16	Front Fan Stall Margin at Constant Flow	SM2
17	Second Fan Stall Margin at Constant Flow	SM22
18	HP Compressor Stall Margin at Constant Flow	SM25
19	Front Fan Inlet Air Flow	WA2
20	Bypass Duct Total Air Flow	W15B
21	Net Thrust	FN
22	Uninstalled Specific Fuel Consumption	SFC

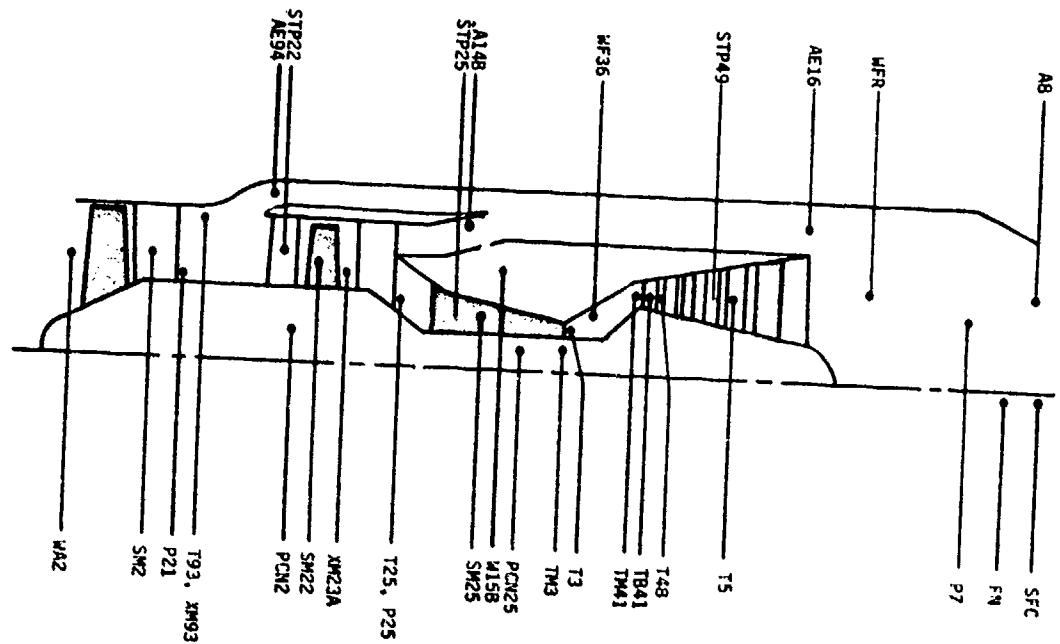


Figure 5.3 Variable Cycle Engine - Controls and Outputs

### 5.1.3 Model Reduction

As described in Section 5.1.2, the linear models generated by the engine manufacturer are 11th order. Using linear analysis techniques, it is possible to identify those modes of these models that are within (or near) the desired bandwidth of a closed loop controller. It is then possible to generate reduced order models which include only the dynamical interactions relevant to control law development. By eliminating "unimportant" dynamics, this procedure can: (1) yield models that are in their simplest form (important for gaining physical insight), and (2) reduce the computational complexity required in control law calculations.

One point must be remembered, however. Any control law developed using these reduced order models must be verified when applied to the full order model. It is possible the controls will affect the higher modes - perhaps leading to an instability. A check with the full nonlinear model (e.g., hybrid simulation) is

also required to assure that no adverse effects arise due to unmodeled nonlinearities.

#### 5.1.3.1 Eigensystem Analysis

The objectives of an eigensystem analysis are: (1) to identify the modes of the linear model that are within the bandwidth of the desired closed loop system (0 to  $20 \text{ sec}^{-1}$ ), and (2) to identify the state variables which dominate those modes. This information forms the basis for the model reduction procedure employed in Section 5.1.3.3.

Eigenvalues for the eleventh order full power, sea-level-static linear model are presented in Table 5.6. (These eigenvalues have been normalized by the time constant of the collective response mode of the spools). A clear frequency separation is apparent. Only five of the eleven modes are in the frequency range of interest of the controller. These modes are isolated in Table 5.7.

The rotor response is dominated by a second order system with two real roots. Examination of the eigenvectors (Figure 5.4) shows that the faster response can be associated with the rotor speeds differentially rematching, i.e., the fan spool decelerating while the compressor accelerates. The slower root involves the collective or rigid body response of the two shafts. The differential and collective response is characteristic in the motion of two heavily damped and heavily coupled inertia elements. (The two spools are aerodynamically coupled in the turbines.) The characteristic motion is present in all regions of the operating envelope. The three temperature response modes shown in Table 5.7 are essentially first order lags resulting from the thermal capacitance and resistance of the engine components.

Eigenvalue locations are functions of flight condition. However, the frequency separation demonstrated above is maintained throughout the flight envelope. Figures 5.4 through 5.7 demonstrate this. Figure 5.4 is a display of the collective and differential response modes of the spools for the first six flight conditions. Figure 5.5 displays the same information for the three temperature roots associated with TM3, TM41 and TB41. Figures 5.6 and 5.7 display the eigenvalues associated with the remaining six gas dynamic modes. These are clearly much faster.

Note that all the eigenvalues have been normalized by the collective response mode time constant at sea-level-static, full-power.

The state variables which dominate each mode can be found by an examination of its associated eigenvectors. In order to reduce the system order, an equal number of states and modes must be chosen. Furthermore, the states chosen must be able to describe the retained modes if the model reduction procedure of Section 3.6.1 is to be possible.

Table 5.6  
Eigenvalues of VCE at SLS - Maximum Power

NUMBER	VALUE *	DESCRIPTION
1	-0.13	Compressor Metal Temperature Response
2	-0.39	Turbine Metal Temperature Response
3	-0.47	Turbine Blade Temperature Response
4	-1.00	Collective Response Mode of Spools
5	-3.24	Differential Response Mode of Spools
6,7	-22.7±;2.83	Gas Dynamics ↓
8,9	-60.75±19.30	
10	-65.35	
11	-131.22	

\*Normalized by Collective Response Mode Eigenvalue

Table 5.7  
Principal Dynamic Modes of VCE at SLS - Maximum Power

MODE	TIME CONSTANT*	DESCRIPTION
1	0.271	Differential Response Mode of the Spools
2	1.000	Collective Response Mode of the Spools
3	6.368	Compressor Metal Temperature Response
4	2.206	Turbine Metal Temperature Response
5	1.975	Turbine Blade Temperature Response

\*Normalized by collective response mode time constant.

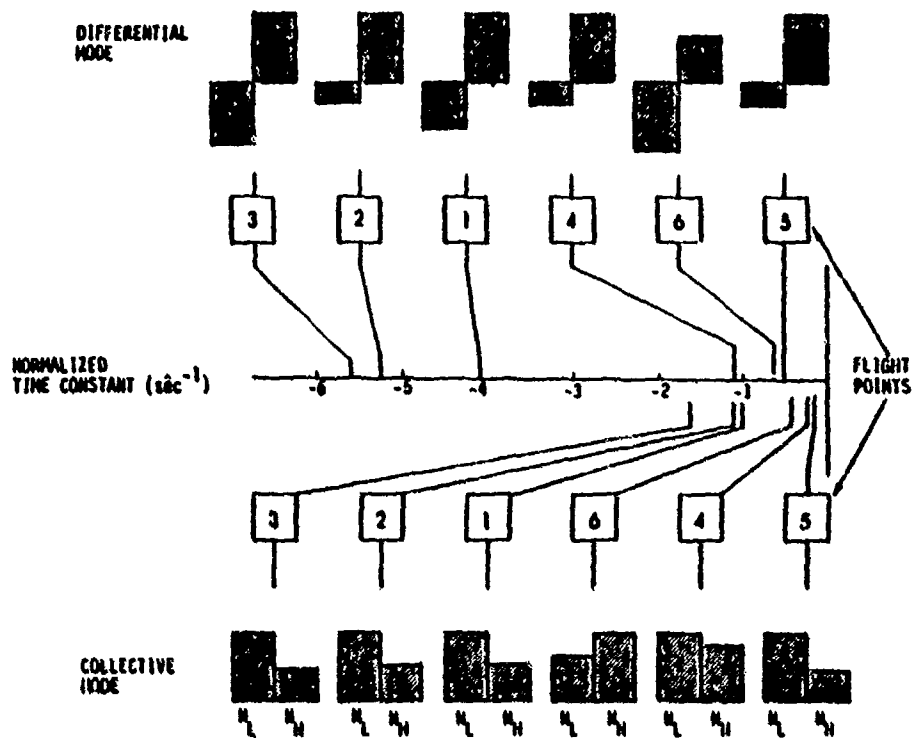


Figure 5.4 Differential and Collective Spool Response Time Constants at Flight Points 1 Through 6

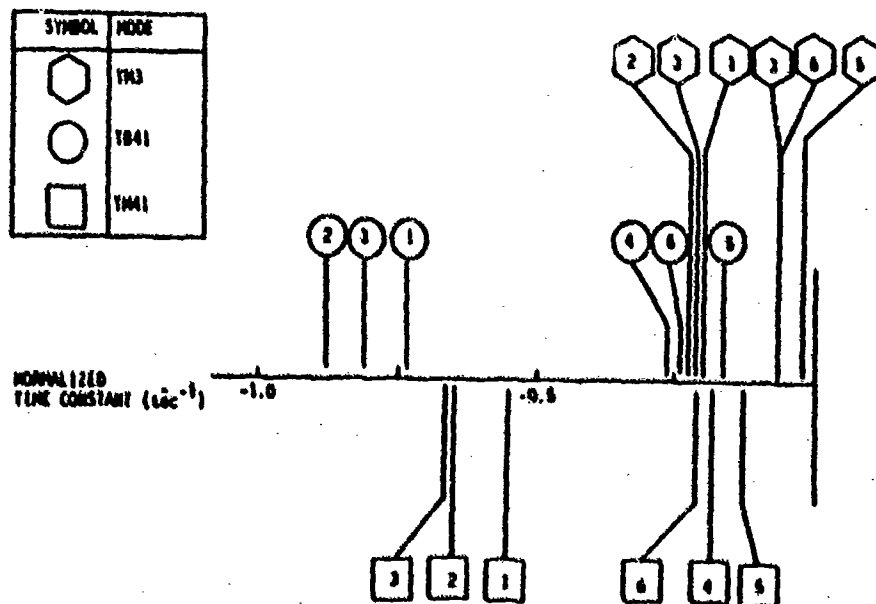


Figure 5.5 Temperature Response Time Constants at Flight Points 1 Through 6

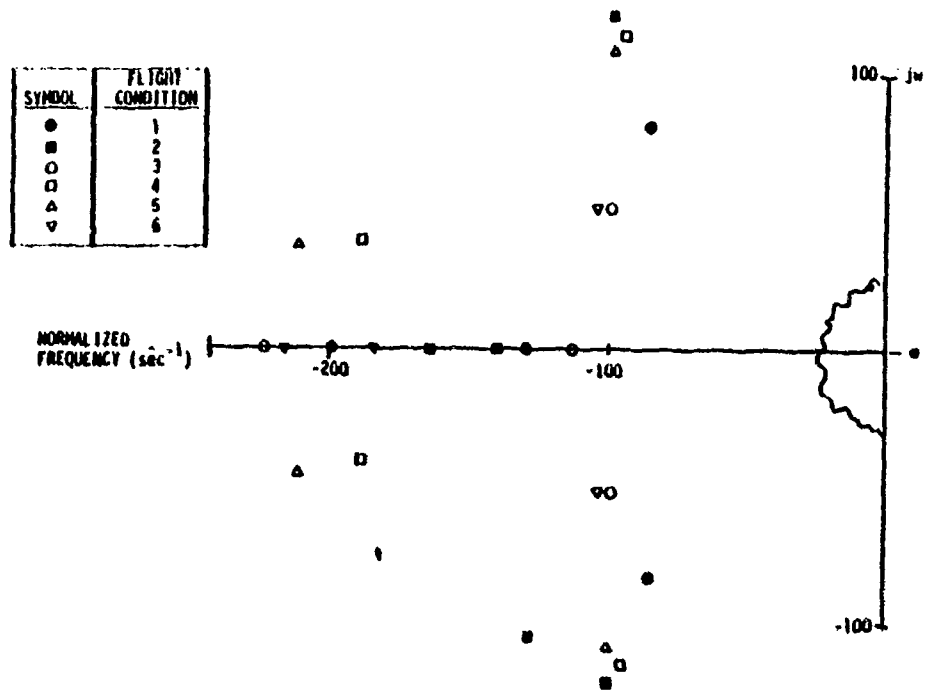


Figure 5.6 Eigenvalues Corresponding to Engine Gas Dynamics at Each of Six Flight Conditions

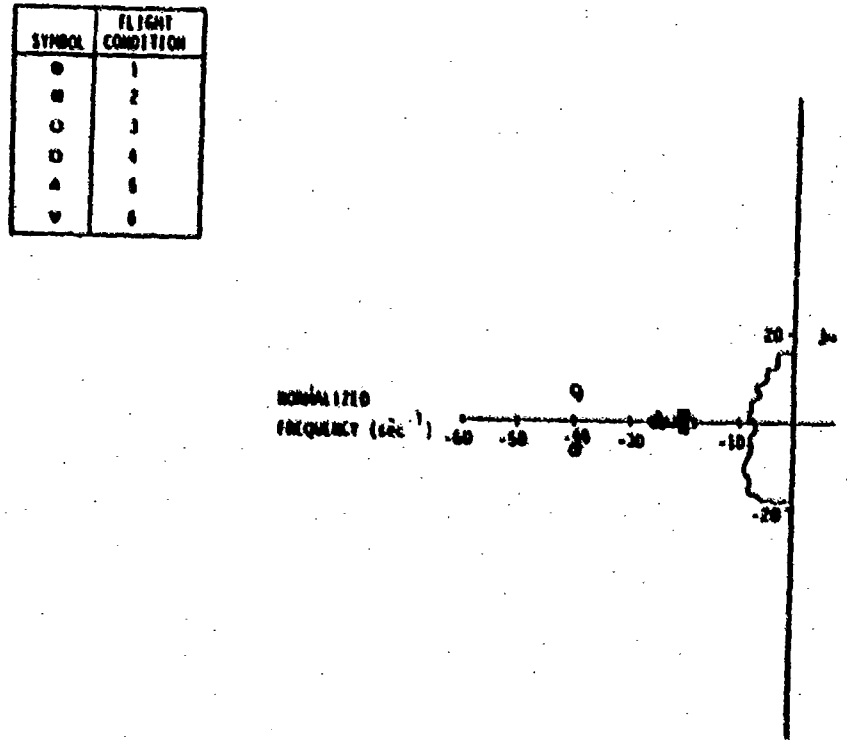
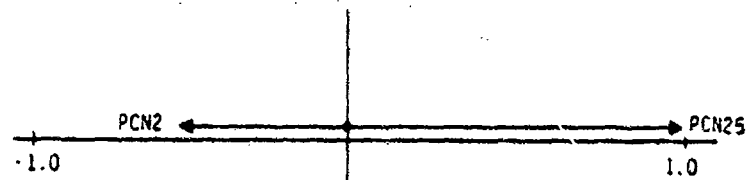
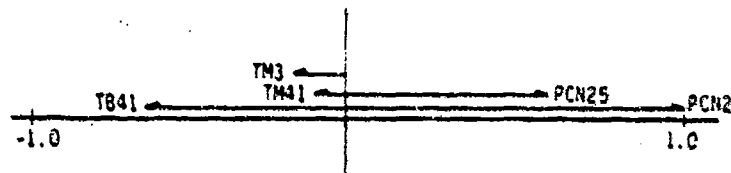


Figure 5.7 Eigenvalues (Gas Dynamics) Vs. Flight Conditions

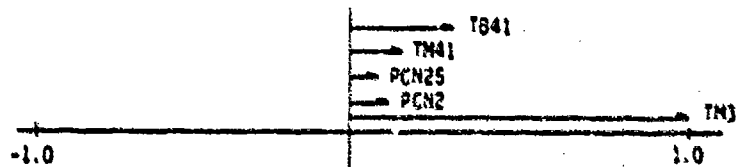
Results are presented in Figure 5.8 and Table 5.8. The figures picture the eigenvectors, and the table lists the states chosen.



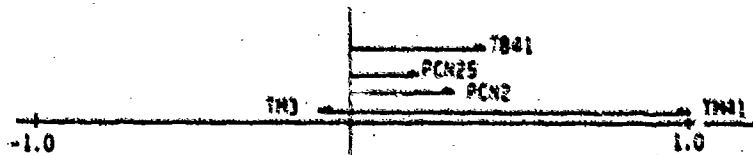
(a) Eigenvector of Mode 1 (Differential Spool Response)



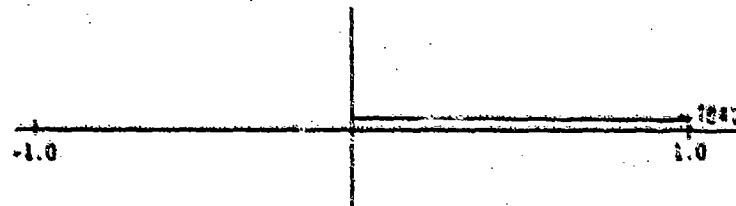
(b) Eigenvector of Mode 2 (Collection Spool Response)



(c) Eigenvector of Mode 3 (Compressor Metal Temperature)



(d) Eigenvector of Mode 4 (Turbine Metal Temperature)



(e) Eigenvector of Mode 5 (Turbine Blade Temperature)

Figure 5.8 Eigenvector Composition of the Five Principal Modes at SLS/Maximum Power (Table 5.7)

Table 5.8  
State Variables for Reduced Order System

NUMBER	VARIABLE	SYMBOL
1	Front Fan Percent Corrected Speed	PCN2
2	HP Compressor Percent Corrected Speed	PCN25
3	HP Compressor Metal Temperature	TM3
4	HP Turbine Metal Temperature	TM41
5	HP Turbine Blade Temperature	TB41

### 5.1.3.2 Transfer Function Analysis

The eigensystem analysis above is most useful in determining the system modes which might be important in the controller design. It is entirely possible, however, that some of these modes may be ignored. That is, they may not contribute significantly to the output quantities which are to be controlled. This subject is most easily addressed using transfer function analysis techniques.

Transfer function techniques examine the structure of the input-output relations. They rely on an investigation of the system zeroes, residues and dc gains.

The transfer function from an input,  $u(s)$ , to an output,  $y(s)$ , may be written as

$$\frac{y(s)}{u(s)} = \frac{(s+z_1)(s+z_2) \dots}{(s+p_1)(s+p_2) \dots}$$

or, equivalently, as

$$\frac{y(s)}{u(s)} = K_{DF} + K_1 \frac{p_1}{s+p_1} + K_2 \frac{p_2}{s+p_2} + \dots + K_N \frac{p_N}{s+p_N}$$

Here,  $K_{DF}$  is the direct feedthrough component, and the  $K_i$  define the various modal components of the dc response ( $K_i p_i$  is the

residue at the  $i^{\text{th}}$  pole). An examination of the relative magnitudes of these  $K_{DF}$  and  $K_i$  will determine those modes which must be retained for an accurate description of the engine's output response.

Figure 5.9 summarizes an analysis of transfer functions at flight conditions one through six. Shown are  $K_{DF}$  and the  $K_i$  for  $\frac{PCN2}{A8}$ ,  $\frac{PCN2}{WF}$ ,  $\frac{FN}{A8}$  and  $\frac{FN}{WF}$ . The modes indicated were summarized in Table 5.7. In the figure  $\lambda_d$  refers to the differential response mode of the spools;  $\lambda_c$  refers to the collective response mode;  $\lambda_3$  refers to the compressor metal temperature mode; and  $\lambda_{41}$  refers to the turbine metal temperature mode.

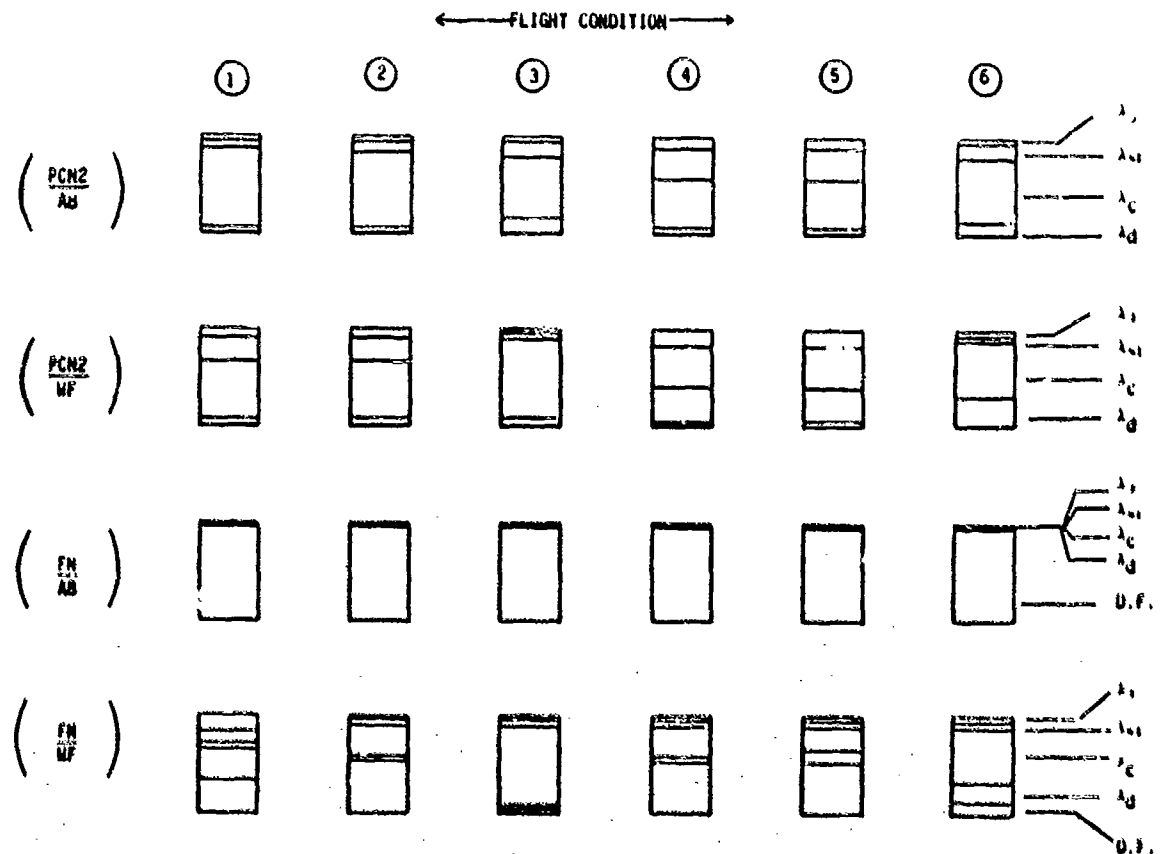


Figure 5.9 Residue Spectra of Selected Transfer Functions

The results shown in Figure 5.9 are characteristic. Several of the transfer functions are dominantly low order, but every mode is important. For example,  $\frac{FN}{A8}$  is zeroth order (direct feedthrough dominates) at all flight points; and  $\frac{PCN2}{A8}$  is first order at flight conditions 1 and 2, but second order at flight condition 4. The modal composition of each transfer function is different; however, every mode contributes significantly to at least one transfer function.

The turbine blade temperature mode is excited by the controls, but is observable in TB41 only. The reason this mode must be retained is that turbine blade temperature is important to engine protection constraints.

The conclusion which must be drawn is that none of the five modes of Table 5.7 can be ignored in an accurate description of the engine.

#### 5.1.3.3 Modal Reduction

Based on the above analysis, a fifth order model of the engine which incorporates the five modes listed in Table 5.7 and the five states listed in Table 5.8 will characterize the engine's dynamic behavior sufficiently well for control purposes. The procedure for generating this reduced order model is highly automatic. It was explained in Section 3.6.1.

During Phase I of this program 28 linear models were generated by the engine manufacturer and processed at SCI (Vt).

#### 5.1.4 Second Stage Reduction

As explained in Section 3.6.2, not all of the elements in the system dynamics matrix, F, are important. Specifically, the sensitivity of the dynamic response (initial conditions) to a particular

element may be small. If so, that element could be fixed at zero with little effect. Furthermore, the remaining elements can be adjusted to minimize any error that does occur. A procedure for performing these calculations is presented in Appendix B.

Before elements in the F matrix can be eliminated, however, it is first required to determine the response sensitivities. This can be done as follows. Let the integral square response be defined as

$$J_0 = \frac{1}{2} \int_0^{\infty} x^T A_x x dt.$$

where

$$\dot{x} = Fx$$

and

$$x(0) = x_0$$

with

$$E \begin{bmatrix} x_0 & x_0^T \end{bmatrix} = X \quad (X = I \text{ for random initial conditions})$$

The object is then to find  $\frac{\partial J_0}{\partial F}$ .

This is easily accomplished. Consider the following substitutions:

$$G_{eq} = I$$

$$H_{eq} = I$$

$$C_{eq} = \Delta F.$$

Then finding  $\frac{\partial J_o}{\partial C_{eq}}$  for the system

$$\dot{x} = Fx + G_{eq} u_{eq}$$

$$y_{eq} = H_{eq} x$$

$$u_{eq} = C_{eq} y_{eq}$$

is the same as finding

$$\frac{\partial J_o}{\partial \Delta F} = \left. \frac{\partial J_o}{\partial F} \right|_{\Delta F=0}$$

in the system

$$\dot{x} = Fx + \Delta Fx$$

$$\dot{x} = (F+\Delta F)x.$$

In other words, the output regulator algorithm discussed in Section 3.5.3 may be used.

The values of  $\frac{dJ_o}{dF}$  have been calculated throughout the flight envelope, and the results are presented in Figure 5.10. The figure is arranged in a matrix format so that the diagram in the (1,1)

block of the figure corresponds to  $\frac{\partial J_o}{\partial F_{11}}$ , etc. Those elements which may be eliminated are indicated by shading in the figure.

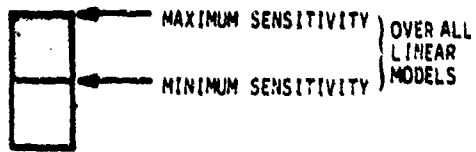
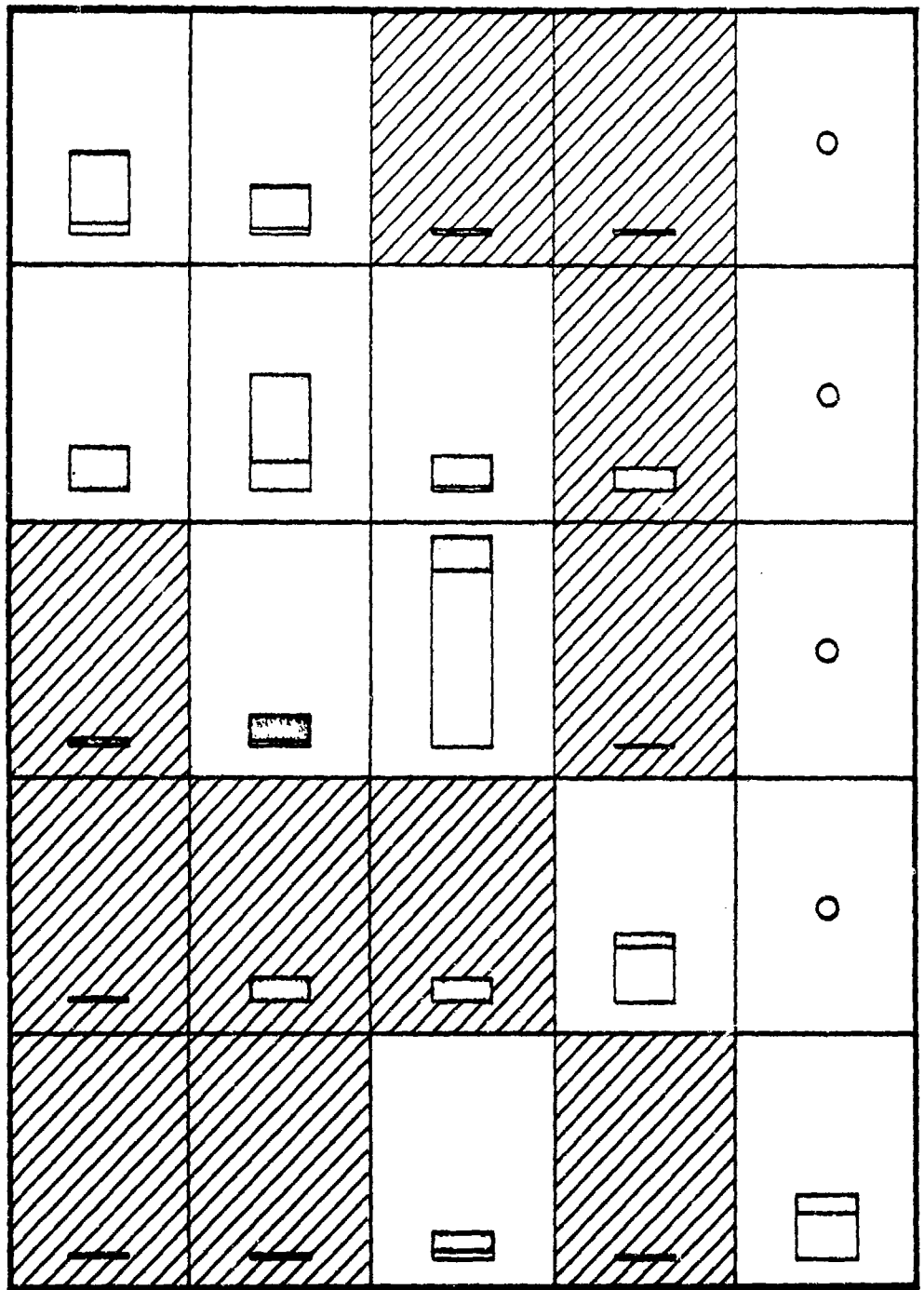


Figure 5.10 Sensitivity of Mean-Square Response to Elements in F-Matrix

Example:

Here the second stage reduction procedure is applied to a fifth order linear model of the GE23-JTDE. The model chosen has the following F matrix:

$$F = \begin{bmatrix} -5.6600E+00 & 4.6230E+00 & 1.1860E-01 & 2.3240E-01 & 0. \\ 2.6860E+00 & -8.8090E+00 & 1.8910E-01 & 4.2300E-01 & 0. \\ 6.8520E-02 & 2.6050E-01 & -4.6350E-01 & 9.0940E-03 & 0. \\ 6.4180E-03 & -1.0110E+00 & 1.0520E-01 & -1.2150E+00 & 0. \\ 1.6360E-01 & -1.6780E-01 & 3.2950E-01 & 9.7680E-02 & -1.6220E+00 \end{bmatrix}$$

It is desired to eliminate as many  $F_{ij}$  elements as possible, yet still retain an acceptable fit to the original response. Step 1 of the procedure is to identify the sensitivity of the system response,  $J_0$ , to each element in the F matrix. For

$$J_0 = \frac{1}{2} \int_0^{\infty} x^T x dt$$

and  $x_0 = I$  (random initial conditions)

the result is

$$\frac{dJ_0}{dF_{ij}} \frac{F_{ij}}{J_0} = \begin{bmatrix} 1.1 \times 10^{-1} & -5.3 \times 10^{-2} & -6.5 \times 10^{-3} & -6.5 \times 10^{-4} & 0 \\ -3.7 \times 10^{-2} & 9.7 \times 10^{-2} & -1.1 \times 10^{-2} & 4.2 \times 10^{-3} & 0 \\ -5.5 \times 10^{-3} & -1.5 \times 10^{-2} & 6.0 \times 10^{-1} & -7.1 \times 10^{-4} & 0 \\ -5.2 \times 10^{-5} & 5.8 \times 10^{-3} & -7.81 \times 10^{-3} & 2.0 \times 10^{-1} & 0 \\ -1.4 \times 10^{-3} & 9.1 \times 10^{-4} & -3.68 \times 10^{-2} & -1.4 \times 10^{-3} & 1.9 \times 10^{-1} \end{bmatrix}$$

Clearly, the diagonal elements must not be eliminated. For example, setting  $F_{33} = 0$  would cause a 60% change in  $J_0$ . However,  $F_{34}$  should be eliminated since this would produce only a 0.07% change in  $J_0$ . Using this logic, the elements chosen for elimination are

$$F_{13}, F_{14}, F_{24}, F_{31}, F_{34}, F_{41}, F_{42}, F_{43}, F_{51}, F_{52}, F_{54} .$$

This leaves ten non-zero elements which must be optimized.

The results of this optimization are

$$\hat{F} = \begin{bmatrix} -5.7207 & 4.7626 & 0 & 0 & 0 \\ 2.7746 & -9.1784 & 0.3494 & 0 & 0 \\ 0 & 0.3294 & -0.4651 & 0 & 0 \\ 0 & 0 & 0 & -1.2885 & 0 \\ 0 & 0 & 0.3357 & 0 & -1.6212 \end{bmatrix}$$

Note that the original  $J_0$  was

$$J_0 = 1.03$$

Setting the indicated elements to zero and performing no optimization yielded only a 1.0% change in  $J_0$ . Performing the optimization reduced this already small error to 0.9%. This confirms the "unimportance" of those terms which were eliminated and thus provides a much simplified  $\bar{F}$  matrix for use in the controller.

The eigenvalues of the original and reduced systems are presented for comparison in Table 5.9.

Table 5.9  
Comparison of Eigenvalues\* between F and  $\hat{F}$

ORIGINAL EIGENVALUES (F)	REDUCED EIGENVALUES ( $\hat{F}$ )
-0.49	-0.49
-3.38	-3.50
-1.00	-1.05
-0.41	-0.39
-0.14	-0.14

\*Eigenvalues normalized by collective response mode eigenvalue.

## 5.2 NONLINEAR MODEL GENERATION

The reduced parameter models developed from the nonlinear simulation have been described. The procedure for developing a nonlinear model of the engine from these matrices was described in Section 3.7. Twenty-eight linear matrices have been used to generate a low order nonlinear model of the VCE valid throughout the operating envelope. These preliminary results are presented below and a comparison of the linear and nonlinear response is shown.

### 5.2.1 Regression for Dynamic Parameters

The model generation procedure is shown in Figure 5.11.

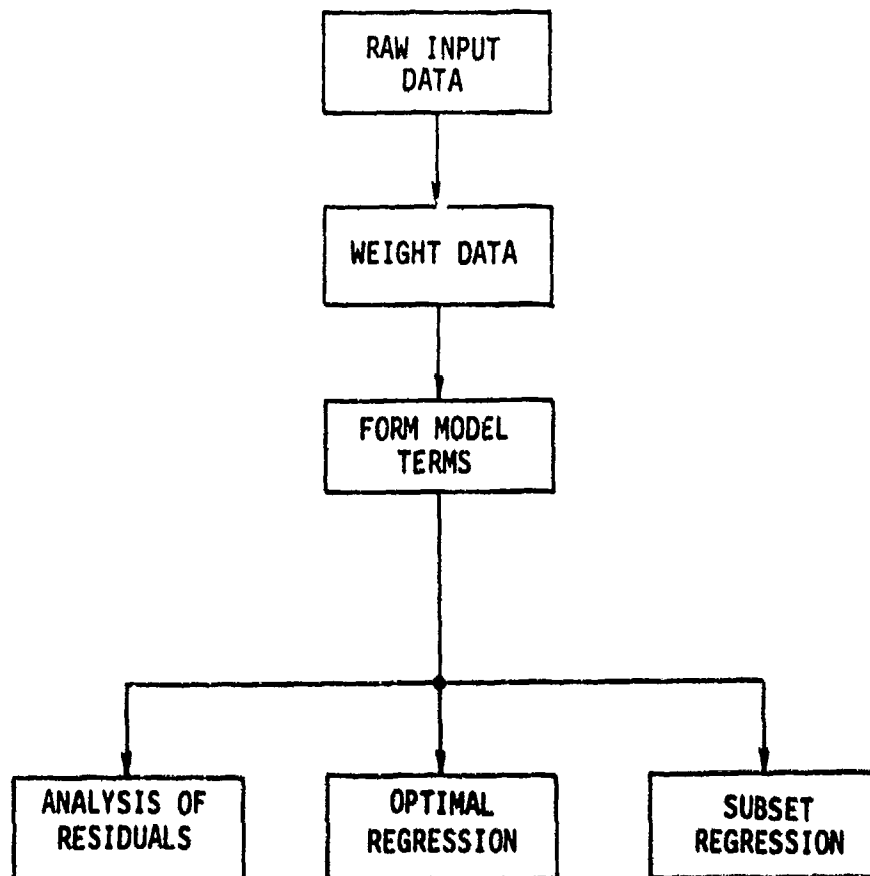


Figure 5.11 Nonlinear Model Generation Procedure

The reduced parameter models discussed in Section 5.1 represented fifth order engine dynamics and were parameterized with 10 nonzero elements. Curves were derived for each dynamic element using subset selection methods. Independent variables were chosen as transgenerated groupings of engine running variables. A typical set of operating variables was initially established by using the stepwise regression procedure on a large set of candidate terms (e.g., 80-100). The variables selected during this procedure are then used as the generators for a regression using the optimal subset selection method. This approach limits the number of 25 regressed terms because the computational overhead increases exponentially with the number of terms.

The models derived for the elements of the dynamics matrix form the basis for the nonlinear model. Table 5.10 shows the preliminary model selected to represent engine dynamics throughout the operating envelope. Thirty-three (33) terms are sufficient to match the linearized dynamics at all flight points. The model's

Table 5.10  
Preliminary Nonlinear Model Structure

MATRIX ELEMENT	MODEL FORM	RMS ERROR*
F11	$a_1 P_{s3c} + a_2 P_2^2 + a_3$	1.0
F33	$b_1 P_{s3c} + b_2 N_2 T_2 + b_3$	0.3
F12	$c_1 P_2 + c_2 T_2 + c_3 N_2 P_2 + c_4$	1.7
F21	$d_1 P_2 + d_2 P_{21} + d_3 P_{s3c} + d_4$	1.5
F22	$e_1 F_{11} + e_2 P_2^2 + e_3 N_2 P_2 + e_4$	1.2
F23	$f_1 P_2 + f_2 P_{21} + f_3 F_{33} + f_4$	1.5
F32	$g_1 P_2 + g_2 P_{21} + g_3 P_{s3c} + g_4$	1.2
F44	$h_1 F_{33} + h_2$	0.3
F53	$k_1 P_{s3c} + k_2 F_{33} + k_3$	0.4
F55	$\lambda_1 F_{33} + \lambda_2$	0.1

\* Percentage of mean

accuracy is summarized in Figure 5.12, which shows a comparison of the actual engine time constants and those calculated from the curve fit model of the dynamics matrix. This procedure represents a significant simplification over other linear modeling methods and allows a tractable simulation of nonlinear dynamics.

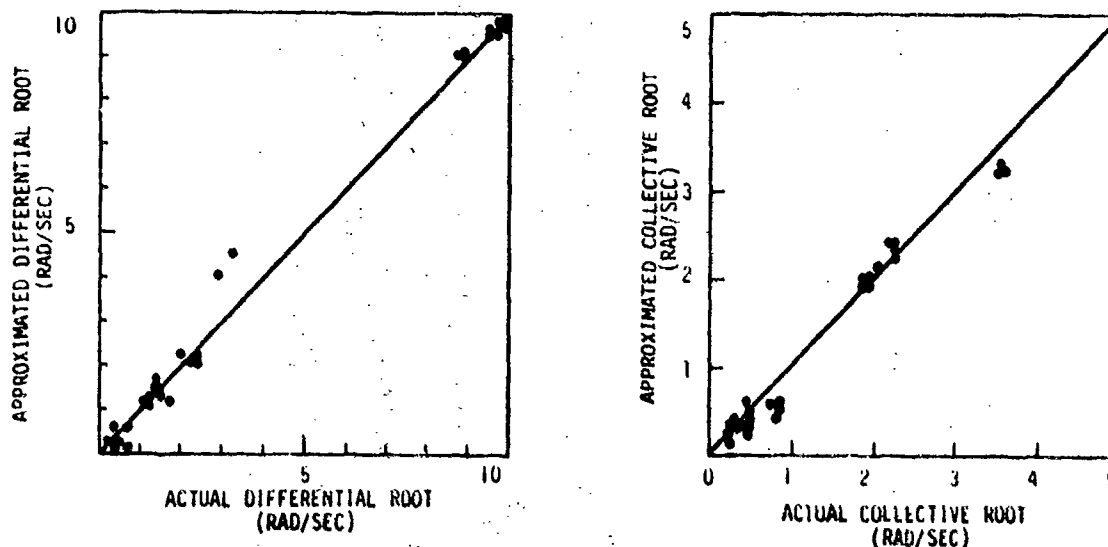
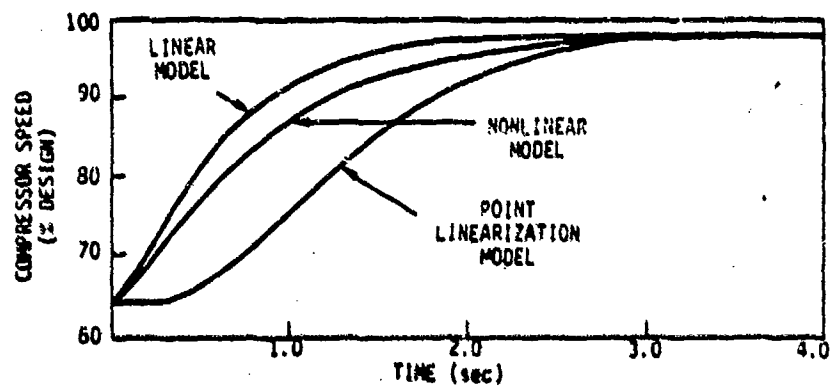
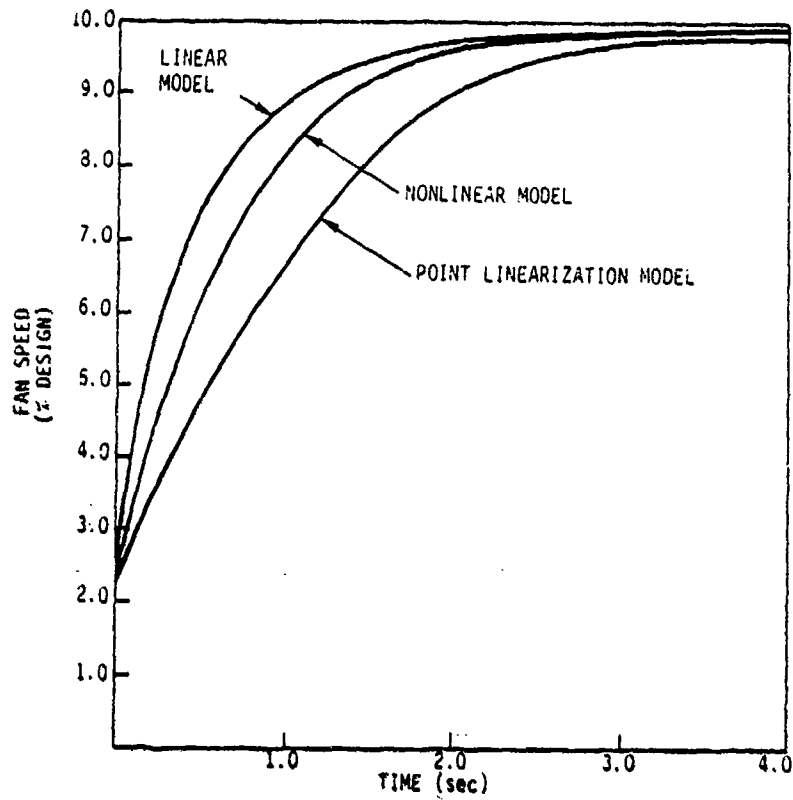


Figure 5.12 Comparison of Linear Eigenvalue Locations and Root Locations Found by Linearizing the Nonlinear Model at 28 Flight Points Spanning the Operating Envelope. The Three Remaining Temperature Modes Had Less Error Than the Collective/Differential Response Models Shown Above

The nonlinear dynamics matrix developed from the linear models was used in a nonlinear simulation of the engine response for a large acceleration from idle to military power. A step input of the control variables was used in this test because the definitions of the control logic governing such a maneuver has not been developed. The response of the nonlinear simulation is compared to a linear model derived at intermediate power and a model which uses a linearization at the trajectory point. (Figure 5.13) It is observed that the response of the nonlinear equations falls



**Figure 5.13 Comparison of Idle to Military Power Step Response Simulated Using Linear Model Derived at Intermediate Power, the Nonlinear Model Derived from Linear Matrices and a Model Using Linearizations at Each Point along the Trajectory**

between the fixed linear and pointwise linear simulation. Further comparison of the approximate nonlinear response to the detailed digital simulation will be made during the next phase of the program.

### 5.3 ACTUATOR SERVO VALVE COMPENSATION

As part of Phase I, compensation for the actuator servo valves has been designed and a detailed simulation performed. The purpose of the simulation was to determine: (1) the sensitivity of the proposed compensation to known errors (e.g., bias and gain), and (2) the effects of variable sample and computation intervals (i.e., the impact of not having a clock).

Two systems have been simulated. They are based on the original and revised versions of the servo valve characteristic respectively. These characteristics are reproduced in Figures 5.14 and 5.15.

The control design specifications for both systems were assumed to be the same. Specifically required were:

- (1) bandwidth of 10 rad/sec (linear operating region)
- (2) linear response (no saturation) for  $\pm 10\%$  of full scale step changes in commanded fuel flow
- (3) dc hangoff error of 0.1% stroke

#### 5.3.1 Simulation

The simulation performed involves a detailed description of the loop error sources and nonlinearities. Included are the

- (1) valve characteristic (nonlinear)
- (2) servo valve time constant
- (3) servo valve gain error
- (4) variable bias ( $\pm 2$  ma)

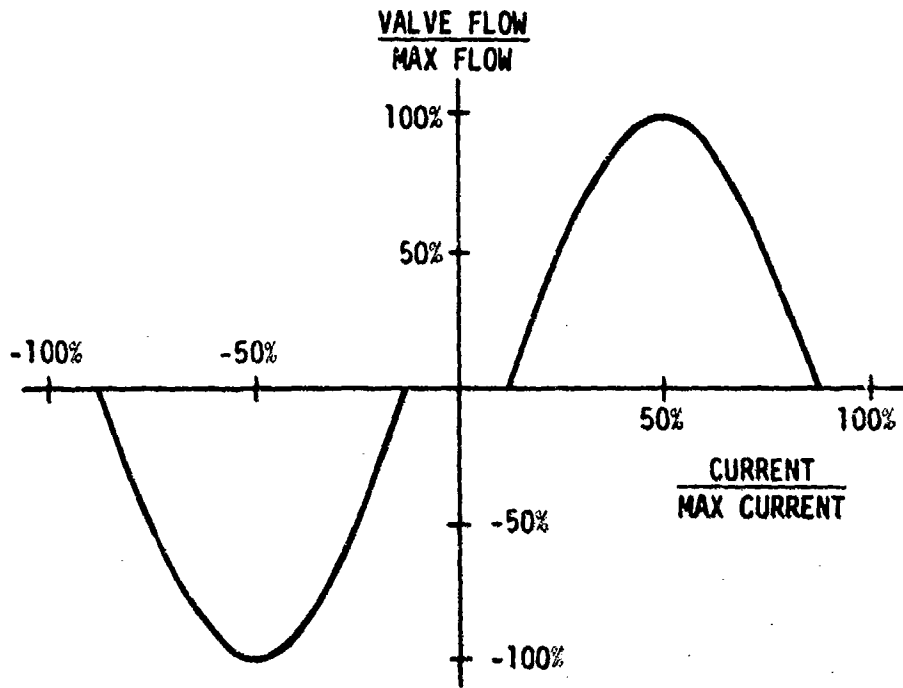


Figure 5.14 Failed-Fixed Servo Valve Characteristic

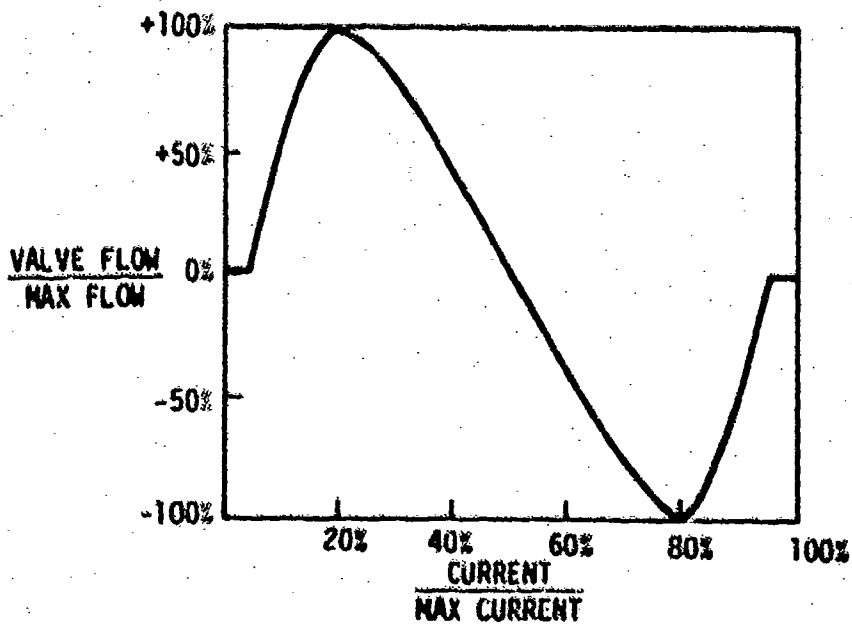


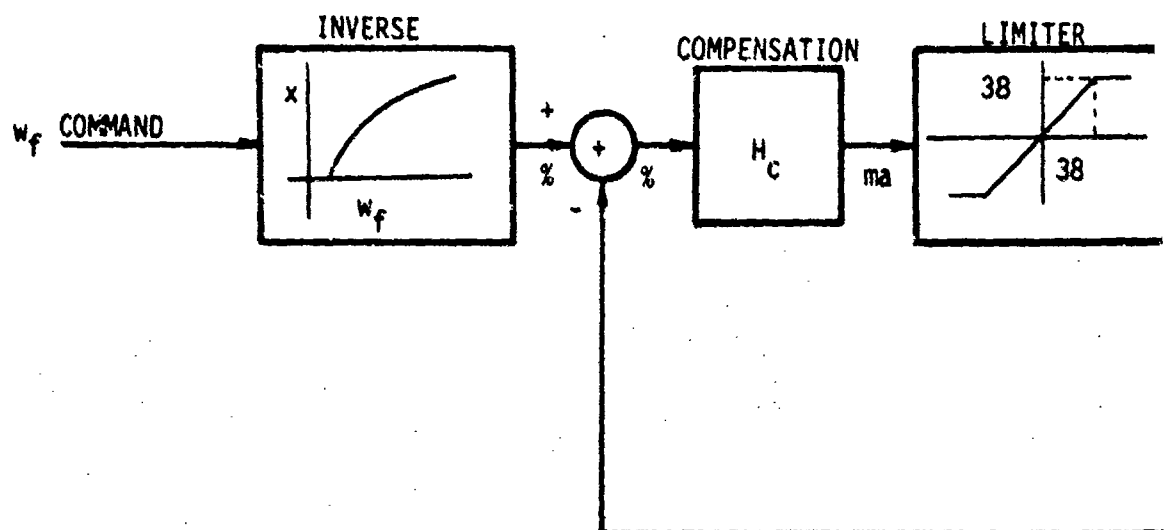
Figure 5.15 Revised Failed-Fixed Servo Valve Characteristic

- (5) 2 ma hysteresis
- (6) additive white measurement noise
- (7) 8 bit quantizer
- (8) 12 bit sampler
- (9) variable loop sample time
- (10) variable control computation time
- (11) 427.25 Hz pulsewidth modulator

A block diagram showing these terms is presented in Figure 5.16. Note that the variable times and modulation interval introduce effective time delays (variable) to the system. These delays and the hysteresis are sources of phase lag which adversely affect loop stability.

The simulation was designed specifically to mimic operation of an actual digital control loop. Implementation of the variable sample interval, modulation time (23.5 ms), and control computation time is described with the aid of Figures 5.17 and 5.18. Figure 5.17 describes the sequence of events in time. Note that the sample intervals shown are not constant (this is intended to describe operation without a clock). The sample interval is assumed to be randomly distributed between 5 and 15 ms. At the beginning of each sample interval the computer memory location containing the LVPT output is sampled. However, this memory location is updated only every 2 ms. Consequently, since the sample interval is not synchronized with this update interval, the information contained in memory will lag the actual LVPT output. This delay is evenly distributed between 0 and 2 ms.

After sampling the LVPT memory location, the computer must compute the commanded control input. This takes time. Currently, this time interval is assumed to be randomly distributed between 5 and 15 ms.



FIGURE

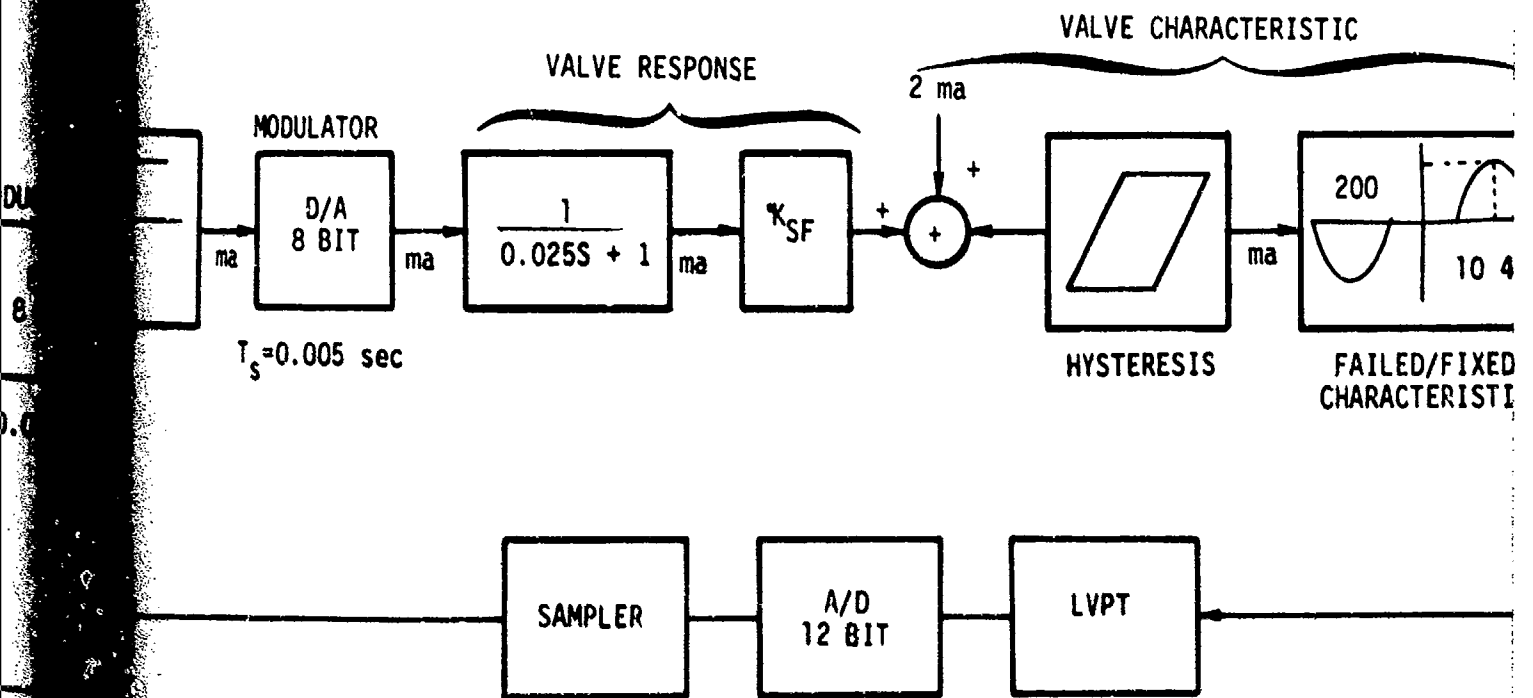
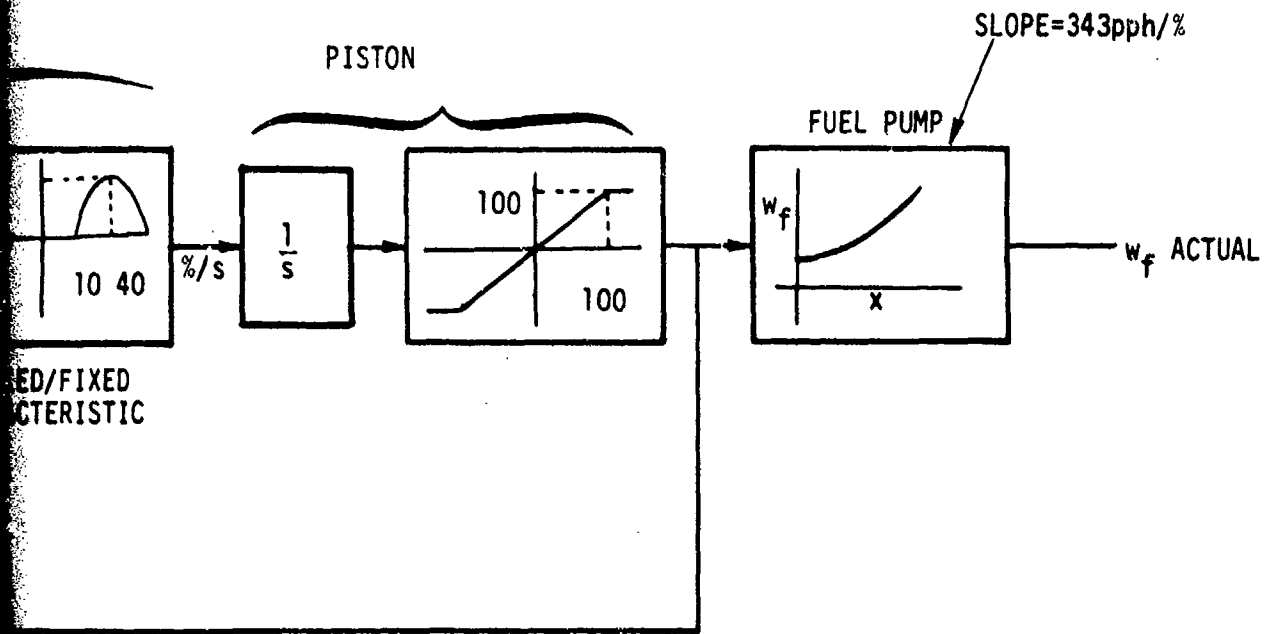


FIGURE 5.16 BLOCK DIAGRAM OF ACTUATOR VALVE SERVOLOOP



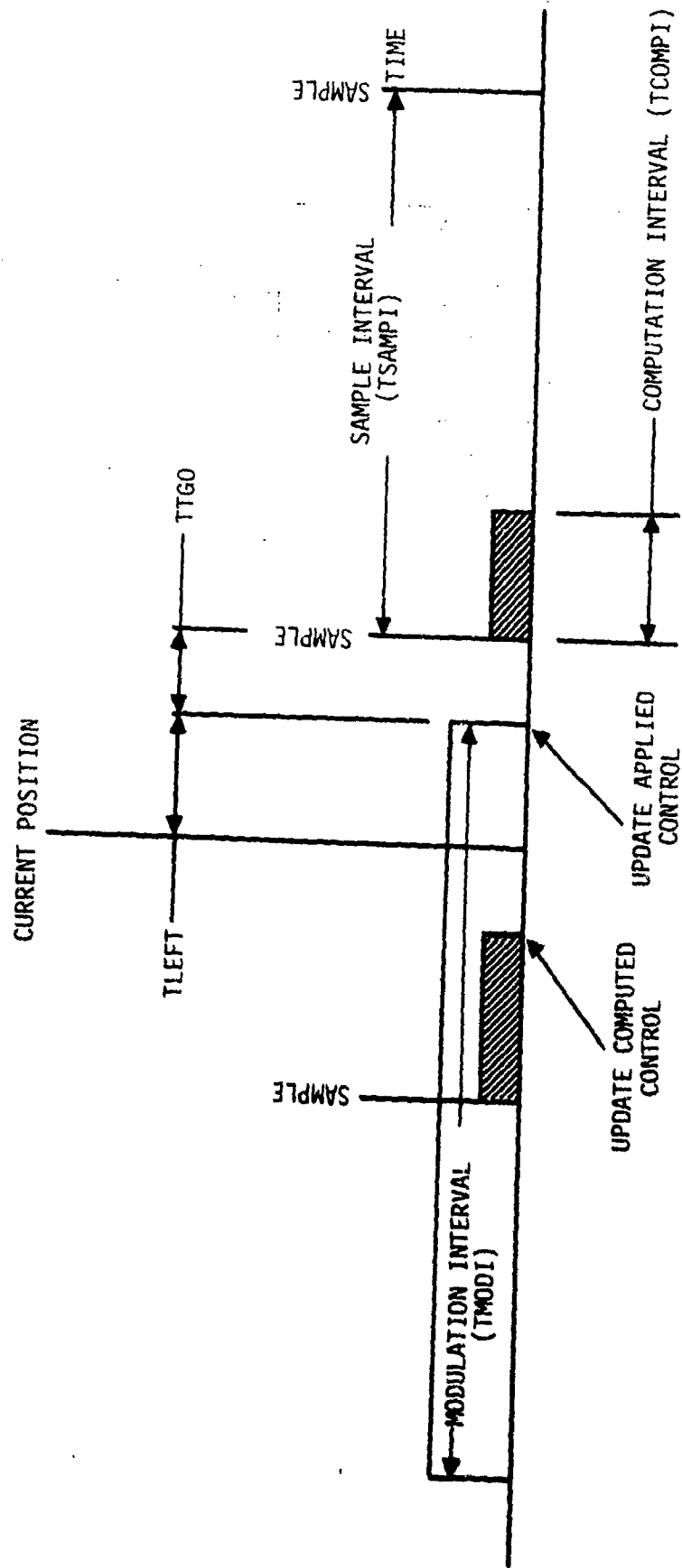


Figure 5.17 Modulation Interval, Sample Interval and Computation Interval

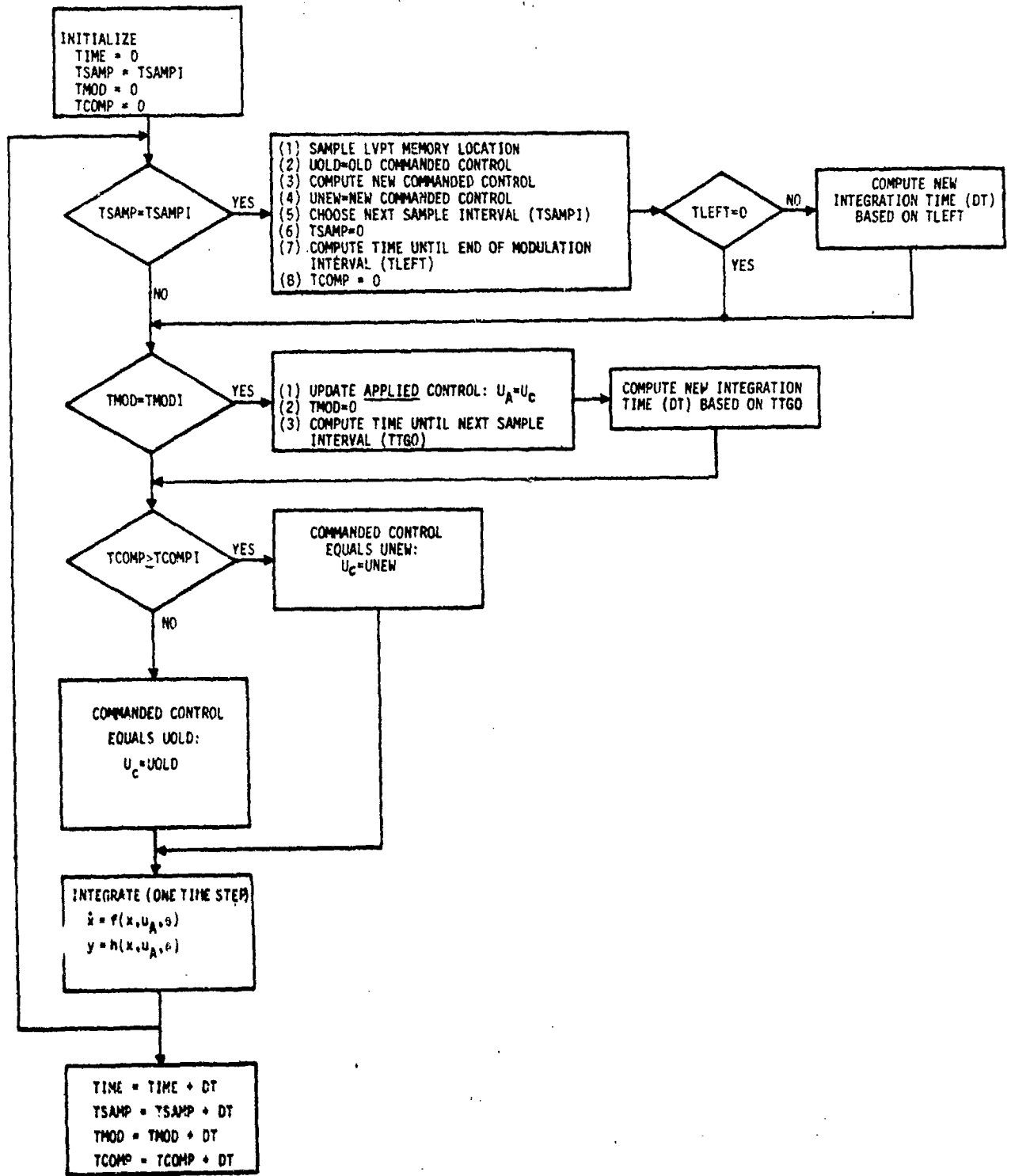


Figure 5.18 Flowchart of Actuator Valve Servo Loop Simulation

After the commanded control input has been calculated, it is applied to the pulsewidth modulator. This modulator, however, only outputs a new pulse at 23.5 ms intervals. Consequently, there is a further delay (up to 23.5 ms) before the actuator sees the new control. Note that it is possible for a second commanded control to be computed before the first has been applied to the torque motor.

Figure 5.18 is a flow chart of the computer code which simulates the process described above. Variable names in the figure are:

- (1) TSAMPI: Sample Interval
- (2) TSAMP: Running Sum for Comparison with TSAMPI
- (3) TMODI: Modulation Interval (23.5 ms)
- (4) TMOD: Running Sum for Comparison with TMODI
- (5) TCOMPI: Computation Interval
- (6) TCOMP: Running Sum for Comparison with TCOMPI

Fourth order Runge Kutta integration is used. The integration time step is varied during execution to assure that the end of each sample interval and the end of a modulation interval both coincide with an integration time (variables TLEFT and TTGO).

### 5.3.2 FADEC Valve I

The preliminary compensation designed for the failed-fixed servo valve (Figure 5.1) is presented in Figure 5.19. This compensation is essentially a stabilized inverse dead zone. With this compensation, the 10 rad/sec bandwidth requirement is easily satisfied. However, in a worst-case error configuration (hysteresis and bias), the dc hangoff specification is not met.

The design proceeds as follows. In the linear operating region, two approximations are first made: (1) the failed/fixed

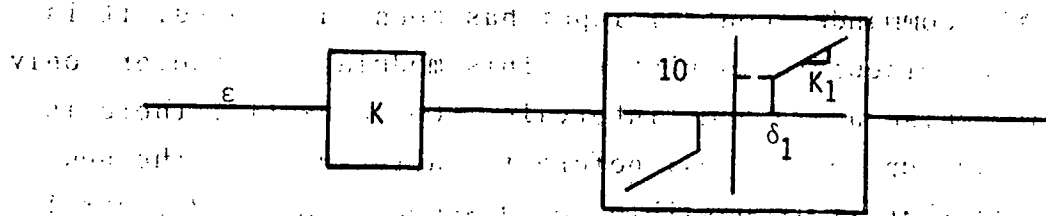


Figure 5.19 Nonlinear Compensation for Actuator Servovalve (FADEC I)

characteristic is roughly a constant gain (10%/sec/ma), and (2) the compensation,  $H_c$ , is a constant gain ( $KK_1$ ). The open-loop transfer function is, therefore,

$$G = \frac{KK_1(10)}{s(0.025s+1)}$$

and the closed-loop transfer function is

$$\frac{\text{piston position}}{\text{commanded position}} = \frac{400 KK_1}{s^2 + 40s + 400 KK_1}$$

The closed-loop pole locations are, therefore,

$$s_1 = -20 - 20 \sqrt{1 - KK_1}$$

$$s_2 = -20 + 20 \sqrt{1 - KK_1}$$

The bandwidth requirement is met if

$$s_2 = -10 = -20 + 20 \sqrt{1 - KK_1}$$

or

$$KK_1 = 0.75$$

The dc hangoff error specification ( $\epsilon \leq 0.1\%$ ) requires (no bias or hysteresis)

$$\delta_1 \leq K\epsilon$$

or

$$\delta_1 \leq 0.1K$$

A set of parameters which satisfies all the requirements is

$$K_1 = 1.00$$

$$K = 0.75$$

$$\delta_1 = 0.075$$

This compensation has been incorporated in the detailed simulation discussed above. The results are presented in Figure 5.20. Shown are two responses. In the first, there are no time delays. In the second, all the error terms in the simulation were included.

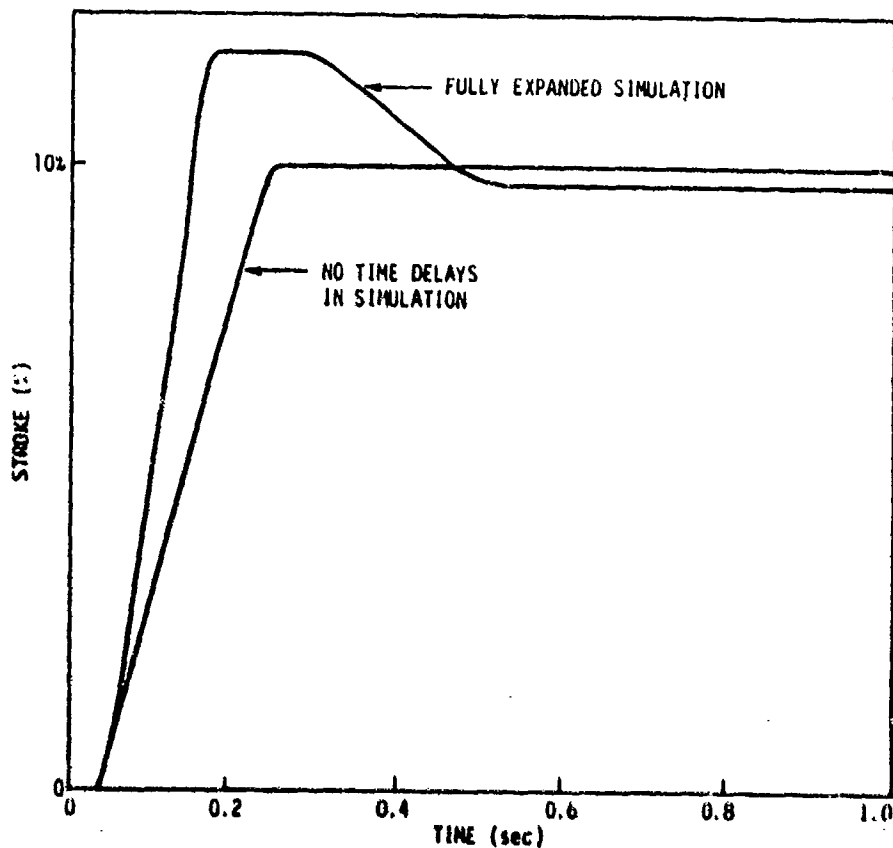


Figure 5.20 Step Response of FADEC Valve #1 to a 10% of Full Scale Step in Commanded Stroke (Measurement Noise Equals 1% of Full Scale Stroke)

The destabilizing effect of the phase lag associated with the hysteresis and time delays is evident. Note that measurement noise signal to 1% of the full scale stroke has been assumed.

### 5.3.3 FADEC Valve II

During the Phase I effort, the engine manufacturer revised the servovalve characteristic to that presented in Figure 5.15. This new characteristic does not have the large deadband of the FADEC Valve I; consequently, it may be compensated using linear techniques.

For this valve, both the dc hangoff error and bandwidth requirements are easily met. The dc hangoff error requirement is satisfied by specifying a lower limit on the dc gain of the compensation  $H_C(s)$ . Specifically, a dc current error of 4 ma is possible (2 ma in bias and 2 ma in hysteresis). This requires

$$x_{ss} [\%] = \frac{4 [\text{ma}]}{H_C(o) [\text{ma}/\%]} = 0.1 [\%]$$

or

$$H_C(o) = 40 \text{ ma}/\%.$$

The bandwidth requirement of 10 rad/sec is satisfied using a compensation of the form

$$H_C(s) = \frac{H_C(o)(\tau_s s + 1)}{(\tau_p s + 1)}.$$

The time constants,  $\tau_s$  and  $\tau_p$ , are easily found using Bode analysis. One set which satisfies the constraints is

$$\begin{aligned} H_C(o) &= 40.0 \\ \tau_s &= 1.59 \text{ sec} \\ \tau_p &= 20.0 \text{ sec} \end{aligned}$$

This compensation loop has been simulated. The results are presented in Figure 5.21.

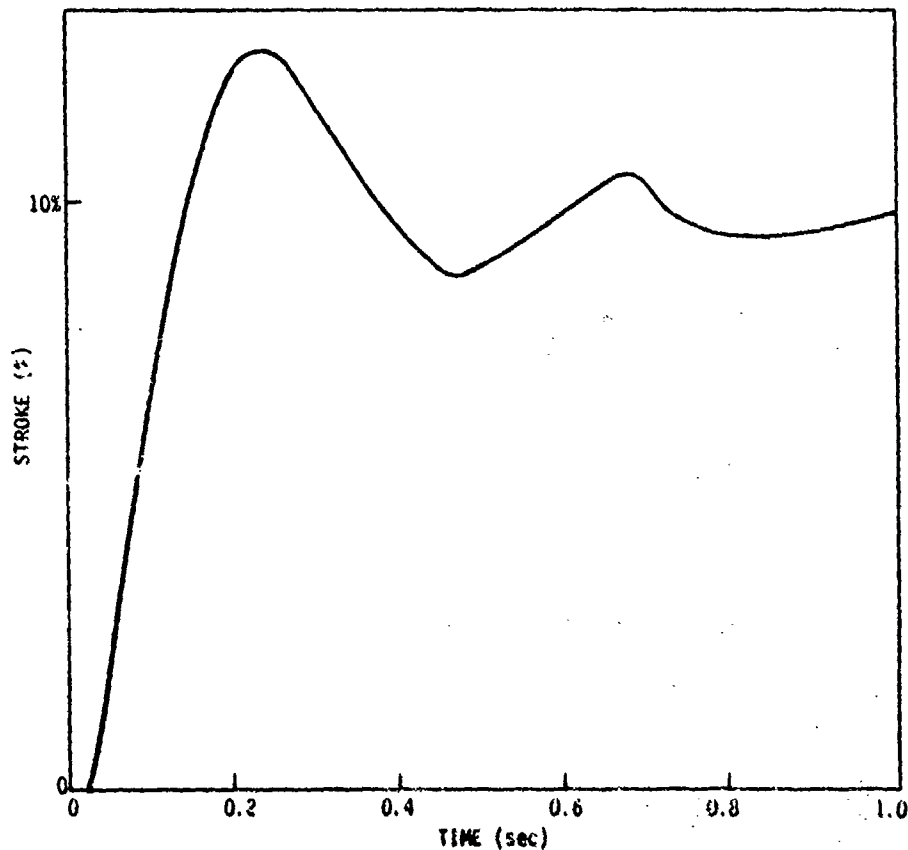


Figure 5.21 Step Response of FADEC Valve #2 to a 10% of Full Scale Step in Commanded Stroke (Measurement Noise Equals 1% of Full Scale Stroke)

The destabilizing phase resulting from the time delays, hysteresis and sampling is apparent. Furthermore, the effect of the noise' passing through the linear compensation is obvious in that the final valve position tracks the noise. This effect was not observed in the FADEC Valve #1 response due to the presence of the dead zone (see Figure 5.20). The final compensation for FADEC Valve #2 will include a deadzone.

#### 5.4 TRANSITION GENERATOR DEMONSTRATION

Trajectory generator logic was designed and demonstrated at one flight condition to evaluate the concept (see Section 4.1.5). A linear model of the engine at sea levels, static, intermediate power was used as the engine simulator. An "acceleration" from 90% intermediate power to intermediate power was performed using fuel flow as the only modulated variable. While this test did not exercise the full flexibility of the general system, it served to illustrate feasibility and provide a prototype software implementation for the final system.

The response of the engine to a step input is compared to the linear servomechanism response in Figure 5.22. The structure of this demonstration system is shown in Figure 5.23. The compensation for the command generator will be designed from the output regulator processes described above. It is observed that the compensated command generator produces a faster thrust response at the cost of a temperature overshoot and unacceptable surge margin loss.

The nonlinear variable rate limit design was also implemented using the  $T_{4.1}$  (turbine entrance) gas temperature limit and the compressor surge margin limits as inputs to the system. The response is shown in Figure 5.24. It can be seen that the trajectory generated with this system provides a fast response without causing a predicted overtemperature or unacceptable surge margin loss in the model. The implementation of the final form of the system will include several limit schedules driving variable rates in each of the compensated command servos used to produce the nominal control and output time histories.

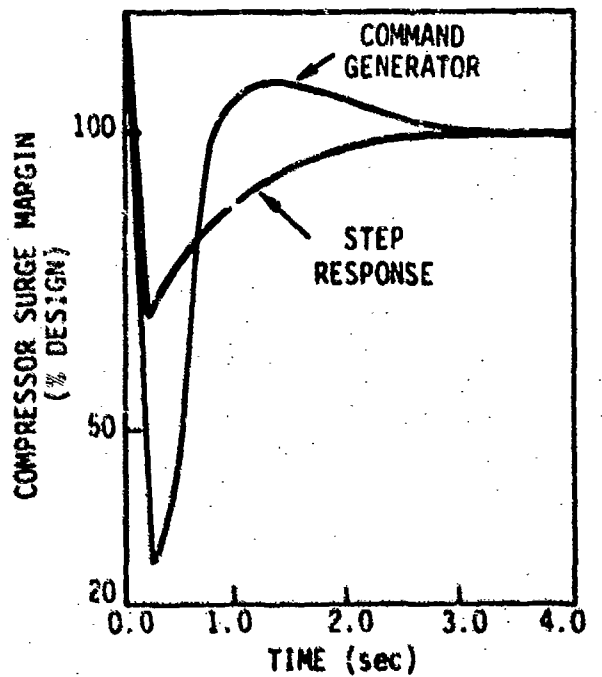
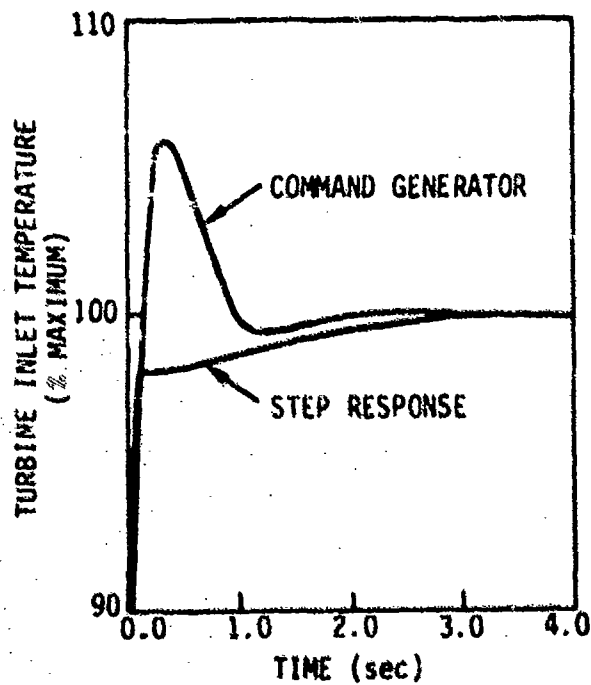
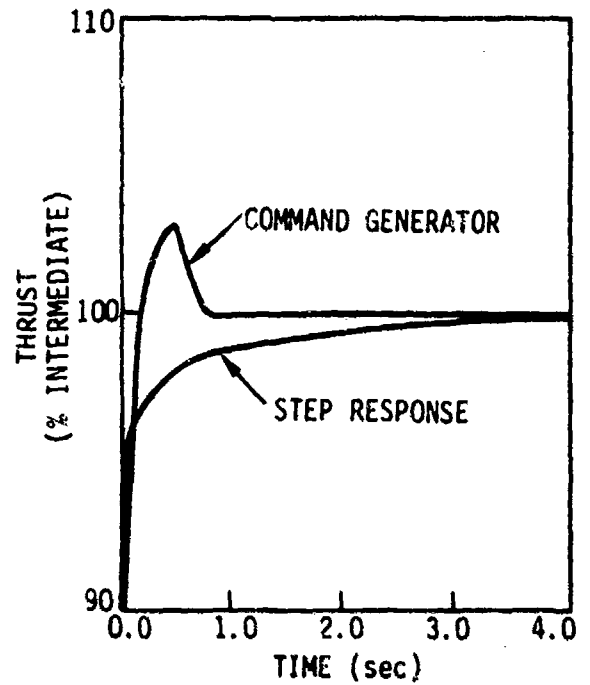
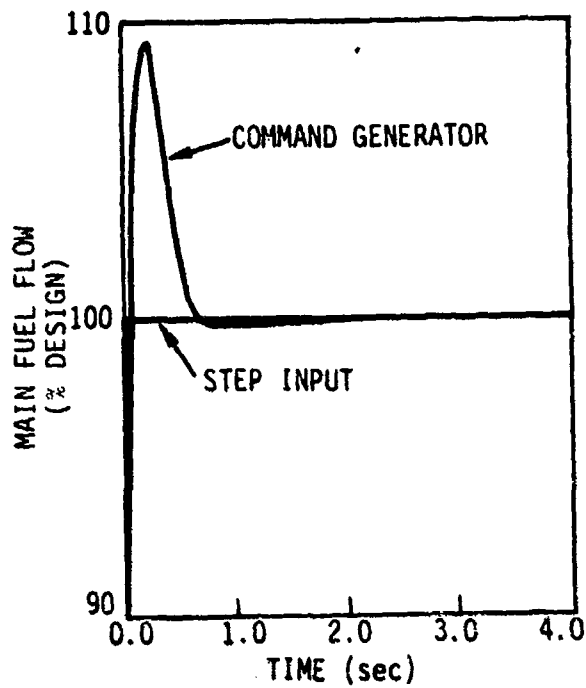


Figure 5.22 Comparison of Step Response and Linear Servomechanism Response for a Ten (10) Percent Acceleration to SLS, Intermediate Power

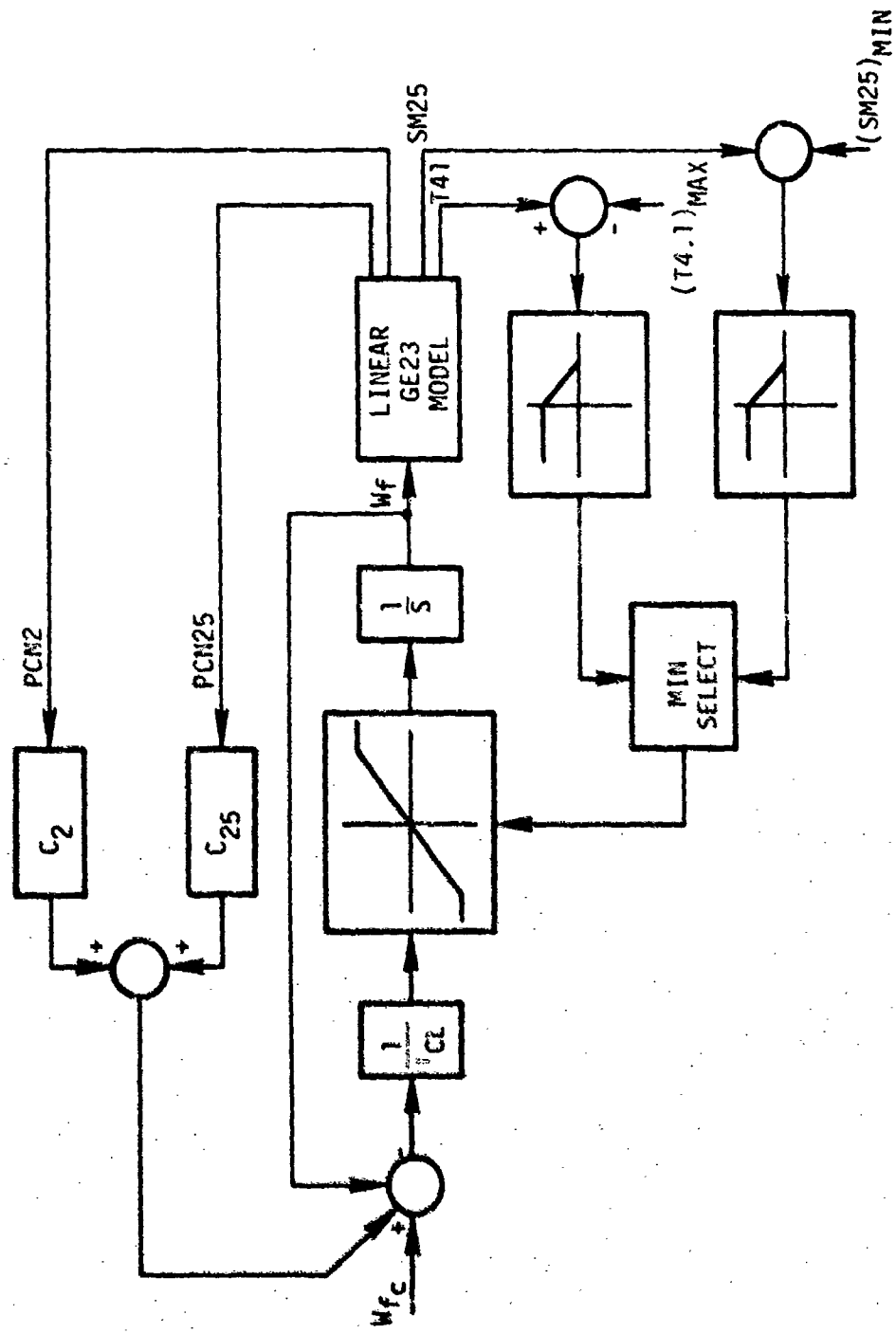


Figure 5.23 Demonstration Trajectory Generator for VCE Linear Simulation Using a Fuel Flow Actuator and Two Nonlinear, Variable Rate Feedbacks

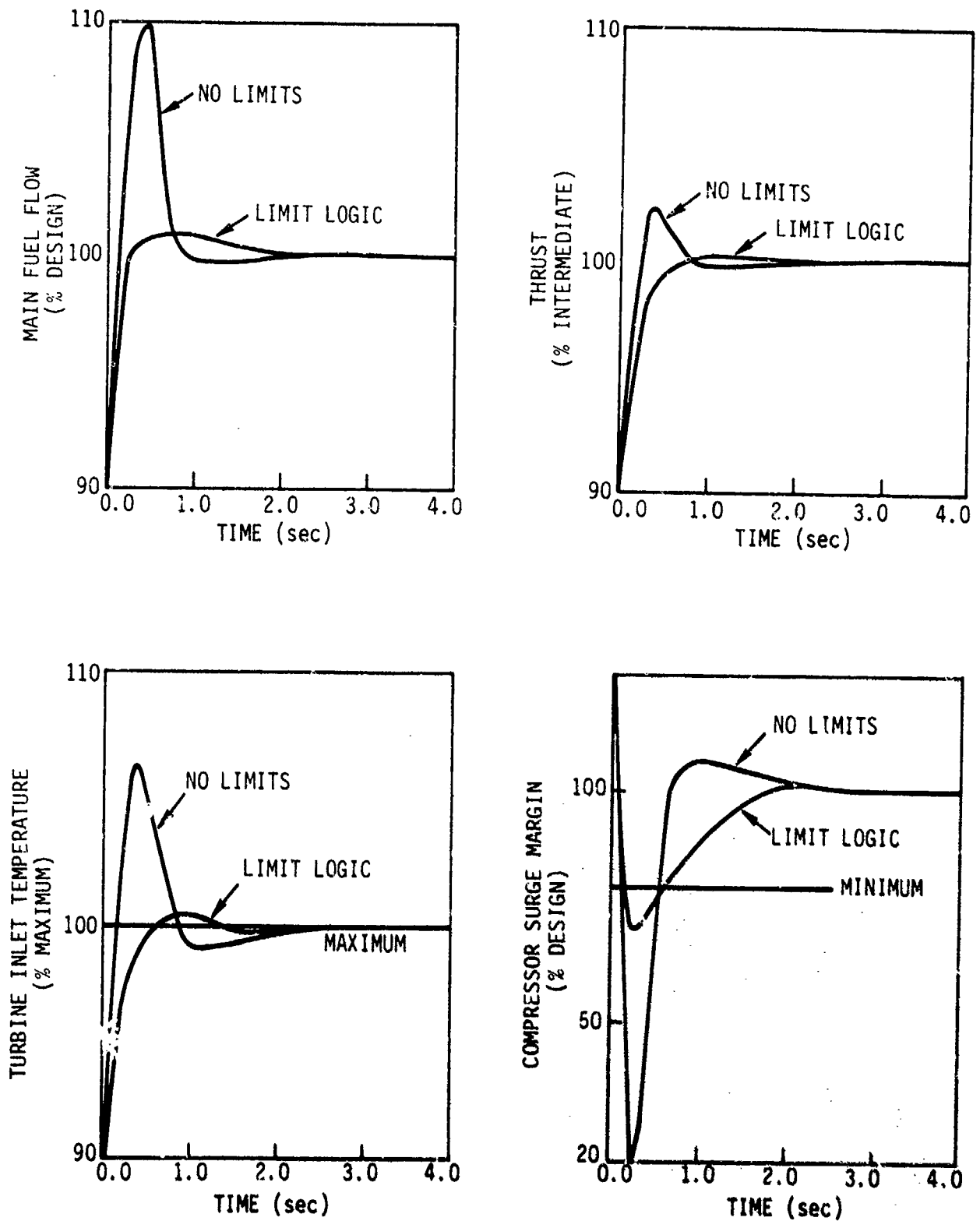


Figure 5.24 Demonstration of Temperature and Surge Limiting Acceleration Trajectory Using Nonlinear, Variable Rate Feedback

SECTION VI  
SUMMARY AND PROGRAM STATUS

6.1 SUMMARY

The development of a multivariable control structure for the GE23-JTDE variable cycle engine has been described. The variable cycle engine provides the necessary performance flexibility to meet advanced mission requirements specified for the Grumman design 623 fighter. A digital control processor is used in conjunction with a hydromechanical backup control and a variety of actuating and sensing devices to produce this capability. The specified hardware represents a major step forward in complexity and versatility in propulsion system design.

A multivariable control design methodology has been presented which addresses each functional requirement. Linear dynamic models form the basis of the design methods. Output regulator synthesis, failure detection and accommodation and nonlinear model development are presented as they address the major specifications of the digital control. Preliminary design results are described in regulator design, actuator compensation, model reduction and nonlinear model development.

The multivariable control structure has been defined. A reference point schedule uses power commands and ambient conditions to estimate the operating point quantities. A trajectory generator produces optimized paths between operating points which respect engine limits. An output regulator provides compensation for modeling errors and disturbances. Failure detection and accommodation is provided by a fault tolerant filter algorithm to compensate for arbitrary sensor failures; engine protection logic is provided to coordinate transfer to the hydromechanical backup; and a failure accommodating actuator compensation module provides a high performance

interface to the GE23 fail-fixed actuators. The specified control structure and design methodology in conjunction with the sophisticated engine hardware has the potential to realize substantially improved performance, reliability and flexibility in the next generation propulsion systems.

## 6.2 PROGRAM STATUS

The multivariable design program for the GE23 is being performed in two phases. The Phase I study results have been documented in this report. They represent the control structure definition and an analysis of linear dynamics of the engine. The results of this study indicate that the proposed design methods have the potential for quickly and efficiently developing the digital multivariable control software in Phase II of the program.

The development, validation and evaluation of the control design will be undertaken in the second phase of the program. The nonlinear simulation will be used as the test bed for the control logic design. The developed software will be transferred to the engine manufacturer for evaluation on a hybrid computer model of the engine. A careful analysis of the results will validate the system for future test in prototype engine programs.

APPENDIX A  
DERIVATION OF  $\frac{dJ}{dC}$

PROBLEM:

Given  $J = J(\bar{C}(C))$

and

$$\frac{dJ}{d\bar{C}}$$

find

$$\frac{dJ}{dC}$$

where

$$\bar{C} = C(I - DC)^{-1}$$

or

$$C = (I + \bar{C}D)^{-1}\bar{C}$$

$J$  is scalar

$C$  is  $m \times p$

$\bar{C}$  is  $m \times p$

$D$  is  $p \times m$

Presented first is a summary of notations described in detail in Refs. 17 and 18. Specifically

$E_{ij}$  = matrix whose  $(i,j)$ <sup>th</sup> element equals one; rest of matrix is zero

$E$  = matrix whose  $(i,j)$ <sup>th</sup> block =  $E_{ij}$

$rsA$  = row string of  $A = [a_{1*} \mid a_{2*} \mid \dots \mid a_{p*}]$   
 $p \times q$  (l x p q)

$csA$  = column string of  $A = \begin{bmatrix} a_{*1} \\ \vdots \\ a_{*q} \end{bmatrix}$   
 $p \times q$  (p x l)

*Preceding Page Blank*

$a_{i*}$   $i^{\text{th}}$  row of A

$a_{*i}$   $i^{\text{th}}$  column of A

Derivative of one matrix with another

$$\begin{matrix} (d/dB) \{A\} & = & \langle dA/db_{kl} \rangle & k \downarrow = 1, 2, \dots, s \\ \text{sxt} & \text{pxq} & \text{spxtq} & l \rightarrow = 1, 2, \dots, t \end{matrix}$$

Kronecker product

$$\begin{matrix} A \times B & = & \langle a_{ij} B \rangle & i \downarrow = 1, 2, \dots, p \\ \text{pxq} & \text{sxt} & \text{psxqt} & j \rightarrow = 1, 2, \dots, q \end{matrix}$$

The derivation proceeds as follows.

From  $J = J(\bar{C}(C))$ , chain rule differentiation yields:

$$\frac{dJ}{dC} = \left( I_m \times \frac{dJ}{d[rs\bar{C}]} \right) \left( \frac{d[rs\bar{C}]}{dC} \times I_1 \right)$$

or

$$\frac{dJ}{dC} = \left( I_m \times \frac{dJ}{d[rs\bar{C}]} \right) \left( \frac{d[rs\bar{C}]}{dC} \right)$$

but

$$\frac{dJ}{d[rs\bar{C}]} = rs \frac{dJ}{d\bar{C}}$$

therefore

$$\frac{dJ}{dC} = \left( I_m \times rs \frac{dJ}{d\bar{C}} \right) \left( \frac{d[rs\bar{C}]}{dC} \right) \quad (\text{A.1})$$

$\text{m} \times \text{p} \qquad \qquad \text{l} \times \text{m} \times \text{p} \qquad \qquad \text{m} \times \text{p} \times \text{p}$

$\frac{dJ}{dC}$  is known. The problem is to find  $\frac{d[rs\bar{C}]}{dC}$ .

First, find

$$\frac{d\bar{C}}{dC}$$

From

$$\bar{C} = C(I-DC)^{-1}$$

$$\frac{d\bar{C}}{dC} = \frac{d}{dC} [C(I-DC)^{-1}].$$

Let

$$B \equiv (I-DC)^{-1}$$

pxp

and

$$F \equiv (I-DC)$$

pxp

Then, the product rule yields

$$\frac{d\bar{C}}{dC} = \frac{dC}{dC} \underset{m \times p}{(I \times B)} + \underset{m}{(I \times C)} \frac{dB}{dC} \quad (A.2)$$

To find  $\frac{dB}{dC}$  use

$$\frac{d(BF)}{dC} = \frac{dI}{dC} = [0].$$

Using the product rule

$$\frac{d(BF)}{dC} = \frac{dB}{dC} \underset{p}{(I \times F)} + \underset{m}{(I \times B)} \underset{p \times p}{\frac{dF}{dC}} = [0].$$

Therefore

$$\frac{dB}{dC} = - \left( I \begin{array}{c} \diagdown \\ \diagup \end{array} B \right) \frac{dF}{dC} \left( I \begin{array}{c} \diagdown \\ \diagup \end{array} F \right)^{-1}$$

or

$$\frac{dB}{dC} = - \left( I \begin{array}{c} \diagdown \\ \diagup \end{array} B \right) \frac{dF}{dC} \left( I \begin{array}{c} \diagdown \\ \diagup \end{array} B \right). \quad (A.3)$$

Now

$$\frac{dF}{dC} = \frac{d}{dC} (I - DC) = [0] - \frac{d}{dC} (DC).$$

Using the product rule again

$$\frac{dF}{dC} = - \frac{dD}{dC} \left( I \begin{array}{c} \diagdown \\ \diagup \end{array} C \right) - \left( I \begin{array}{c} \diagdown \\ \diagup \end{array} D \right) \frac{dC}{dC}$$

or

$$\frac{dF}{dC} = - \left( I \begin{array}{c} \diagdown \\ \diagup \end{array} D \right) \frac{dC}{dC} \quad (A.4)$$

Inserting Eq. (A.4) into Eq. (A.3)

$$\frac{dB}{dC} = \left( I \begin{array}{c} \diagdown \\ \diagup \end{array} B \right) \left( I \begin{array}{c} \diagdown \\ \diagup \end{array} D \right) \frac{dC}{dC} \left( I \begin{array}{c} \diagdown \\ \diagup \end{array} B \right) \quad (A.5)$$

Inserting Eq. (A.5) into Eq. (A.2)

$$\frac{dC}{dC} = \frac{dC}{dC} \left( I \begin{array}{c} \diagdown \\ \diagup \end{array} B \right) + \left( I \begin{array}{c} \diagdown \\ \diagup \end{array} C \right) \left( I \begin{array}{c} \diagdown \\ \diagup \end{array} B \right) \left( I \begin{array}{c} \diagdown \\ \diagup \end{array} D \right) \frac{dC}{dC} \left( I \begin{array}{c} \diagdown \\ \diagup \end{array} B \right)$$

which can be written

$$\frac{d\bar{C}}{dC} = [I_m + (I_m \times C)(I_m \times B)(I_m \times D)] \frac{dC}{dC} (I_p \times B)$$

or

$$\frac{d\bar{C}}{dC} = (I_m \times A) \frac{dC}{dC} (I_p \times B) \quad (A.6)$$

where

$$A \equiv I + CBD$$

Noting that

$$\frac{dC}{dC} = E_{m \times p}$$

where the  $(i,j)^{th}$  block of  $E$  is  $E_{ij}$  and  $E$  is  $m$  by  $p$  blocks.

Then Eq. (A.6) may be written

$$\frac{d\bar{C}}{dC} = (csA) \times (rsB) \quad (A.7)$$

By expanding Eq. (A.7) it may be shown that

$$\frac{d[rs\bar{C}]}{dC} = (csA) \times B^T \quad (A.8)$$

By substitution of Eq. (A.8) into Eq. (A.1)

$$\frac{dJ}{dC} = (I_m \times rs \frac{dJ}{dC}) (csA \times B^T)$$

which equals

$$\frac{dJ}{dC} = A^T \frac{dJ}{dC} B^T .$$

The solution is, therefore,

$$\frac{dJ}{dC} = (I+CBD)^T \frac{dJ}{dC} (I-DC)^{-T} \quad (A.9)$$

APPENDIX B  
SECOND STAGE MODEL REDUCTION

Given the system

$$\dot{x} = Fx \quad x(0) = x_0, \quad (B.1)$$

the problem of "second stage reduction" may be stated as: Find the elements of a matrix,  $\bar{F}$ , (which has a different structure than  $F$ ) such that the response of the system

$$\dot{\bar{x}} = \bar{F} \bar{x} \quad \bar{x}(0) = x_0 \quad (B.2)$$

most nearly matches the response of the system defined by Eq. (B.1). Specifically, if the error in the response is defined as

$$z \equiv \overset{\Delta}{x} - \bar{x}, \quad (B.3)$$

then the object is to minimize

$$J = 1/2 \int_0^{\infty} z^T A_2 z \, dt. \quad (B.4)$$

For example, it might be desired to find an  $\bar{F}$  of the form

$$\bar{F} = \begin{bmatrix} \bar{F}_{11} & 0 \\ \bar{F}_{21} & \bar{F}_{22} \end{bmatrix} \quad (B.5)$$

which most nearly matches the dynamic response of the original system

$$F = \begin{bmatrix} f_{11} & f_{12} \\ f_{21} & f_{22} \end{bmatrix} \quad (B.6)$$

That is, the object is to find the optimum system with the  $F_{12}$  element fixed at zero.

A convenient procedure for solving this problem follows. First, define a matrix,  $\Delta F$ , as

$$\Delta F = F - \bar{F} \quad (B.7)$$

Then, from Eqs. (B.1)-(B.3)

$$\begin{aligned} \dot{z} &= \dot{x} - \dot{\bar{x}} \\ &= Fx - \bar{F} \bar{x} \\ &= Fx - (F - \Delta F)(x - z) \\ &= Fz - \Delta F(x - z) \end{aligned} \quad (B.8)$$

where  $z(0) = 0$ . An equivalent statement of the problem now becomes:

Find  $\Delta F$  in

$$\frac{d}{dt} \begin{bmatrix} x \\ z \end{bmatrix} = \begin{bmatrix} F & 0 \\ 0 & F \end{bmatrix} \begin{bmatrix} x \\ z \end{bmatrix} + \begin{bmatrix} 0 \\ I \end{bmatrix} \begin{bmatrix} \Delta F & 0 \\ 0 & 0 \end{bmatrix} \begin{bmatrix} I & -I \\ 0 & I \end{bmatrix} \begin{bmatrix} x \\ z \end{bmatrix} \quad (B.9)$$

which minimizes

$$J = 1/2 \int_0^{\infty} \begin{bmatrix} x^T & z^T \end{bmatrix} \begin{bmatrix} 0 & 0 \\ 0 & A_z \end{bmatrix} \begin{bmatrix} x \\ z \end{bmatrix} dt \quad (B.10)$$

In the example used above,  $\Delta F$  would be of the form

$$\begin{bmatrix} -\delta f_{11} & f_{12} \\ -\delta f_{21} & -\delta f_{22} \end{bmatrix} \quad (B.11)$$

and the problem becomes finding  $\delta f_{11}$ ,  $\delta f_{21}$ , and  $\delta f_{22}$ .

An interesting observation can be made at this point. If the following equivalences are made

$$x_{eq} = \begin{bmatrix} x \\ z \end{bmatrix} \quad (B.12)$$

$$F_{eq} = \begin{bmatrix} F & 0 \\ 0 & F \end{bmatrix} \quad (B.13)$$

$$G_{eq} = \begin{bmatrix} 0 \\ I \end{bmatrix} \quad (B.14)$$

$$H_{eq} = \begin{bmatrix} I & -I \\ 0 & I \end{bmatrix} \quad (B.15)$$

$$D_{eq} = [0] \quad (B.16)$$

$$C_{eq} = [\Delta F; 0] \quad (B.17)$$

$$A_{y_{eq}} = \begin{bmatrix} 0 & 0 \\ 0 & A_z \end{bmatrix} \quad (B.18)$$

$$x_{eq}(0) = \begin{bmatrix} I & 0 \\ 0 & 0 \end{bmatrix} \quad (B.19)$$

then the optimization problem is identical to the output regulator problem with a fixed structure gain matrix. Specifically, the problem is finding  $C_{eq}$  in the system

$$\dot{x}_{eq} = F_{eq} x_{eq} + G_{eq} u \quad (B.20)$$

$$u = C_{eq} y_{eq}$$

and

$$y_{eq} = H_{eq} x_{eq} \quad (B.21)$$

with

$$J = 1/2 \int_0^{\infty} y_{eq}^T A y_{eq} y \, dt \quad (B.22)$$

and

$$E\{x_{eq} x_{eq}^T\} = X_{eq}(0) \quad (B.23)$$

Consequently, this problem may be solved with the same algorithm used for the calculation of output regulator gains.

APPENDIX C  
MODELING PROCEDURES FOR THE VARIABLE CYCLE ENGINE

C.1 INTRODUCTION

A critical part of the multivariable control law is a dynamical model of the engine response. While this model does not predict engine response exactly, the closer to the real behavior, the better. The VCE is a complex engine and an accurate mathematical model could be far too complex to implement on the digital processor. An approach to model synthesis is described below which appears to balance accuracy and complexity considerations in a straightforward fashion.

The modeling problem has been solved in several other applications. It is useful to review these before discussing the VCE in particular. Simulation modeling in a hybrid computer environment has been around a long time. Thermodynamics and rig data are combined to give the best match of engine response as measured on prototype engines or previous models. Simplified phenomenological models can be written and solved in the processor. This approach is the basis of the Spang-Corley [19] fault detection algorithm for the QCSEE engine. In this case, maps are simplified and the thermodynamic equations are incorporated directly. This procedure has been used by several people to model static engine response for fault monitoring purposes. Control of the accuracy and complexity trade-offs is not apparent.

Linear behavior of the engine is used to design the control logic. Direct application of the linear dynamics matrices is not generally used for simulation because of the poor steady state response of the models to moderate inputs. It has been

suggested that the linear dynamic matrices, along with accurate set point information, could be used to simulate the nonlinear response of the engine in a more accurate fashion than using constant coefficient, linear dynamical equations. This procedure is attractive to MVC design since there is already a reference point generator requirement in the synthesis procedure.

## C.2 COMPARISON OF LINEAR AND NONLINEAR RESPONSE

To clarify the following sections, the utilization of linear dynamics matrices for simulation is compared to integration of the actual nonlinear equations. Engine dynamics can be represented by the  $n$ th order set of nonlinear equations:

$$\dot{x} = f(x, u, \theta) \quad (C.1)$$

$$y = h(x, u, \theta) \quad (C.2)$$

where  $m$  quantities  $u$  (controls) and  $q$  inputs  $\theta$  (ambients) determine the states and state rates,  $x$  and  $\dot{x}$  respectively. These quantities appear as nonlinear algebraic functions in the output equations for  $p$  quantities,  $y$  of interest. Much is known about the steady state engine response. This can be written:

$$0 = f(x_{ss}, u, \theta) \quad (C.3)$$

$$y = h(x_{ss}, u, \theta) \quad (C.4)$$

Most of the modeling effort should go into matching steady state response since it is at these points that engine performance is usually evaluated. Dynamical response is also important to the overall description of the behavior since these dynamical properties determine stability.

A linear approximation to Eq. (C.1) can be evaluated if derivative matrices of  $f$  are available. The function in

Eq. (C.1) can be expanded to first order about an equilibrium point  $(x_0, u_0)$  as follows:

$$\dot{\delta x} = f_x(x_0, u_0)\delta x + f_u(x_0, u_0)\delta u \quad (C.5a)$$

$$\delta x = x - x_0 \quad (C.5b)$$

$$\delta u = u - u_0$$

If it is assumed that  $u(t)$  is piecewise constant on an interval  $[nT, (n+1)T]$ , Eq. (C.5) can be rewritten relative to the constant value of  $u$  and the value of  $x$  which could be attained if  $u$  remained at that value, or,

$$\dot{x} = F_x(x_{ss}, u(n))(x(t) - x_{ss}) \quad (C.6)$$

where  $x_{ss}$  must satisfy the nonlinear equilibrium relationship

$$0 = f(x_{ss}, u(n), \theta) \quad (C.7)$$

or, equivalently,

$$x_{ss} = g(u(n), \theta) \quad (C.8)$$

where  $g(u(n), \theta)$  came from the reference schedules.

The time interval,  $T$ , can be made small relative to the dynamics and the equation used to solve for the response for an arbitrary function,  $u(t)$ .

The principal drawbacks of this approach are the accuracy and the storage requirements necessary to implement Eq. (C.6). The accuracy limitation arises because it is typically true that  $\|x - x_{ss}\|$  may be quite large if  $u(n)$  changes quickly. This produces large errors in the prediction of the engine response. Also, the gradient matrices must be written as functions of the operating line variables.

### C.3 A NEW APPROACH TO SIMPLE ENGINE MODELS

Linear models are simple and accurate near the linearization point. Extension of these models to larger operating regions should be approached systematically to achieve the most accurate results. Steady state accuracy is extremely important in evaluating the model results. A procedure for allowing accurate dynamic and static models to be combined is attractive.

One approach to the problem would be to generate engine data (from a simulation) of the form

$$(\dot{x}_i, x_i, u_i) \quad i=1, N$$

Then, the nonlinear relationships shown in Eq. (C.1) could be fit with a suitable model using curve fitting techniques. Data weighting could be used to assure that points where  $\dot{x}=0$  were matched accurately. The primary problem in this procedure is that weighting the static data points degrades the dynamic performance significantly. Direct modeling of the process results in these types of equations with presumably the same problems.

An alternate approach appears more attractive and is based on the linearization in Eq. (C.6). The linearized matrices,  $f_x(x, u)$  are easily generated from the nonlinear simulation. These matrices can be generated along the static operating line. Sensitivity calculations and multivariate regression techniques can be applied to develop accurate, and simple representations of these matrices as low order polynomial forms. The models determine only the dynamics and there is no trade off between dynamic and static performance. These curve fitting techniques are not pursued here. Consider that these functions have been derived and can be represented as follows:

$$\left. \frac{\partial f}{\partial x}(x, u) \right|_{\dot{x}=0} = F(x, u) \quad (C.9)$$

The equilibrium points are modeled by a separate equation.

$$x_{ss} = g(u_{ss}, \theta) \quad (C.10)$$

It is tempting to combine Eqs. (C.9) and (C.10) as follows:

$$\dot{x} = F(x, u_{ss})(x - x_{ss}) \quad (C.11)$$

and integrate away. A related equation can be used to accurately match the true nonlinear dynamic behavior in Eq. (C.1) without a specific representation of the dynamics,  $f(x, u, \theta)$ .

#### C.4 MODELING NONLINEAR DYNAMICS BY GRADIENTS

A comparison of Eqs. (C.1) and (C.11) can be made by considering a Taylor series expansion of Eq. (C.1) around the equilibrium point  $(x_{ss}, u_{ss})$ . First, define the perturbation

$$\delta x = x(t) - x_{ss} \quad (C.12)$$

Then,

$$\dot{x} = F(x_{ss}, u_{ss})\delta x + \frac{1}{2} \left. \frac{\partial F}{\partial x} \right|_{\substack{x=x_{ss} \\ u=u_{ss}}} \delta x \delta x + \dots + \frac{1}{n!} \left. \frac{\partial^{n-1} F}{\partial x^{n-1}} \right|_{\substack{x=x_{ss} \\ u=u_{ss}}} \delta x \dots \delta x$$

where dyadic notation is used. This can be more conveniently written as follows:

$$\dot{x} = [F_0 + \frac{1}{2}F_1\delta x + \frac{1}{6}F_2\delta x\delta x + \frac{1}{24}F_3\delta x\delta x\delta x]\delta x + ||0(\delta x^5)|| \quad (C.13)$$

Note that Eq. (C.13) represents the true dynamics up to order,  $||\delta x||^5$ . Suppose Eq. (C.11) is modified so that it matches Eq. (C.13). In this case, Eq. (C.11) would match the true dynamics to order  $||\delta x||^5$ . As it is, it matches only to order  $||\delta x||$ . Write Eq. (C.11) in a slightly different form as follows:

$$\dot{x} = [\alpha_1 F(x_0 + \frac{\delta x}{q_1}, u_{ss}) + \alpha_2 F(x_0 + \frac{\delta x}{q_2}, u_{ss})] (x - x_{ss}) \quad (C.14)$$

An expansion of one of the terms in Eq. (C.14) would look as follows:

$$F(x_0 + \frac{\delta x}{q}, u_{ss}) = F_0 + F_1 \frac{\delta x}{q_1} + \frac{1}{2} F_2 \frac{\delta x}{q_1} \frac{\delta x}{q_1} + \dots \quad (C.15)$$

By matching terms in Eqs. (C.14) and (C.13) an equivalence can be attained. There are four parameters,  $\alpha_1$ ,  $\alpha_2$ ,  $q_1$ , and  $q_2$ . Thus, Eq. (C.14) can be made to match the first four terms in Eq. (C.13) - resulting in the desired accuracy. The coefficients yield the following equations:

$$\alpha_1 + \alpha_2 = 1 \quad (C.16)$$

$$\left(\frac{1}{q_1}\right)\alpha_1 + \left(\frac{1}{q_2}\right)\alpha_2 = \frac{1}{2} \quad (C.17)$$

$$\left(\frac{1}{2q_1^2}\right)\alpha_1 + \left(\frac{1}{2q_2^2}\right)\alpha_2 = \frac{1}{6} \quad (C.18)$$

$$\left(\frac{1}{6q_1^3}\right)\alpha_1 + \left(\frac{1}{6q_2^3}\right)\alpha_2 = \frac{1}{24} \quad (C.19)$$

The solution to these equations is as follows:

$$\alpha_1 = \frac{1}{2} \quad (C.20)$$

$$\alpha_2 = \frac{1}{2} \quad (C.21)$$

$$q_1 = 3 - \sqrt{3} = 1.268 \quad (C.22)$$

$$q_2 = 3 + \sqrt{3} = 4.732 \quad (C.23)$$

The resulting form of equations which match the nonlinear system to order  $||\delta x||^5$  can now be written as follows:

$$\dot{x} = \frac{1}{2} \left[ F\left(x_{ss} + \frac{x - x_{ss}}{3 - \sqrt{3}}, u_{ss}\right) + F\left(x_{ss} + \frac{x - x_{ss}}{3 + \sqrt{3}}, u_{ss}\right) \right] (x - x_{ss}) \quad (C.24)$$

$$x_{ss} = g(u_{ss}, \theta) \quad (C.25)$$

The simulation procedure can be derived by assuming  $u$  constant on a small interval and solving a set of constant coefficient equations at each step. Higher order approximations can be derived directly from matching the expansions.

Example: An explicit equation

Suppose the engine model had the following form (which was unknown):

$$\dot{x} = x^4 - 2x^3u^2 + u^3 \quad (C.26)$$

Gradients were available and the linearized models were fit to form the "simulated model":

$$F(x,u) = (4x^3 - 6x^2u^2) \quad (C.27)$$

The reference point schedule indicates that  $u_{ss} = 1$ ,  $x_{ss} = 1$ , in a static equilibrium. The "engine simulation" for a step input to this equilibrium for any initial condition would be as follows:

$$\dot{x} = \frac{1}{2} \left( F\left(1 + \frac{x-1}{3+\sqrt{3}}, 1\right) + F\left(1 + \frac{x-1}{3-\sqrt{3}}, 1\right) \right) (x-1) \quad (C.28)$$

The accuracy of this model can be verified by expanding Eq. (C.28):

$$\begin{aligned} \dot{x} &= \frac{1}{2} \left( 4 \left[ \left(1 + \frac{x-1}{3+\sqrt{3}}\right)^3 + \left(1 + \frac{x-1}{3-\sqrt{3}}\right)^3 \right] \right. \\ &\quad \left. - 6 \left[ \left(1 + \frac{x-1}{3+\sqrt{3}}\right)^2 + \left(1 + \frac{x-1}{3-\sqrt{3}}\right)^2 \right] \right) (x-1) \\ &= (x^3 + x^2 + x + 1 - 2(x^2 + x + 1))(x-1) \\ &= x^4 - 1 - 2(x^3 - 1) \\ &= x^4 - 2x^3 + 1 \end{aligned} \quad (C.29)$$

In this case, the resulting equation (C.29) is identical to the unknown equation (C.26) at the equilibrium because Eq. (C.26) does not have terms higher than  $O(\delta x^5)$  and the form used is exact. The fits for the derivative matrix, Eq. (C.27), can be implemented in subroutine form and evaluation of Eq. (C.28) is straightforward during simulation.

Example 2: Matrix Case

A complex nonlinear set of differential equations is listed below:

$$\dot{x}_1 = -x_1^4 u_1 + x_2^3 - x_1^2 x_3 - x_1 u_2^4 + u_1 + u_2 \quad (C.30)$$

$$\dot{x}_2 = -x_2^3 - x_1 x_2 x_3 x_4 u_1 - x_1 x_4 u_2^3 - u_1^2 u_2^2 x_3 + 2u_1 + 2u_2^2 \quad (C.31)$$

$$\dot{x}_3 = -x_3 u_2^3 - x_1 u_1 u_2 - x_2 u_2^4 u_1^4 - x_4 u_1^8 + 6u_2^3 u_1^3 \quad (C.32)$$

$$\dot{x}_4 = -x_4^4 u_1 u_2 - x_2 x_3^3 u_1 - x_1 x_2 u_1 u_2 - x_1 x_4 - x_4 + 5 \quad (C.33)$$

These equations, for example, might represent an approximation to engine dynamics derived from a nonlinear dynamic simulation. These equations could be replaced by the trim map or steady state schedules and a functional representation of the time derivatives. The equivalent linear dynamics function is shown below:

$$F(\underline{x}, \underline{u}) = \begin{bmatrix} -4x_1^3 u_1 - 2x_1 x_3 - u_2^4 & 3x_2^2 & -x_1^2 & 0 \\ -x_2 x_3 x_4 u_1 - x_4 u_2^3 & -x_1 x_3 x_4 u_1 - 3x_2^2 & -x_1 x_2 x_4 u_1 - u_1^2 u_2^2 & -x_1 x_2 x_3 u_1 - x_1 u_2^3 \\ -u_1 u_2 & 0 & -u_2^3 & -u_1^8 \\ -x_2 u_1 u_2 - x_4 & -x_3^3 u_1 - x_1 u_1 u_2 & -3x_2 x_3^2 u_1 & -6x_4^3 u_1 u_2 - x_1 - 1 \end{bmatrix} \quad (C.34)$$

The procedure is verified for the equilibrium point,

$$x_1 = x_2 = x_3 = x_4 = u_1 = u_2 = 1 \quad (\text{C.35})$$

The "simulation" procedure integrates the following equations:

$$\dot{\underline{x}} = \frac{1}{2} \left( F\left(\underline{1} + \frac{\underline{x}-\underline{1}}{3+\sqrt{3}}, \underline{1}\right) + F\left(\underline{1} + \frac{\underline{x}-\underline{1}}{3-\sqrt{3}}, \underline{1}\right) \right) (\underline{x}-\underline{1}) \quad (\text{C.36})$$

for any  $\underline{x}(0) = \underline{x}_0$ . In this case, the nonlinear equations are of lower order than  $x^5$  so the solutions are identical. The equations can be integrated numerically to verify the results. Notice that inaccuracies in  $F(\underline{x}, \underline{u})$  do not affect the equilibrium point of the simulation equations.

## REFERENCES

1. Szuch, J.S., Soeder, J.F., Seldner, K., and Cwynar, D.S., "F100 Multivariable Control Synthesis Program - Evaluation of a Multivariable Control using a Real-Time Engine Simulation," NASA Final Report, Proposed Technical Memo, June 1977.
2. De Hoff, R.L., Hall, W.E., Adams, R.J. and Gupta, N.K., "Design of a Multivariable Controller Utilizing Linear Quadratic Methods," AFAPL-TR-77-35, June 1977.
3. Miller, Ronald J. and Hackney, Ronald D., "Research on F100 Multivariable Control," AFAPL Contract F33615-75-C-2048, Final Report for Period 1 June 1975-31 August 1976, AFAPL-TR-76-4, November 1976.
4. Kast, H.B., Hurtle, J.E., and Poppel, G.L., "Backup Control for a Variable Cycle Engine," Phase I Interim Technical Report, AFAPL-TR-77-92, December 1977.
5. Barclay, B.A. and Richards, J.C., "FADEC Preliminary Design Overview for Variable Cycle Engine Control," AIAA/SAE 13th Propulsion Conference, No. 77-837, July 1977.
6. Wanger, R., Corley, R., and Anderson, R., "Variable Cycle Engine Multivariable Control Synthesis," Phase I General Electric Interim Technical Report, August 1978.
7. Beattie, E.E., Carlisle, L.B., Katzer, T.J. and Spock, W.R., "Attitude Control/Engine Control Systems," Final Report, NAPTC Contract N00019-72-C-0612, December 1975.
8. Teren, F., "Solution of Transient Optimization Problems by using an Algorithm Based on Nonlinear Programming," NASA TM X-73618, June 1977.
9. Bryson, A.E. and Hall, W.E., "Optimal Control and Filter Synthesis by Eigenvector Decomposition," Stanford University, SUDAAR No. 436, November 1971.
10. Bryson, A.E. and Ho, Y.C., Applied Optimal Control, Ginn Blaisdell, Waltham, Mass., 1969.
11. Merrill, W.C., "Design of Turbofan Engine Controls using Output Feedback Regulator Theory," presented at the 1977 JACC, San Francisco, CA, June 1977.

12. Gill, P.E., Murray, W., and Pitfield, R.A., "The Implementation of Two Revised Quasi-Newton Algorithms for Unconstrained Optimization," National Physics Laboratory, NAC11, April 1972.
13. Twine, W.S. and Athans, M., "On the Determination of the Optimal Constant Output Feedback Gains for Linear Multivariable Systems," IEEE Transactions on Automatic Control, Vol. AC-15, No.1, p.44, February 1970.
14. Choi, S.S. and Sirisena, H.R., "Computation of Optimal Output Feedback Gains for Linear Multivariable Systems," IEEE Transactions on Automatic Control, Vol. AC-19, No. 3, p.257, June 1974.
15. De Hoff, R.L. and Hall, W.E., "Systems Identification Principles Applied to Multivariable Control Synthesis of the F100 Turbofan Engine," presented at the 1977 JACC, San Francisco, CA, June 1977.
16. De Hoff, R.L. and Hall, W.E., "Advanced Fault Detection and Isolation Methods for Aircraft Turbine Engines," Office of Naval Research Report ONR-CR-215-245-1, February 1978.
17. Vetter, W.J., "Derivative Operations on Matrices," IEEE Transactions on Automatic Control, April 1970.
18. Athans, M. and Schweppe, F. C., "Gradient Matrices and Matrix Calculations," MITLL TN 1965-53, November 1965.
19. Spang, H.A. III and Corley, R.C., "Failure Detection and Corrections for Turbofan Engines," General Electric Report No. 77CRD159, June 1977.